Study on the Inhibition Mechanism of Histone Deacetylases by Design of Inhibitors with Various Functional Groups

Md. Shahidul Islam

Graduate School of Life Science and Systems Engineering
Kyushu Institute of Technology, Japan

March, 2011

Study on the Inhibition Mechanism of Histone Deacetylases by Design of Inhibitors with Various Functional Groups

A dissertation in partial fulfillment of the requirements for the degree of Doctor of Philosophy

Md. Shahidul Islam

Student Number: 08897004

Graduate School of Life Science and Systems Engineering

Kyushu Institute of Technology, Japan

March, 2011

Contents

Chapter 1. Histone deacetylase inhibitors

Chapter 1

Histone Deacetylase Inhibitors

1. Introduction

The organization of DNA in eukaryotic cells is accomplished with the help of histones. Histones are found in octameric form with DNA wrapped around the exterior of the octamer. This DNA/histone complexes are called nucleosomes which are packed together to form chromatin. DNA must be unwound from the histones before it can be accessed by the large complexes responsible for transcription and replication. Nucleosomes exist in either a condensed conformation, where transcription is repressed, or in an open conformation that is transcriptionally active (Figure 1).[1] Regulatory proteins cause changes in nucleosome conformation through chemical modification of the histones.

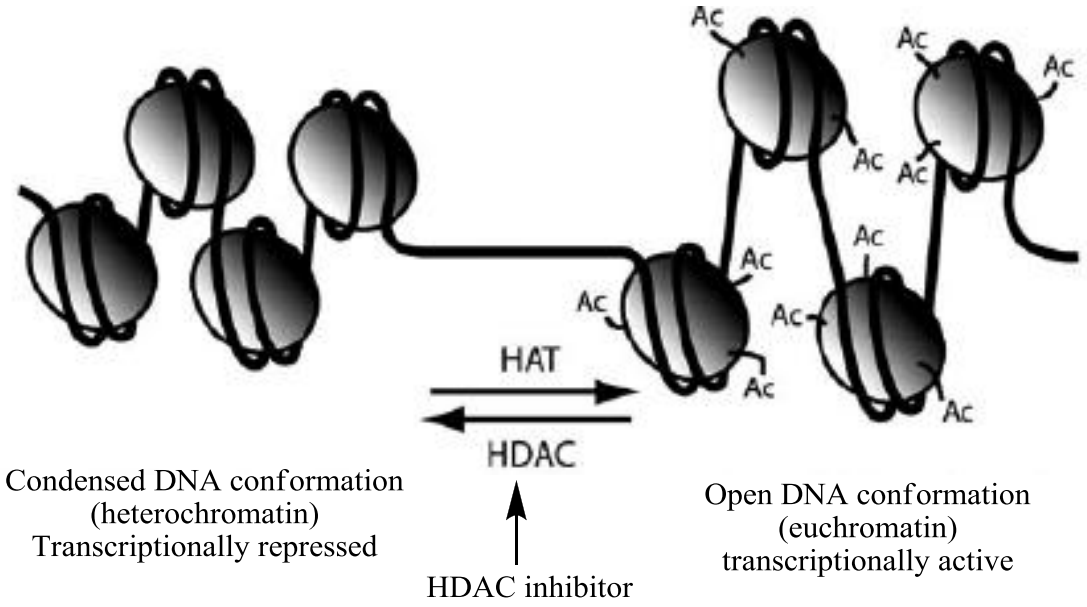

Figure 1. Dynamic histone acetylation and deacetylation.

These modifications include phosphorylation, methylation, ribosylation and acetylation. Many of the modifications to the histones occur at lysine residues near the amino terminus of the histone protein. These lysine residues are positively charged at physiological pH. The charged lysine residues interact with the oxygen anions of the

DNA phosphate backbone, forming strong ionic interactions that keep the DNA wound tightly around the histones. Histone acetyltransferase (HAT) is responsible for transfer of an acetyl group to the side chain amine of the lysine residues which neutralizes the positive charge and allows the DNA to unwind from the histone. In this unwound conformation, the DNA is transcriptionally active. Histone deacetylase (HDAC) catalyzes the reverse reaction, the removal of acetate from the lysine residues which restores the ionic interaction and causes DNA to return to the transcriptionally repressed, condensed conformation.[2] In brief, HAT promotes gene transcription and HDAC promotes gene repression. Up to date studies and growing evidences support that the imbalance in histone acetylation can lead to transcriptional deregulation of genes that are involved in the control of cell cycle progression, differentiation and/or apoptosis. Aberrant histone acetylation caused by the disrupted HAT activity or abnormal recruitment of HDACs has been related to carcinogenesis and cancer progression. Inappropriate recruitment of HDACs provides a molecular mechanism by which genes necessary for proper differentiation or growth arrest can be silenced leading to excessive proliferation. Owing to the link between transcriptional repression and the recruitment of HDACs, inhibitors of this enzymatic activity are expected to reverse repression and to induce re-expression of differentiation-inducing genes.

2. Reversible acetylation and deacetylation

Among the several posttranslational modifications, reversible acetylation of the ε-amino groups of lysine residues clustered near the amino terminus of nucleosomal histones has been the most studied and appreciated histone modification. Acetylation of specific lysine residues in the amino termini of the core histones plays a fundamental role in transcriptional regulation. All core histone proteins are reversibly and dynamically acetylated at multiple sites in their N-terminal tails (Lysine 9, 14, 18 and 23 in H3; and 5, 8, 12 and 16 in H4). Hyperacetylated histones (euchromatin) are generally found in transcriptionally active genes and hypoacetylated histones in transcriptionally silent regions, such as heterochromatin. The level of histone acetylation at a particular locus in chromatin reflects the competing activities of the enzymes histone acetyl transferases (HATs) and histone deacetylases (HDACs).[3-5] Thus HAT and HDAC activity control the level of acetylation and in turn, can regulate the gene expression and its biological

functions (Figure 1). Any alteration in the enzyme activity leads to aberrant acetylation. Aberrant acetylation has been linked to cellular transformation and in development of cancer suggesting that both HATs and HDACs play an important role in carcinogenesis.[6-9]

3. Histone acetyl transferases (HATs)

Acetylation of histones by HAT effectively neutralizes the positive charge on lysine which results in the destabilization of both the inter-nucleosomal interactions and the association of the histone with the negatively charged phosphate backbone of DNA.[10-14] Thus acetylation results in the unwinding of the nucleosomal array, decreases the interaction between histone and DNA which loosens the nucleosome structure. This conformational change activates transcription by promoting the access of RNA polymerase, transcription factors, regulatory complexes and other transcriptional machinery to the DNA template. This process can be regulated by the presence of HDACs which control the amount of acetylation by opposing the action of HATs and thereby control the extent to which transcription can occur.

4. Role of histone deacetylases (HDACs)

When the gene no longer needs to be transcribed, the HDACs are recruited to key locations in nucleosomes through their interaction with transcription complexes and remove the acetyl group in the lysines added by HATs.[7-9,12,15-18] The removal of the chemical group restores the positive charge of ε-amino group of lysines and enables histone to interact electrostatically to the negatively charged phosphate backbone of DNA. In this way, DNA binds tightly to histone and restricting access of transcription factors to silence genes.

5. Histone deacetylation and cancer

The modification level of histone acetylation and its consequences have received enormous interest in recent years and increased evidences support their importance for basic cellular functions such as DNA replication, transcription, differentiation and apoptosis. HDACs and HATs usually act with other proteins in suppressing or activating transcription. Abnormal activities of HATs and HDACs have been linked to

the pathogenesis of cancer. Although inactivating mutations of HATs and over expression of HDACs have been described,[8,9,12,15-19] the best link between HDACs and cancer progression comes from models of acute promyelocytic leukemia's where chromosomal translocations result in chimeric proteins that alter transcriptional events and thereby interfere with normal cell growth, differentiation and apoptosis. Chromosomal translocations between RARa (retinoic receptor a) and PLZF (promyelocytic leukemia zinc finger) or PML (promyelocytic leukemia protein), for example, lead to inappropriate recruitment of co-repressors and HDACs and abolish the ability of RARa to mediate myelocytic differentiation. Another well-documented example is AML1-ETO where ETO recruits N-CoR and mSin3A together with HDACs which also interferes with retinoic acid functions and myeloid differentiation. In addition, a gene frequently deregulated in lymphomas is BCL-6 which recruits a complex containing SMRT, mSin3A and HDAC. Together, these examples have in common the aberrant recruitment of HDACs to promoters mediating transcriptional repression which strengthens the rationale for the development of HDAC inhibitors as cancer therapeutics.[19]

6. The HDAC family

HDAC1 was identified using the HDAC inhibitor trapoxin as an affinity from nuclear extract in 1996.[20] It was found that HDAC1 shares high sequence homology with yeast Rpd3 (Reduced potassium dependency 3), a global gene regulator and transcriptional co-repressor with histone deacetylase activity.[21] Subsequently, 18 HDAC family members have been identified in the human genome. HDACs are divided into class I-IV based on their sequence homology to their yeast orthologues Rpd3, HdaI and Sir2 (silent information regulator 2) respectively.[22,23] Class I (HDACs 1, 2, 3, and 8) and class II (HDACs 4, 5, 6, 7, 9, and 10) HDACs are Zn^{2+}-dependent amidohydrolases with a conserved catalytic core but differing in size, domain structure and tissue expression pattern. Class III HDACs are NAD^{+} dependent, unrelated in sequence and mechanism to classes I and II. Class IV consists of HDAC11. Very little information is available about its expression and function.[24] Zn^{2+} dependent enzymes harbor a catalytic pocket with a Zn^{2+} ion at its base that can be inhibited by Zn^{2+} chelating compounds. In contrast, these compounds are not active against sirtuins as class III enzymes have a

different mechanism of action requiring NAD^+ (nicotinamide adenine dinucleotide) as an essential cofactor.[22] Class II HDAC family members are further subdivided into IIA (HDACs 4, 5, 7 and 9) and IIB (HDACs 6 and 10). Class IIA members are defined by a large, functionally important N-terminal domain regulating nuclear-cytoplasmic shuttling and specific DNA-binding. Class IIB HDAC contains two tandem deacetylase domain and C-terminal zinc finger. HDAC6 has emerged as a major deacetylase functioning as an α-tubulin deacetylase.[25] HDAC10 structurally related to HDAC6, but contains one additional catalytically inactive domain. Its function is largely unknown.[24]

7. HDAC structural study and concept of inhibitor design

Class I HDACs are 350-500 amino acid proteins, while class II enzymes are usually about 1000 amino acid long. Due to the larger size of class II HDACs, they posses many additional structural features, including a lengthy N-terminal sequence. The class I and class II HDACs share a 320 residue region of homology, corresponding to the section of the enzyme that forms the catalytic pocket.[26] The highly conserved catalytic pocket presents challenges to development of selective HDAC inhibitors. However, some structural differences have been found useful in generating class selective and isoform selective inhibitors.[27]

HDAC is typically found in the nucleus, at the location of the histone substrates, but can also be found in the cytoplasm. A nuclear import signal (NIS) is required for the HDAC to be transported into the nucleus, and a nuclear export signal (NES) is necessary for transportation out of the nucleus. Regarding the class I enzymes, HDAC1 and 2 are primarily found in the nucleus, as they lack an NES, although HDAC3 can be exported to the cytoplasm, as they contain an NES. Class II HDACs are generally cytoplasmic proteins, but they may be chaperoned into the nucleus. The 14-3-3 protein forces HDAC enzymes to remain in the cytoplasm. Binding of 14-3-3 to nuclear localization sequences on the class II enzymes interferes with the nuclear import and export signals and confines the enzymes to the cytoplasm. 14-3-3 binding is regulated by phosphorylation of serine residues on the HDAC.[28,29] Class I HDACs tend to be found in all tissue types, while class II enzymes are more tissue specific. This observation has led researchers to speculate that class II enzymes may have an important role in cellular

differentiation and development.[17] HDAC6 is the most frequently expressed isoform which may be related to its ability to deactylate a variety of targets, including histones, tubilin and heat shock protein. The HDAC4 enzyme is quite rare in normal tissues, but is found with much higher incidence in tumor tissues.[22] HDAC6 is exceptional in that it has two independent catalytic sites. Mutagenesis studies have demonstrated that each site is independent and has a unique set of substrates. Additonally, one site can remain active even if the other is disabled by mutation. A truncated form of HDAC6 that contains no N-terminal catalytic domain retains activity in the C-terminal domain. Mutagenesis and inhibitor studies confirmed that tublin deacetylation takes place only at the C-terminal catalytic site.[30,31] With the exception of HDAC6, histone deacetylases must form multiprotein complexes with regulatory proteins to be active *in vivo*. Crystal structures of the HDACs and their homologues provide essential information for rational drug design of selective HDAC inhibitors. Currently, crystal structures have been reported for HDAC8,[32] HDAC7[33] and a variety of histone deacetylase homologues including HDLP[34] and FB188 HDAH.[35]

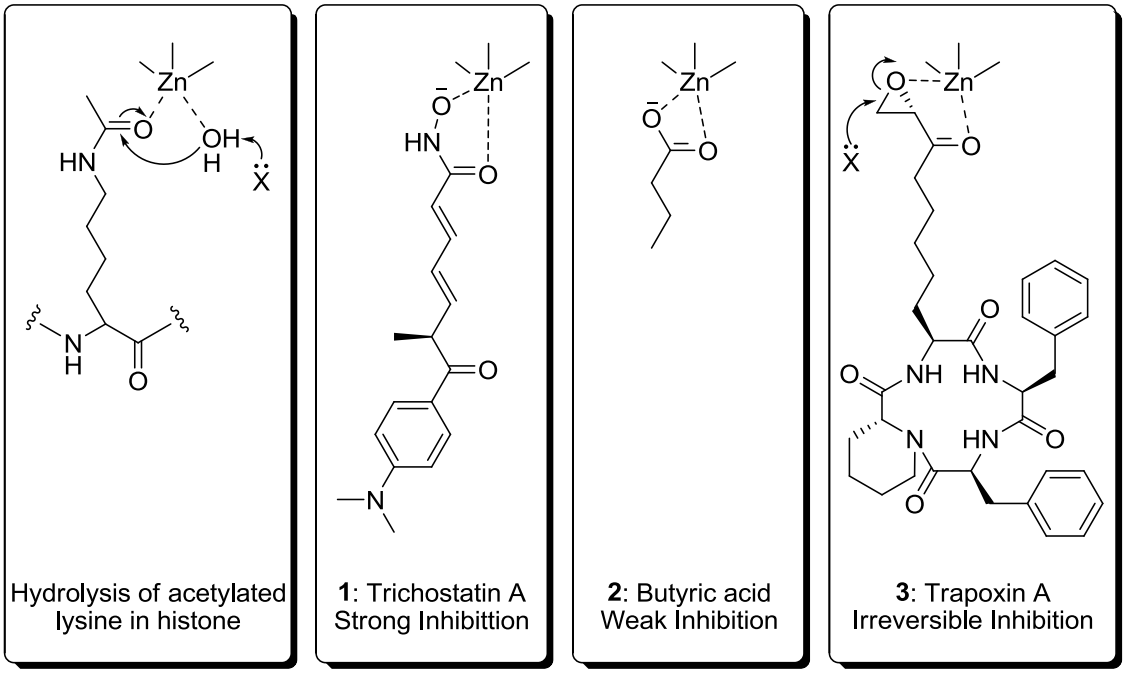

Figure 2. Concept of HDAC inhibitory mechanism.

In 1990s, Yoshida and coworkers found that three different compounds with various functional groups and with different characteristics inhibit HDAC in different extents.[36]

One of the inhibitors, trichostatin A (**1**, TSA), is a strong inhibitor of HDAC, on the other hand, butyric acid (**2**) is a weak inhibitor and trapoxin A (**3**) is an irreversible inhibitor. On the basis of the inhibitory activities of the hydroxamic acid **1**, carboxylic acid **2** and epoxy ketone **3**, they proposed that HDAC is a metalloprotease enzyme and suggested the reason for the difference in the activities of these three compounds (Figure 2).

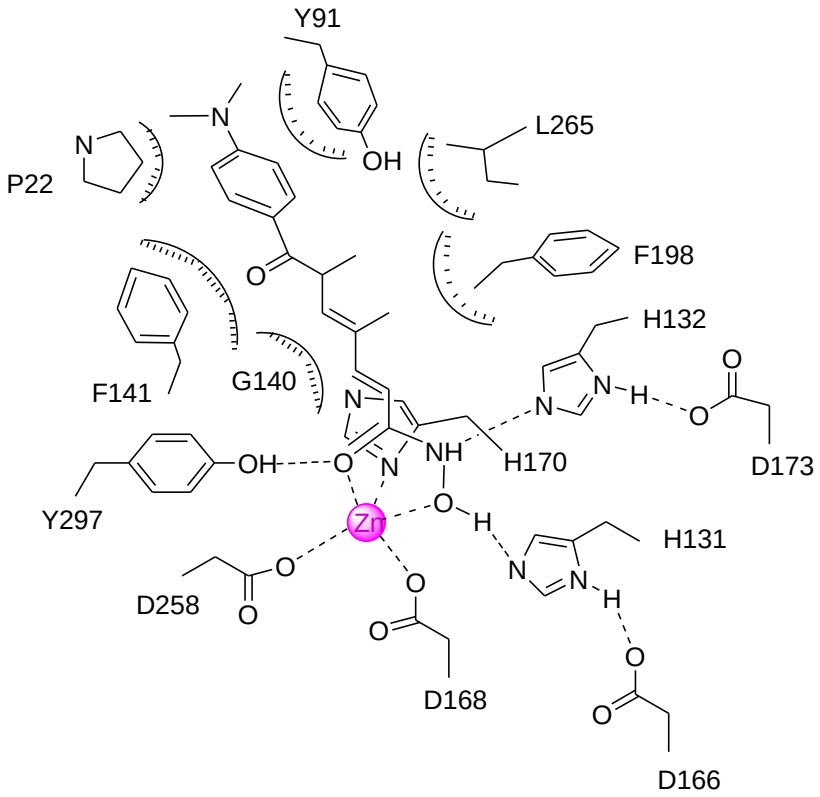

Figure 3. Crystal structure of TSA bound to the HDLP.

Based on this hypothesis, Yoshida *et al*. synthesized a series of potent HDAC inhibitors with activity in the nanomolar range.

The structural details of the class I/II HDAC inhibitor-enzyme interactions were first elucidated by Finnin *et al*. in 1999.[34] The crystal structure of histone deacetylase-like protein (HDLP), which was isolated from a hyperthermophilic bacterium, *Aquifex aeolicus*; a homologue of mammalian class I/II HDAC with 35.2% sequence identity over 375 residues, was solved with the HDAC inhibitor (*R*)-trichostatin A (TSA, **1**) (Figure 3) bound to the active site. This structural information provided the first

concrete evidence that this enzyme indeed contained an active site zinc-binding pocket, consistent with previous observations[26] that HDAC activity was contingent upon the presence of a metal cofactor and strongly supported by the pronounced activity of certain hydroxamic acid-based inhibitors. The crystal structure reveals that HDLP has a single-domain structure belonging to the open α/β class of folds and the catalytic domain is very closely related to that of HDACs. The enzyme contains two Asp-His charge-relay systems, a structural feature which is conserved across the HDAC family. The prominent architectural feature of the ligand binding site shows the presence of a gently curved tubular pocket approximately 11Å deep (Figure 4) whose walls are lined with hydrophobic and aromatic residues identical to those found in HDAC1. The cavity narrows to ~7.5Å near its center, constrained by the parallel disposition of Phe141 and Phe198. In the crystal structure of the zinc-reconstituted enzyme, the zinc ion is positioned near the bottom of the pocket. It is coordinated by Asp168, His170, Asp258 and a water molecule. In the crystal structure of HDLP-TSA complex, TSA binds by inserting its long aliphatic chain into the HDAC pocket, making multiple contacts to the tube-like hydrophobic portion of the pocket. The hydroxamic acid group at one end of the aliphatic chain reaches the polar bottom of the pocket where it coordinates the zinc in a bidentate fashion and also contacts active site residues. The aromatic dimethylamino-phenyl group at the other end of the TSA chain makes contacts at the pocket entrance and in an adjacent surface groove, capping the pocket. The length of the aliphatic chain is optimal for spanning the length of the pocket and allowing contacts at the bottom and at the entrance of the pocket. The structural information mentioned above facilitates elucidation of the precise deacetylation reaction mechanism. The carbonyl and hydroxyl groups of hydroxamic acid along with three tetrahedral-disposed residues (Asp168, His170, Asp258), coordinates the zinc atom and results a penta-coordinated Zn^{2+} and the sole coordinated water molecule is shifted ~25°

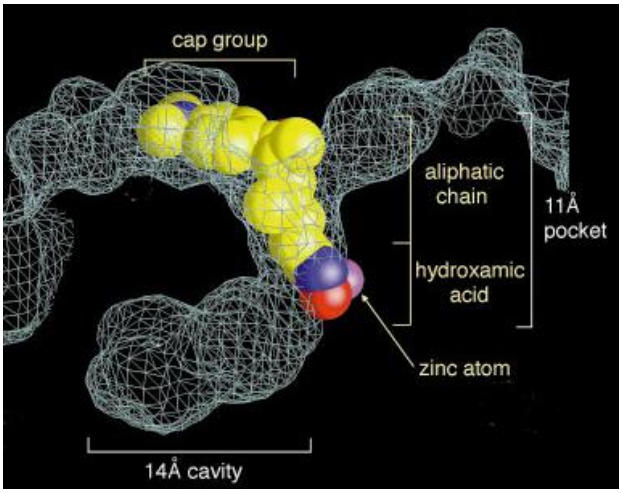

Figure 4. Space-filling representation of TSA in the active-site pocket.

away from ideal geometry. The catalytic mechanism proposed by Finnin and colleagues is shown in Scheme 1. In HDLP, Tyr297 and zinc form bonds with the carbonyl oxygen of the acetyl group, causing an increase in the electrophilicity of the carbonyl group. Two charge transfer complexes made up of His132 and Asp173, and also His131 and Asp166 hydrogen bond with the free water molecule, increasing the nucleophilicity. Water is further activated by binding with zinc which lowers the pKa of water. At this point, the various interactions between the enzyme and the substrate have sufficiently lowered the activation energy of the reaction and a nucleophilic attack occurs by the water nucleophile upon the carbonyl carbon of acetyl-lysine, generating a tetrahedral intermediate. The tetrahedral intermediate is stabilized by Tyr297 and Zn^{2+}. Collapse of the tetrahedral intermediate eliminates lysine and the free acetate picks up a proton from the enzyme. Lysine dissociates from the enzyme and the enzyme eliminates acetate by shuttling it out of the enzyme through the interior cavity. Hydrogen bonds between an Asp residue on the enzyme surface and two NH groups of the substrate lock the substrate in place for catalysis.

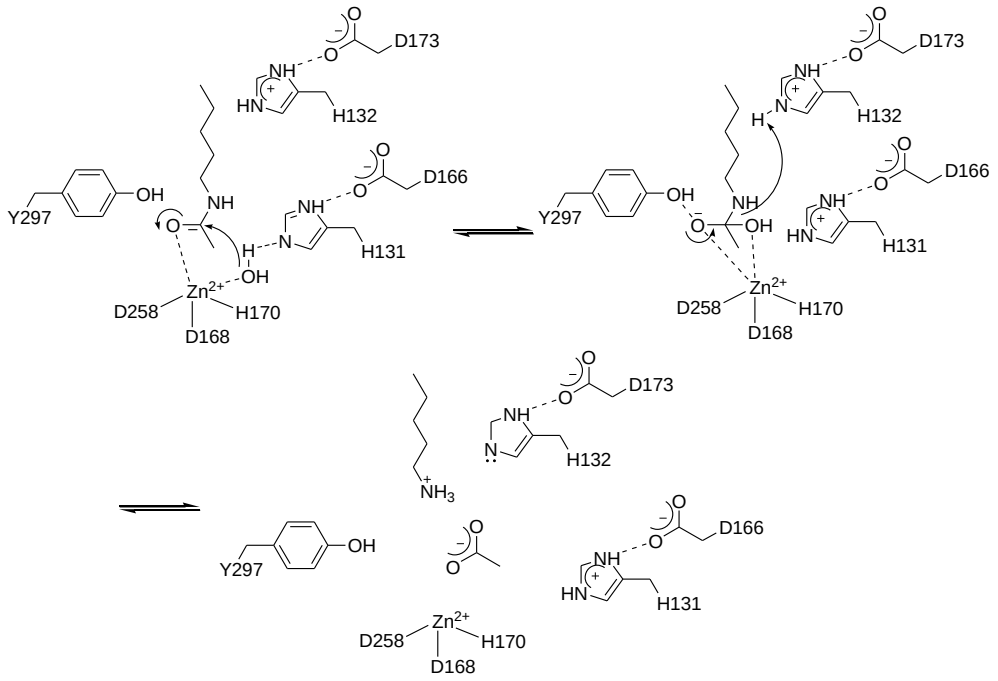

Scheme 1. Mechanism of deacetylation of acetylated lysine.

In addition, separate mutagenesis experiments established that replacement of the two Asp-His charge-relay system profoundly disrupted the enzyme's biological activity.[37]

More interestingly, the crystal structure showed that upon TSA binding the side chain of one tyrosine (Tyr91) which is at the periphery of the pocket and mostly solvent exposed, changes conformation to make space for the dimethylamino-phenyl group of TSA.

8. Structure of inhibitor

The histone deacetylase enzymes are able to be inhibited by small molecules. The inhibitor binds tightly to the active site and likely chelates the zinc cofactor, so that catalysis cannot occur. Most HDAC inhibitors, including those in clinical trials, are reversible, although irreversible inhibitors are known.[38] HDAC enzymes have three primary domains (functional group or metal binding domain, spacer or linker domain and cap group or surface recognition domain), each with a specific function relating to the structure of the enzyme. The basic functional domain of an HDAC inhibitor is the functional group or metal binding domain which chelates the zinc ion and engages in multiple hydrogen bonds with the residue at the active site. The functional groups/zinc ligands are typically a thiol, hydroxamic acid, carboxylic acid, ketone or substituted aniline. Recently, HDAC inhibitors with boronic acid functional group have also been reported.[39] The zinc binding region is analogous to the acetyl group of the N-acetylated-lysine substrate and it interacts with many of the same residues of the enzyme. Irreversible inhibitor have an electrophilic group, usually a keto-epoxide in the zinc binding region that may become covalently attached to a nucleophilic residue, such as His, Asp or Tyr in the active site.[40,41] The cyclic tetrapeptide trapoxin was shown experimentally to irreversibly inhibit the HDAC enzymes through reduction of the epoxide.[41] The linker domain is generally a hydrophobic chain, homologous to the hydrophobic portion of the lysine side chain. The linker bridges the zinc binding group and the surface recognition domain or cap group. The cap group is connected to the linker through a connecting unit, typically an amide bond. The cap group frequently contains one or more aromatic or heteroaromatic ring systems, although many structurally diverse cap groups have been reported. Inhibitors with multiple cap groups are frequently made and some of these compounds show enhanced potency and selectivity.[42] Because, the residues on the enzyme surface which surround the binding pocket are much less conserved than those in the active site, making the enzyme surface an important source of selectivity.[35] Difference at the enzyme surface between the

HDAC isoforms will cause the inhibitor cap group to interact with the enzyme in different ways. The result is that the inhibitor will have a different activity at each isoform. If the difference in activities between isoforms is large enough, the inhibitor is said to be selective.

9. The inhibitors of HDACs

From the crystal structural studies of HDLP complexed with TSA or SAHA, it is clear that the criteria to be fulfilled by a molecule for an effective inhibitor for HDACs are, a functional group capable of chelating the active site Zn^{2+} ion (e.g., carboxylic acid, hydroxamic acid, sulfhydryl etc.) attached to a hydrophobic scaffold (cap group) by means of a spacer. The functional group, scaffold and spacer play their specified role in the inhibitory activity. The inhibitory activity is determined by several factors, such as, the length of the spacer and interactions of the spacer with the hydrophobic residues in the channels of catalytic site, the nature of scaffold and its interaction with the residues at the rim region of the catalytic site and the strength of bonding between the functional group and the active site. Depending on the functional groups and the construction of hydrophobic surface binding scaffolds, HDAC inhibitors can be roughly categorized into several structural classes. The following is a brief discussion of different HDAC inhibitor classes.

9.1. Carboxylates

Butyric acid (**2**),[43] a natural product generated in man by metabolism of fatty acids and bacterial fermentation of fibre in the colon, was the first identified HDAC inhibitor. The related compounds, such as phenyl butyrate (**5**) and anticonvulsant valproic acid (**6**)[44] were later found as antiproliferative agents and HDAC inhibitors (Figure 5). However, these carboxylates are far less potent in comparison with other inhibitors. The carboxylic acid chelating group is less active than the other functional groups such as hydroxamic acid; may be due to weak coordination with Zn^{+2} ions. Despite being much less potent and their pleitropic effects, these are currently among the best studied HDAC inhibitor. Valproic acid and phenyl butyrate have already been approved for use in treating epilepsy and some cancers respectively, whereas butanoic acid (or its prodrug forms such as pivaloyloxymethylbutyrate) is undergoing clinical trials.

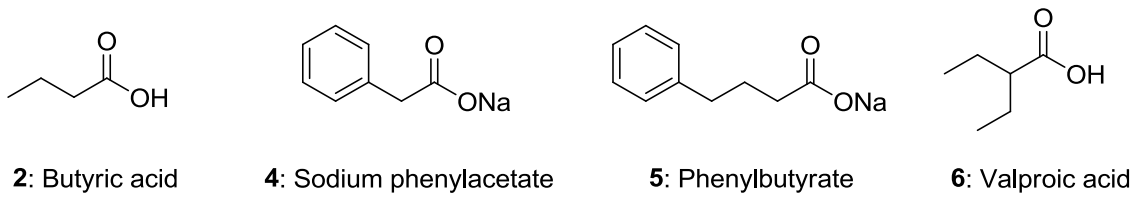

2: Butyric acid **4**: Sodium phenylacetate **5**: Phenylbutyrate **6**: Valproic acid

Figure 5. Carboxylic acids as HDAC inhibitors.

9.2. Hydroxamic acids

Hydroxamic acid, one of the well-studied ligand for the active site Zn^{2+} of HDACs, has constituted the broadest family of HDAC inhibitors. A large number of HDAC inhibitors containing hydroxamic acid as functional group are known, including natural products like trichostatin A (TSA) (**1**). The general structure of these inhibitors consists of a hydrophobic linker that allows the hydroxamic acid moiety to chelate the Zn^{2+} cation at the bottom of HDAC catalytic pocket, while the bulky part of the molecule which is the surface recognition domain, acts as a cap group. The linker domain can consist of linear or cyclic structures, either saturated or unsaturated, is generally a hydrophobic group (Figure 6).

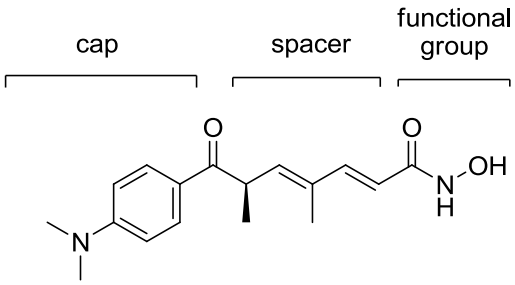

1: Trichostatin A

Figure 6. Structural dissection of TSA based on crystal structure of HDLP-TSA complex.

TSA was first isolated in 1976 by Tsuji *et al*. from S*treptomyces hygrocopicus* as an fungistatic antibiotic active against *trichophytin*[45] and the HDAC activity of TSA was found by Yoshida and coworkers in 1990.[46] TSA is a potent inhibitor of HDACs with activity in the nanomolar concentrations, whereas the corresponding carboxylate, trichostatic acid, was shown to be ineffective as an HDAC inhibitor, indicating that the hydroxamate is inevitable for the activity.[47] Furthermore, the enantiomer (*S*)-TSA which was obtained by total synthesis, was demonstrated to be inactive.[47,48] The interactions of

hydroxamic acid functional group at the active site of HDAC are known from the X-ray structure (Figure 4).

Based on the structure of TSA and its interaction with HDAC, a large number of inhibitors were designed and synthesized. Structurally simple TSA like straight chain hydroxamate, suberoylanilide hydroxamic acid (SAHA, **7**) was reported by Breslow and coworkers, as a cytodifferentiating agent and HDAC inhibitor.[49, 50] After the disclosure of this potent synthetic compound, a large number of synthetic HDAC inhibitors were reported. Examples are, hydroxamates analogous to SAHA, including pyroxamide (**8**), CBHA (**9**) and 3-Cl-UCHA (**10**) (Figure 7).[50,51] These agents have been shown to be effective HDAC inhibitors and antiproliferative agents, both *in vitro* and *in vivo*.

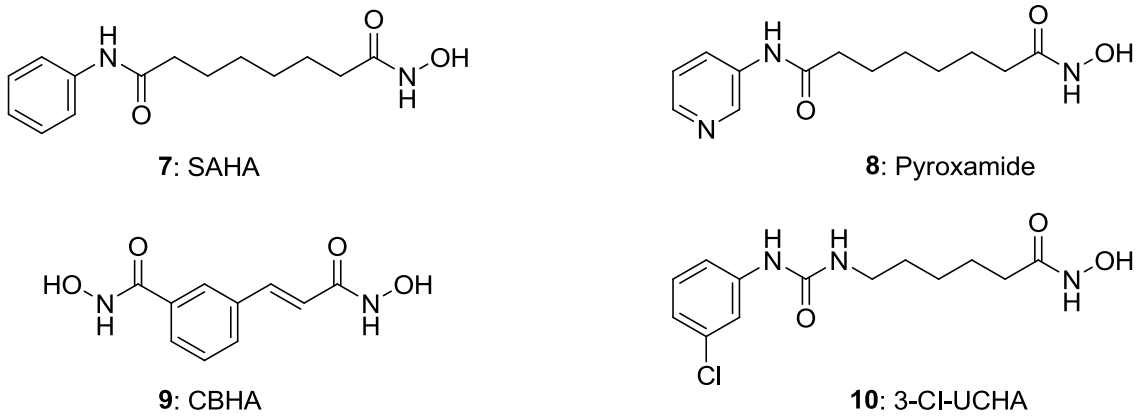

Figure 7. Hydroxamic acid-based HDAC inhibitors having linear linker.

SAHA (**7**), commercially known as vorinostat (Zolinza; Merck), has been approaved by the U.S. FDA for the treatment of cutaneous manifestations in patients with cutaneous T-cell lymphoma.[52] The synthetic SAHA, CBHA and natural TSA which represent the archetypical hydroxamate HDAC inhibitors, have been instrumental in guiding the design of hydroxamate-derived HDAC inhibitors. Structure-activity relationship (SAR) study of these paradigmatic hydroxamate compounds were performed in a focused way by several research groups. In order to understand the importance of the methyl-substituted olefinic linker in TSA hybrids, compounds **12** and **13** has been synthesized and evaluated against HDACs.[53] These agents, along with related analogue **11** (Figure 8), demonstrate a highly sensitive and selective SAR features. As for example, the

designed addition of a methyl group (**12**) and two double bonds (**13**) caused a 2.3- and 33-fold reduction in activity respectively, relative to the linear alkyl linker (**11**).

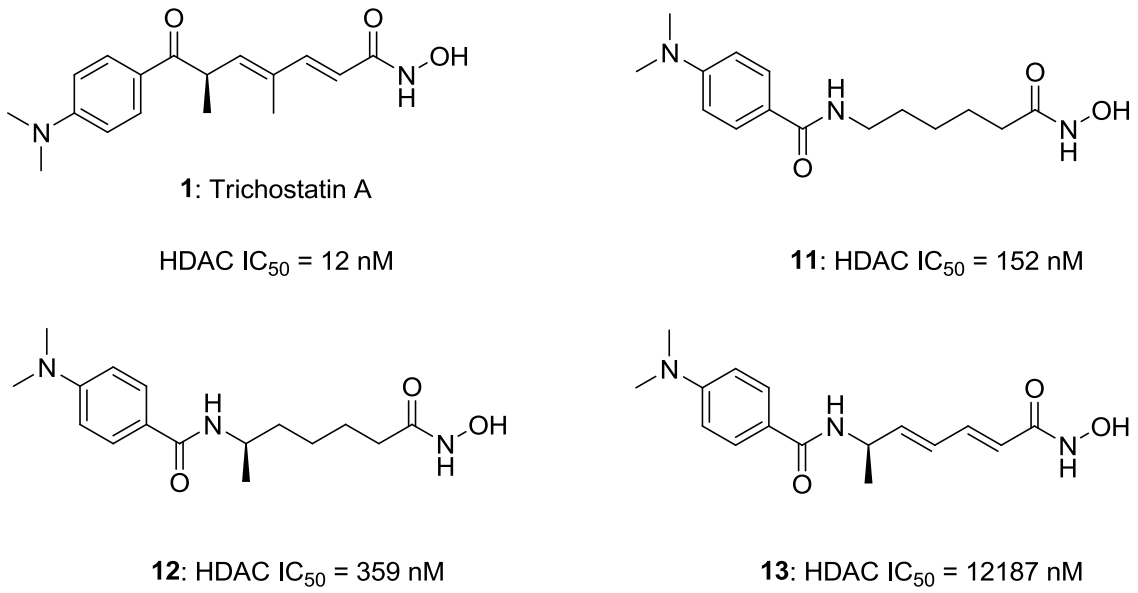

Figure 8. TSA analogues.

Using high-throughput transcriptional screening Kern and coworkers identified scriptaid (**14**) as a potent inhibitor of HDAC (Figure 9).[54] A series of tricyclic molecules related to scriptaid were recently reported and the most potent one (**15**) has IC_{50} = 10 nM.[55]

Figure 9. Inhibitors with tricyclic cap groups.

Jung and coworkers synthesized reverse amide analogues of TSA as HDAC inhibitors.[56] These compounds (Table 1) were tested against both maize histone deacetylase (HD-2) and partially purified rat liver HDAC. Using variation in the substitution at the cap portion of the inhibitor and changing the spacer length, they studied the inhibitory

activity and structure-activity relationship of simple straight chain hydroxamates (**16**) (Table 1).

Table 1. SAR of reverse amide analogues of TSA

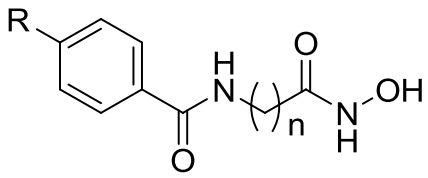

Compounds	R	n	HD-2 IC_{50} (nM)	HDAC IC_{50} (nM)
1: TSA			3	26
11	Me_2N	5	100	244
16a	Me_2N	3	>40000	-
16b	Me_2N	4	2000	>10000
16c	Me_2N	6	100	46
16d	Me_2N	7	300	145
16e	MeO	5	140	-
16f	H	5	900	-
16g	Cl	5	150	369
16h	NO_2	5	180	1566
16i	Ph	5	100	265

This study confirmed the earlier observation that compounds with five and six methylene spacers (**11** and **16c**) are the most active.[49] If the hydroxamic acid is changed to carboxylic acids, the activity of these amide analogues diminished drastically.

The same group studied the structure-activity relationship (SAR) of several SAHA analogues with a phenylalanine at the cap portion (Table 2). They found that the groups

present at the cap region have remarkable effect on the inhibitory activity (**17**).[57] Compounds **17l-o** with bulky hydrophobic side chains, appear to be the best inhibitors and differentiating agents. This series provides insight into the nature of inhibitor-enzyme interaction. The trends in activity against HD-2 are different from those observed in mammalian HDAC. For example, compound **17o** is the most active of the series against HD-2 but does not outperform the others against mammalian HDAC.

Table 2. SAR of SAHA analogues with phenylalanine cap groups

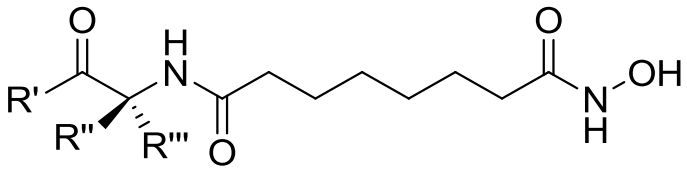

Compounds	R´	R´´	R´´´	IC_{50} (nM) Maize HD-2	IC_{50} (nM) Rat liver HDAC
1: TSA				3	12
17a	CH_3O	Bzl	H	500	800
17b	NH_2	Bzl	H	1100	840
17c	PhNH	Bzl	H	80	790
17d	BzlNH	Bzl	H	140	460
17e	$Ph(CH_2)_2NH$	Bzl	H	330	260
17f	$Ph(CH_2)_3NH$	Bzl	H	380	1010
17g	$Ph(CH_2)_2NH$	H	Bzl	340	390
17h	CH_3O	H	Bzl	760	880
17i	OH	H	Bzl	750	-
17j	CH_3O	4-MeOBzl	H	250	-
17k	CH_3O	4-PhBzl	H	210	-
17l	CH_3O	1-napthyl-methyl	H	360	130
17m	CH_3O	2-napthyl-methyl	H	40	510
17n	CH_3O	3-indolyl-methyl	H	120	320
17o	$Ph(CH_2)_2NH$	1-napthyl-methyl	H	35	310

Finally, inversion of the phenylalanine chiral center (**17e-g** vs **17a** and **17h**) did not affect inhibitor activity against the enzyme or in cells. Woo *et al*. [58] synthesized a series of TSA-SAHA analogues and evaluated these compounds as inhibitors of recombinant human HDAC1 and anti-proliferative agents against a panel of human cell lines.

Table 3. Hydroxamic acids with different cap variations

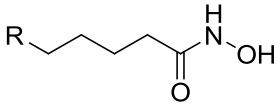

Compounds	R	HDAC1 IC_{50} (nM)	Compounds	R	HDAC1 IC_{50} (nM)
18a	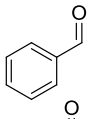	1500	18k	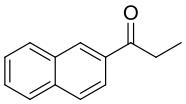	5
18b	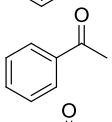	500	18l	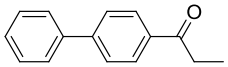	5
18c	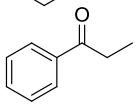	65	18m	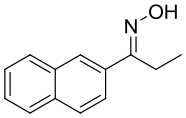	8.5
18d	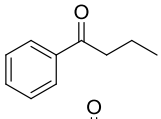	135	18n	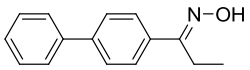	4
18e	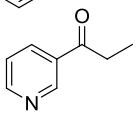	153	18o	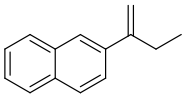	8
18f	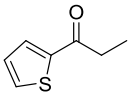	50	18p	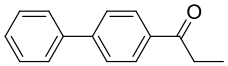	2
18g	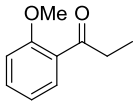	95	18q	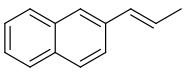	6
18h	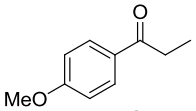	15	18r	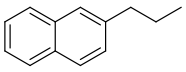	25
18i	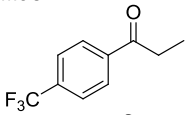	45	18s	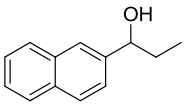	35
18j	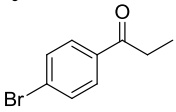	45			
	TSA	5	18t	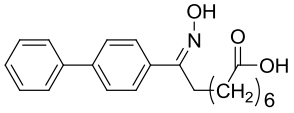	200

Heterocyclic derivatives (**18e and 18f**) were found to be active. Para-substituted aryl derivatives (**18h-18j**) were more active than ortho-substituted derivative (**18g**). The corresponding carboxylic acids were also tested and found to be inactive with the notable exception of **18t**.

Glaser and co-workers identified the biaryl ether hydroxamate **19** as a mimic of transforming growth factor β (TGF- β) with proliferation inhibitory properties (Figure 10). This compound inhibits a mixture containing human HDAC1, HDAC2, and HDAC3 (IC_{50} = 9 nM) and to cause histone hyperacetylation and p21 induction.[59]

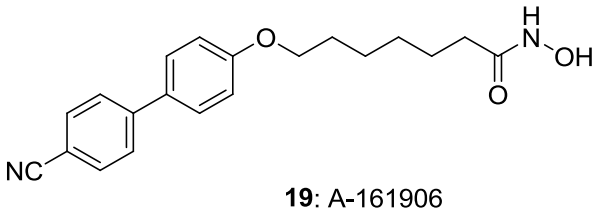

19: A-161906

Figure 10. Biaryl ether hydroxamate.

Curtin and co-workers[60] reported potent inhibitors with a succinimide surface recognition domain. Compound **20** which contains a macrocyclic surface recognition domain, has good HDAC inhibitory activity while other non-macrocyclic succinimides such as, **21** were equipotent (Figure 11).

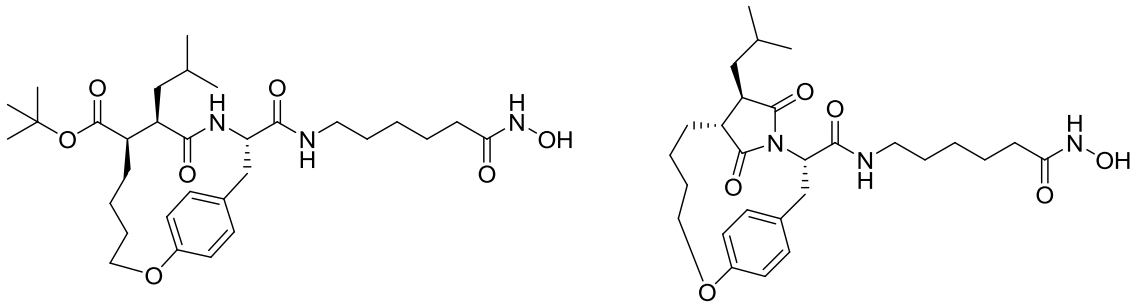

20: HDAC IC_{50} = 2100 nM

21: HDAC IC_{50} = 38 nM

Figure 11. Succinimide as cap group.

To get a complete SAR picture, a series of succinimide hydroxamic acids (**22**) were prepared and assayed against human HDAC1 (Table 4). The number, identity and disposition of macrocycle substituents are vital for activity. The removal of the succinimide substituents (**22b**) or the phenylalanine side chain (**22f**) reduces activity.

Replacement of the succinimide with a lactam or phthalimide also led to reduced activity. The length of the linker domain alkyl group was also found to be critical, with the five-methylene analogue showing maximal activity. This work revealed that the subtle adjustments of the succinimide cap group could lead to large positive changes in the HDAC inhibitory activity.

Table 4. SAR of hydroxamic acids with succinimide cap groups

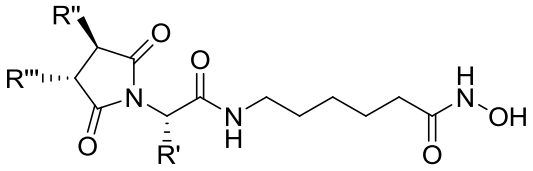

Compounds	R´	R´´	R´´´	HDAC IC_{50} (nM)
7: SAHA				120
22a	Bzl	*i*-Bu	H	99
22b	Bzl	H	H	660
22c	Bzl	*i*-Bu	*n*-Pr	51
22d	Cyclohexyl-CH_2	*i*-Bu	H	640
22e	4-MeO-Bzl	*i*-Bu	*n*-Pr	38
22f	H	*i*-Bu	H	5000

The synthesis of a series of heterocyclic-amide hydroxamic acids (Table 5) revealed the highly potent HDAC inhibitory activity of indole-amide structure **23c**.[61] Further study of the indole-amide series revealed that 2-substituted indole-carboxamides are the most active of the agents studied (**23e, 23f and 23i-k**). Finally, the structure-activity relationship of monosubstituted indole-amide hydroxamic acids led to the discovery of low nanomolar HDAC inhibitors with potent cellular activity.

In 1999, Yoshida and coworkers reported another interesting compound, oxamflatin (**24**) containing a phenyl sulfonyl amine moiety as cap group with a spacer and hydroxamic acid functional group (Figure 12) as HDAC inhibitor.[62] This compound was structurally different from other HDAC inhibitors.

Table 5. Heterocyclic-amide hydroxamic acids activity table

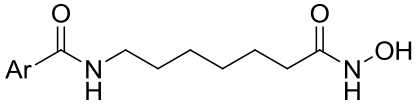

Compounds	Ar	HDAC IC_{50} (nM)	Compounds	Ar	HDAC IC_{50} (nM)
23a	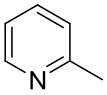	1680	23g	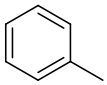	1006
23b	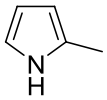	524	23h	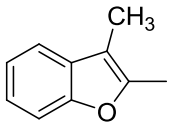	12.5
23c	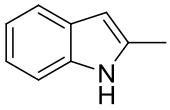	14.6	23i	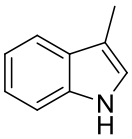	37.5
23d	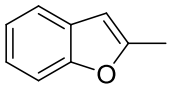	29.6	23j	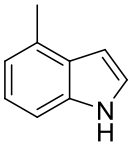	80.3
23e	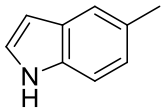	31.4	23k	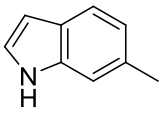	56.5
23f	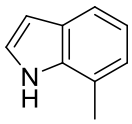	41.0	23l	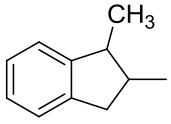	732

Oxamflatin was found to be a potent HDAC inhibitor of partially purified mouse HDAC (IC_{50} = 15.7 nM), although it was found to be less potent than TSA (**1**) (IC_{50} = 1.44 nM) in the same assay.

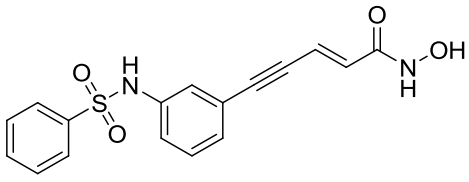

24: Oxamflatin

Figure 12. Phenyl sulfonyl amine moiety as cap group.

The disclosure of the potency of oxamflatin accelerated the research on HDAC inhibitors and hydroxamates bearing sulfonamide moiety in the cap group were reported. Delorme and coworkers developed sulfonamide hydroxamic acid base HDAC inhibitors which showed inhibitory activity in the nanomolar range. They studied the structure-activity relationship, antiproliferative activity and *in vivo* efficacy of these sulfonamide inhibitors (**25**).[63,64]

Table 6. SAR of sulfonamide hydroxamic acid base HDAC inhibitors

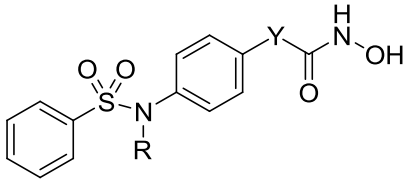

Compounds	Y	R	HDAC IC_{50} (nM)
1: TSA			5
25a	-	H	900
25b	$-CH_2-$	H	1000
25c	$-(CH_2)_2-$	H	100
25d	$-(CH_2)_3-$	H	1000
25e	-CH=CH-	H	200
25f	$-CH=C(CH_3)-$	H	2000
25g	$-CH_2CH(CH_3)-$	H	17000
25h	$-CH_2CH$(i-Pr)-	H	>25000
25i	-CH=CH-	CH_3	600

From their study it became clear that substitution on the sulfonamide or on the double bond α to the hydroxamic acid function was insufficient to confer measurable activity, whereas substitution on the aryl group provided an increase in the HDAC inhibition. The HDAC inhibitory activity of selected compounds of these series is given in Table 6. Compounds containing cinnamic (**25e**) and hydrocinnamic (**25c**) linkers were determined to be the best in a series consisting of various lengths (**25a**-**e**). The presence of the double bond has little effect on activity, while substitution R to the hydroxamate

dramatically decreased activity (**25f-h**). A 3-fold decrease in HDAC inhibitory activity was observed upon methylation of the sulfonamide nitrogen (**25i**).

Table 7. Effect of sulfonylanilides, ureas and sulfonamides on HDAC inhibition

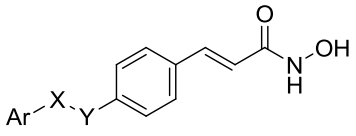

Compounds	Ar	X-Y	HDAC IC_{50} (μM)	Compounds	Ar	X-Y	HDAC IC_{50} (μM)
25e		SO_2NH	0.2	26f	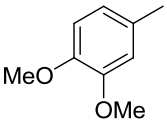	NHCONH	1
26a	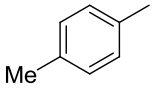	SO_2NH	0.3	26g	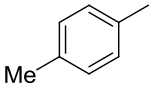	$NHSO_2$	0.2
26b	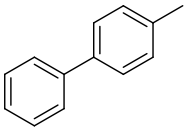	SO_2NH	0.01	26h	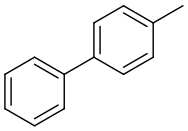	$NHSO_2$	0.04
26c	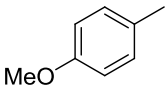	SO_2NH	0.06				
26d	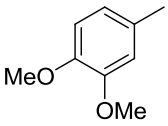	SO_2NH	0.09	26i	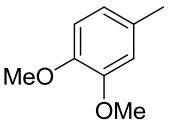	$NHSO_2$	0.05
26e	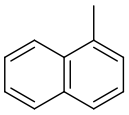	SO_2NH	0.05	1	TSA		0.005

The same group optimized the lead candidates picked from the sulfonamide hydroxamate series, through variation of the aryl substituents, sulfonamide functionality and the zinc chelating moieties. Sulfonylanilides and ureas were developed along with sulfonamides (Table 7).[64] Compounds with low nanomolar activity were obtained by substitution on the phenyl ring of **25e**. In particular, the biphenyl compound **26b** was found to be a 10 nM inhibitor. Inversion of the sulfonamide moiety in **26g-i** did not affect activity relative to **26a**, **26b** and **26d**. However, replacement of the sulfonamide with a urea structure resulted in a 20-fold loss in inhibitory activity (**26f** vs **26i**).

Small molecule inhibitors with 1,4-cyclohexelene or 1,4-phenylene linker and bicyclic aryl groups in the cap position were reported by Uesato *et al*.[65] They found that cyclohexeylene containing inhibitors such as, **28** are less potent than phenylene containing inhibitors like **29** (Figure 13).

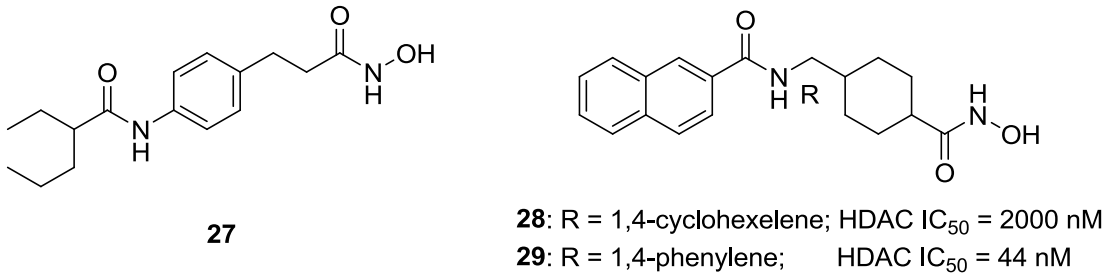

Figure 13. Inhibitors with 1,4-cyclohexelene or 1,4-phenylene linker.

Chen and coworkers reported HDAC inhibitors using a short chain fatty acid such as valproic acid, butyric acid and phenylacetic acid etc.[66] Despite poor enzymatic inhibitory activity, a number of carboxylates, including butyric acid and phenylbutyric acid are in clinical trials for cancer treatment alone and in combination with other agents. Advanced in generating carboxylates with improved HDAC inhibitory potency has provided insights into the field of HDAC inhibitor design. Short chain fatty acids were coupled with Zn^{2+} chelating motifs like hydroxamic acids and *o*-phenylenediamine through aromatic ω-amino acid linkers. These hydroxamic acids (**27**) showed HDAC inhibitory activity in lower micromolar levels.

Research group of Mai and Massa reported pyrrole containing HDAC inhibitors with hydroxamic acid as the zinc binding ligand (Table 8).[67-69] These compounds showed micromolar inhibitory activity toward HDACs. Using extensive docking studies they proposed that the presence of the pyrrole ring in the spacer gave higher flexibility inside the binding pocket of the enzyme. In subsequent work, compound **30h**, in which the benzoyl group on the pyrrole had been replaced by a phenylacetyl, showed a 38-fold increase in enzyme inhibitory activity.[69] The gain in activity was ascribed to the additional flexibility in the surface recognition domain of the inhibitor which allows overall better contact and an improved binding geometry for the hydroxamate in the active site.

Table 8. Pyrrole-containing HDAC inhibitors

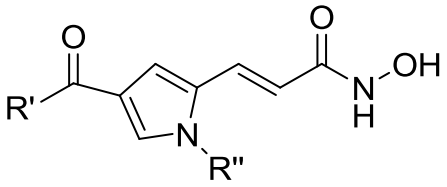

Compounds	R'	R''	HDAC IC_{50} (μM)	Compounds	R''	R''	HDAC IC_{50} (μM)
30a	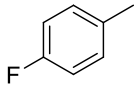	CH_3	3.8	30g	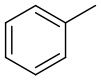	CH_3	2.4
30b	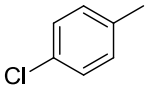	CH_3	3.8	30h	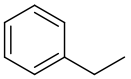	CH_3	0.1
30c	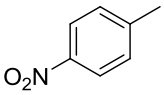	CH_3	2.4	30i	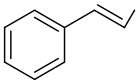	CH_3	1
30d	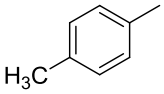	CH_3	3.9	30j	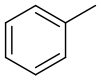	H	5
30e	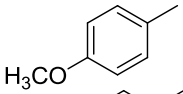	CH_3	1.9	30k	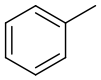	*i*-Pr	53
30f	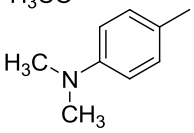	CH_3	2.9	30l	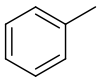	Ph	110

Schreiber and coworkers synthesized a library of 7200 small molecule inhibitors on polystyrene micro beads using one bead one stock solution method.[70] Some of these compounds such as, **31** with a dioxane derived cap group and hydroxamic acid functional group showed micromolar inhibitory activity (Figure 14).

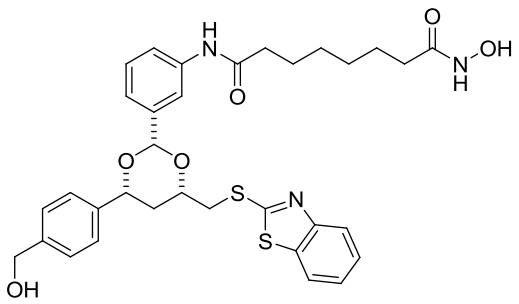

31: HDAC1 IC_{50} = 1.7 μM

Figure 14. Hydroxamic acid inhibitors with dioxane derived cap group.

The research group of C.L.Marson[71] has reported the synthesis of novel series of HDAC inhibitors based on arylsulfinyl 2,4-hexadienoic hydroxamic acids and their derivatives. Herein they carried out *in vitro* inhibition and inhibition of CEM (human leukemic cell) viability studies. In the Table 9, some of potent compounds were being listed.

Table 9. *In vitro* inhibition of HDAC and CEM cell viability

Compounds	Structures	HDAC inhibitory activity		50% viability in CEM cells IC_{50} (μM)
		Purified liver IC_{50} (μM)	CEM cells IC_{50} (μM)	
32a	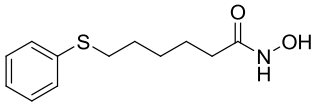	0.12	9.4	>25
32b	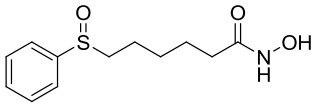	0.06	7.7	>25
32c	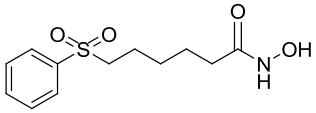	0.04	15.5	>25
32d	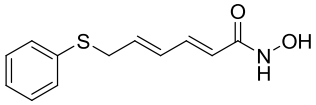	0.39	>25	ND
32e	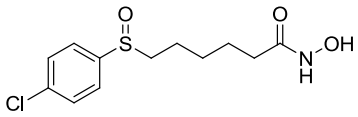	0.15	1.3	2.6
32f	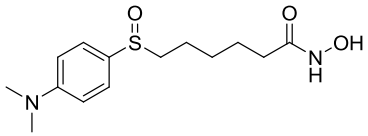	0.18	2.2	3.4
32g	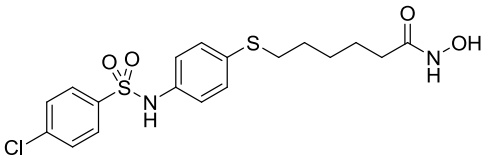	0.11	9.4	>25
32h	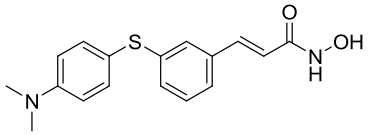	0.16	8.6	3.4
32i	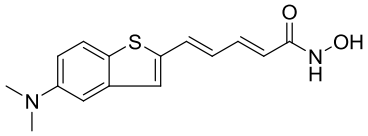	>25	ND	ND
SAHA	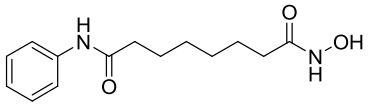	0.44	0.33	1.9

Presence of aromatic thioether units in HDAC inhibitors can make the arylpenta-2,4-dienoic acid hydroxamic acids as efficient inhibitors. Sulfides although less similar to TSA than the corresponding sulfones, were generally more potent than the latter, may be due to greater cellular uptake of sulfides. **32a** was shown to inhibit proliferation of three cell lines by 50% at 0.9-2.7 μM. Saturated chain sulfoxides **32b** and **32f** showed better inhibitory activities than saturated chain sulfide **32g** in all three assays. The cinnamohydroxamic acid type **32h** tolerably good in activity than **32i** in which fused ring is present.

Table 10. SAR of antitumor agents

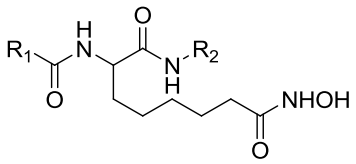

Compounds	R_1	R_2	IC_{50} (μM) NFF	IC_{50} (μM) MM96L	SI
33a	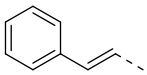	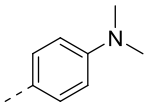	0.24	0.16	1.5
33b	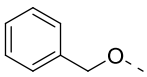	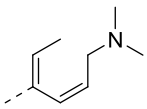	0.65	0.61	1.1
33c	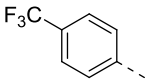	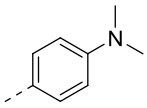	0.4	0.22	1.8
33d	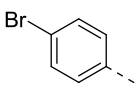	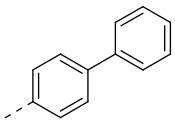	0.19	0.07	2.5
33e	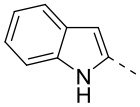	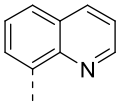	0.337	0.021	16
33f	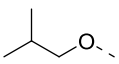	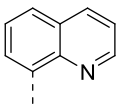	0.081	0.023	3.5

Recently, D.P.Fairlie *et al.*[72] have reported a series of compounds from α-aminosuberic acid which shown potent activity against cancer cell lines. They emphasized on small hydrophobic groups and chosen several basic groups to mimic dimethyl alanine. Some potent compounds were shown in Table 10. Some of these compounds differing from previously reported cysteine derived series.[73]

9.3. Benzamides

Suzuki and coworkers[74,75] was the first to report a series of synthetic benzamide-based non-hydroxamate HDAC inhibitors.

Table 11. SAR of MS-275 analogues

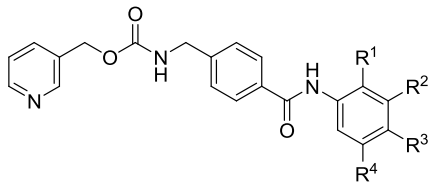

Compounds	R^1	R^2	R^3	R^4	IC_{50} (μM)
34: MS-275	NH_2	H	H	H	4.8
34a	H	H	H	H	>100
34b	H	NH_2	H	H	>100
34c	H	H	NH_2	H	>100
34d	NHAc	H	H	H	>100
34e	OH	H	H	H	2.2
34f	NH_2	CH_3	H	H	>100
34g	NH_2	H	CH_3	H	>100
34h	NH_2	H	OCH_3	H	44
34i	NH_2	H	Cl	H	40
34j	NH_2	H	H	CH_3	2.8
34k	NH_2	H	H	OCH_3	4.6
34l	NH_2	H	H	Cl	7.7
34m	NH_2	H	H	F	6.0
1: TSA					0.0046

Benzamides are the class of compounds which inhibit HDACs by ligating the active site Zn^{2+} ion with a benzamide moiety. These compounds are generally less potent than the corresponding hydroxamate and cyclic tetrapeptide classes. The most potent compound of the series is named as MS-275. It has HDAC inhibitory activity of 5 μM and showed significant anti-tumor activity *in vivo*. The SAR study of the benzanilide functionality revealed that a 2′-amino (**34**) or 2′-hydroxyl (**34e**) moiety is crucial for inhibitory activity against HDACs as illustrated in Table 11. Changing the 2′-amino group on the aryl substituent (**34a-c**) by removing, repositioning or capping with acetate (**34d**) makes the compounds inactive. Incorporation of functionality at the R^4 site was well tolerated (**34j-m**). Additional evaluation of MS-275 (**34**) demonstrated that it could inhibit partially purified human HDAC preparations and cause hyperacetylation of nuclear histones in various cell lines.[75,76] When administered orally to nude mice implanted with tumor lines, seven out of eight lines were strongly inhibited.[75] Importantly, an inactive MS-275 structural analogue was devoid of both *in vitro* and *in vivo* activity, further suggesting that the beneficial biological effects are a result of HDAC inhibition. The MS-275 is under clinical trials now.

Table 12. HDAC inhibitors with sulfonamide cap and benzamide ligand

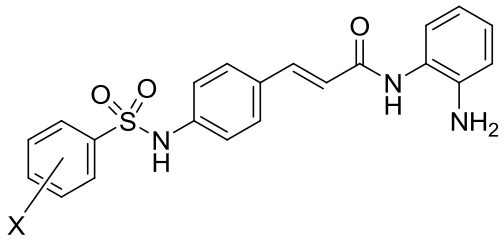

Compounds	X	HDAC IC_{50} (μM)
35a	4-Me	3
35b	4-*t*-Bu	1
35c	4-OMe	1
35d	3,4-di-OMe	4
35e	4-Ph	1

During the course of study on sulfonamide hydroxamic acid and anilide based HDAC inhibitors, the researchers of *MethylGene Inc.*[64] explored benzamides obtained by replaceing the zinc chelating hydroxamic acid moiety. The benzamides showed 10 times reduced activity compared with the parent hydroxamates (Table 12), whereas oxamflatin analogue with benzamide functionality reveals 50 times decrease in activity compared to oxamflatin.

Recently the same research group reported[77] straight chain benzamides (**36**) as HDAC inhibitors having different cap groups. Some of these compounds with hydrophobic cap groups showed HDAC inhibitory activity in low micromolar range as shown in Table 13. However, the *in-vivo* anti-tumor activity of selected compounds from this series is lower than that of MS-275. This is probably due to the short half life and poor bioavailability.

Chen and coworkers have also synthesized benzamides as the functional group as HDAC substrate during their synthesis of hydroxamic acid **27**.[66]

Table 13. SAR of benzamides

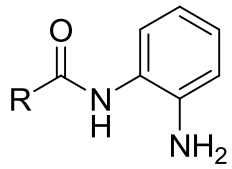

Compounds	R	HDAC IC_{50} (μM)	Compounds	R	HDAC IC_{50} (μM)
36a	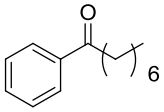	9	36c	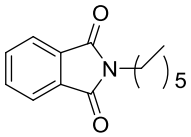	3
36b	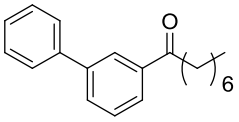	1	36d	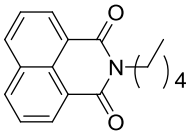	1

These compounds showed only slightly lower inhibitory activity than the corresponding hydroxamic acids. Schreiber and coworkers also synthesized benzamides using the one

bead-one stock solution method with 1, 3-dioxane based structure, that is analogues to the hydroxamic acid **31**.[75] This approach eventually leads to the identification of a paralog selective inhibitor of HDAC1.[78]

Although, some of the benzamide inhibitors showed significant HDAC inhibitory activity, there is no clear evidence that benzamide is acting at the zinc active site and an allosteric binding site cannot be ruled out. Additional studies are required to understand the exact mechanism of action of benzamide-based HDAC inhibitors.

9.4. Electrophilic ketones

There are several electrophilic ketones known to inhibit proteases, including metal-dependent hydrolytic enzymes such as carboxypeptidase-A and metallo-β-lactamase.[79,80] It has been proved that hydrated form of the ketone acts as a transition-state analogue and coordinates the zinc ion in the active site of carboxypeptidase A (Figure 15).[79] A similar mechanism might also be operative for HDAC inhibition by the electrophilic ketones.

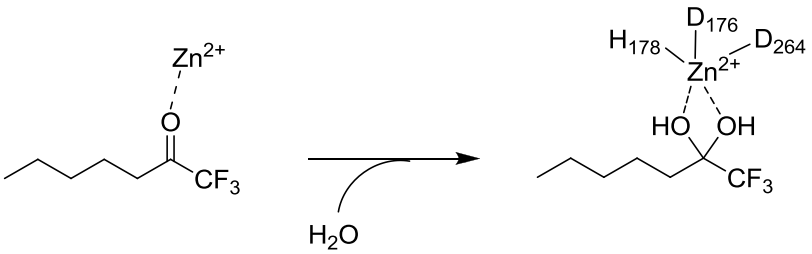

Figure 15. Mechanism of hydration.

Frey and coworkers[81] from Abbott Laboratories reported SAHA based straight chain trifluoromethyl ketones as HDAC inhibitors. They synthesized of various linear molecules containing an aromatic ring in the surface recognition domain, connected via ether or amide bonds to an aliphatic chain in the linker domain and carrying a trifluoromethyl ketone in the metal binding domain (Table 14). These agents were tested against a mixture of HDAC1 and HDAC2 and showed inhibition at low micromolar/high nanomolar concentrations. These agents also posses antiproliferative activities *in vitro* and induce histone hyperacetylation and p21 gene expression. Both the five and six-methylene linkers showed optimal activity in the ether series.

Table 14. Electrophilic ketones with linear cap groups

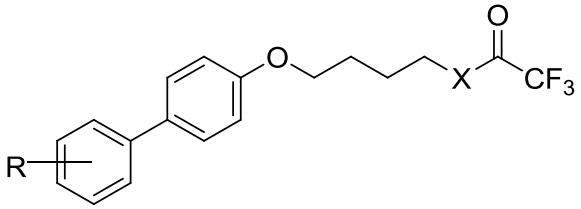

Compounds	R	X	HDAC IC_{50} (μM)
37a	4-Ph	$-CH_2-$	2.6
37b	4-Ph	$-CH_2-CH_2-$	2.9
37c	4-Ph	$-CH_2-CH_2-CH_2-$	72% @ 50
37d	4-Ph	-CH≡CH-	8.6
37e	4-Ph	-CH=CH-	5.0
37f	4-Ph	$-OCH_2-$	11
37g	4-Ph	$-SCH_2-$	4.6
37h	H	$-CH_2-CH_2-$	8.0
37i	3-Ph	$-CH_2-CH_2-$	2.8
37j	4-OPh	$-CH_2-CH_2-$	3.4
37k	Simple ketone analogue	$-CH_2-CH_2-$	>50

α-Ketoesters and amides also have the hydrating property like trifluoromethyl ketones. Based on this property, Wada and coworkers synthesized α-keto esters and amides as HDAC inhibitors. Several compounds (**38-40**, Figure 16) of the series showed good inhibitory activity and by altering the aryl group, nanomolar α-keto amide inhibitors of HDACs were developed.[82] The electrophilic ketone class represents a relatively new group of HDACs substrate that has not yet been fully explored. More efforts need to develop additional structural variants in order to assess optimal design parameters and

tolerances. However, the electrophilic ketone class contains potent inhibitors of HDAC that despite apparent poor stability, possess antitumor effects in animal models.

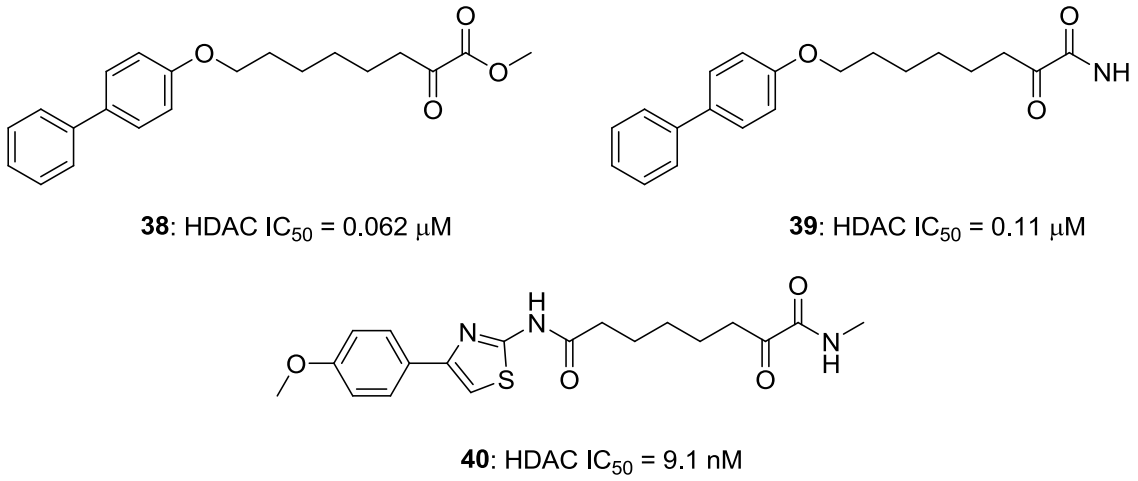

38: HDAC IC_{50} = 0.062 μM

39: HDAC IC_{50} = 0.11 μM

40: HDAC IC_{50} = 9.1 nM

Figure 16. α-Ketoesters and amides.

9.5. Cyclic peptide-based HDAC inhibitors

Cyclic peptide based HDAC inhibitors, a structurally complex class of HDAC inhibitors, are particularly interesting because many of them are naturally occurring, they are relatively less toxic with high pharmacokinetic properties, their structural balance between hydrophilicity and hydrophobicity is optimum and structural features are advantageous for their *in vivo* application. The main structural features of the cyclic peptide-based HDAC inhibitors include a macrocycle containing hydrophobic amino acids in the surface recognition domain, an alkyl chain in the linker domain and a functional group in the metal binding domain. There is some evidence which support that cyclic peptide based HDAC inhibitors bind to the HDAC enzyme in a manner consistent with TSA (**1**). The aliphatic linker passes down the enzyme's tube-like channel positioning the binding moiety in proximity to the active site zinc, while the macrocyclic portion binds to the rim of the active site. The macrocycle in naturally occurring cyclic tetrapeptide inhibitors is arranged with a D-amino acid and a cyclic amino acid (Pro or Pip) flanking the amino acid bearing the linker moiety which generates a constrained 12-membered cyclic structure with extensive internal hydrogen bonding. It is postulated that the D-configuration of the amino acid is necessary for tight

association with the rim of the active site, thereby allowing the linker to align and insert into the enzyme's tube-like channel.[83]

9.5.1. Cyclic tetrapeptide containing epoxyketone moiety

Naturally occurring cyclic tetrapeptide based HDAC inhibitors belong to a class which contain a unique amino acid, (*S*)-2-amino-8-oxo-9,10-epoxydecanoic acid (Aoe). These compounds have two more structural features in common: (i) at least one amino acid with (*R*) configuration and (ii) a proline or pipecolic acid residue. The Aoe side chain is approximately isosteric with an acetylated lysine, suggesting that it functions as a mimic of an acetylated histone protein. Several groups have shown that reduction or hydrolysis of the epoxide results in a complete loss of biological activity, suggesting that Aoe may irreversibly inactivate its receptor through covalent bond formation (Figure 17). HC-toxin I (**41**, commonly referred to as HC-toxin), produced by *Helminthosporium carbonum*, was one of the first cyclic tetrapeptides in this structural class identified. Its structure, initially characterized by Liesch *et al*.,[84] later was revised by Knoche and co-workers.[85,86] Further investigations led to the identification of HC-toxin III (**42**),[87] bearing a *trans*-3-hydroxyproline. Also discovered was HC-toxin II (**43**), an analogue in which one alanine residue was replaced by a glycine.[88] While HC-toxin III was found to be comparable in potency to **41**, HC-toxin II have low activity (EC_{50} = 7 μg/mL) in a maize root inhibition assay) relative to HC-toxin (EC_{50} = 0.2 μg/mL). It is interesting to mention that this 35-fold decrease in efficacy originated from a relatively modest structural change (Ala to Gly). The cyclic tetrapeptides chlamydocin (**44**) and dihydro-chlamydocin (**45**) were first isolated and characterized by Closse and Huguenin.[89] Chlamydocin, produced by *Diheterospora chlamydosphoria*, exhibited pronounced cytostatic activity *in vitro.* It is found to be a highly potent HDAC inhibitor, inhibiting HDAC activity *in vitro* with an IC_{50} value of 1.3 nM, whereas dihydro-chlamydocin (**45**), with its reduced C8-carbonyl was inert. Trapoxins A (**3**) and trapoxin B (**49**), discovered in the fermentation broth of *Helicoma ambiens,*[90] can potentially inhibit cellular transformations. In their structure, they differ solely by the presence of either a cyclic imino acid D-Pip or D-Pro in the tetrapeptide scaffold. The fungal metabolite WF-3161 (**48**), obtained from *Petriella guttulata*, also exhibited interesting antitumor activity *in vitro* and *in vivo*.[91]

The prolyl-substituted Cyl-1 (**46**) as well as its pipecolyl-variant Cyl-2 (**47**) produced by *Cylindrocladium scoparium*, were found as potent plant growth regulators.[92-94]

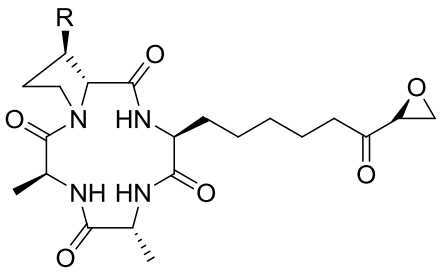

41: HC-Toxin I (R = H)
42: HC-Toxin III (R = OH)

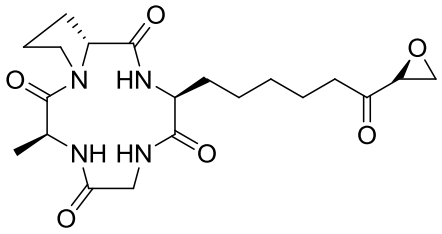

43: HC-Toxin II

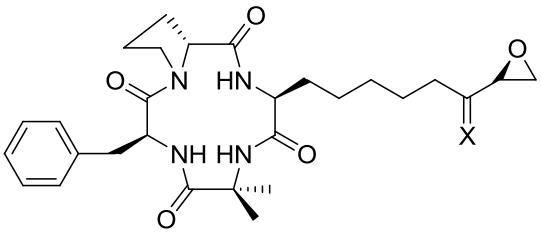

44: Chlamydocin (X = O)
45: Dihydrochlamydocin (X = H, OH)

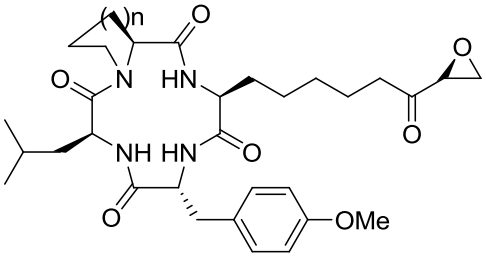

46: Cyl-1 (n = 1)
47: Cyl-2 (n = 2)

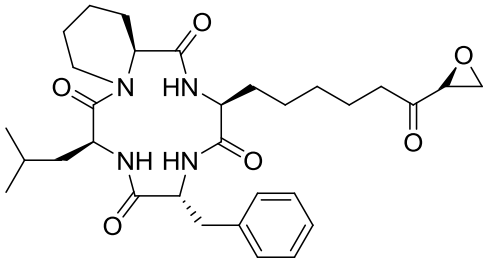

48: WF-3161

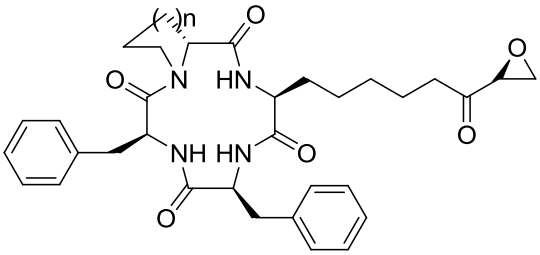

3: Trapoxin A (n = 2)
49: Trapoxin B (n = 1)

Figure 17. Naturally occurring Aoe containing cyclic tetrapeptides.

Three HDAC inhibitors, HC-toxin, chlamydocin and Cyl-2, were directly compared for phytotoxic efficacy to elucidate the relationship between cyclic tetrapeptide structure and biological activity.[95] The shifts in their respective biological activities correlated to overall cyclic peptide polarity. Consequently, it was postulated that these differences could be ascribed to a given analogue's potential ability to penetrate membranes as

increased hydrophobicity enhanced potency. As an example, HC-toxin is 10-fold less potent than chlamydocin against these sensitive maize hybrids.[96] This premise was further supported by the dramatically reduced efficacy of the more polar glycine variant of HC-toxin, cyclic tetrapeptide **43** (approximately 3% as active as HC-toxin). Hydroxamic acids and carboxylic acids are reversible inhibitors of HDAC. On the other hand, trapoxins, chlamydocin, HC-Toxin, Cyl-1, Cyl-2 and WF-3161 have irreversible HDAC inhibitory activity.

On the basis of the irreversible inhibition of trapoxin B with HDAC enzyme, Schreiber and coworkers isolated HDAC1 using affinity chromatography.[97,20] Due to the irreversible nature of the epoxide based inhibitors, they did not receive much attention in the HDAC inhibitor research.

9.5.2. Cyclic tetrapeptide containing hydroxamic acids

Till date the most potent synthetic HDAC inhibitor was reported by Nishino *et al*. This inhibitor contains a hydroxamic acid as the zinc binding group attached to a cyclic tetrapeptide scaffold (CHAPs).[83,98] The biological activity of CHAPs varied by changing the number of the amino acids constituting the ring structure, the pattern of amino acid chiral combinations and the side chain structure of each amino acids. Comparative study of the activity of cyclic tetrapeptide and cyclic octapeptide revealed the importance of the cyclic tetrapeptide scaffold for high HDAC inhibitory activity. Naturally occurring cyclic tetrapeptide based HDAC inhibitors containing epoxyketone functional group demonstrated the importance of the cyclic tetrapeptide moiety for the nanomolar inhibition of HDAC. Further, there was a 1-25 fold decrease in the activity for cyclic octapeptide confirms the importance of the cyclic tetrapeptide scaffold.

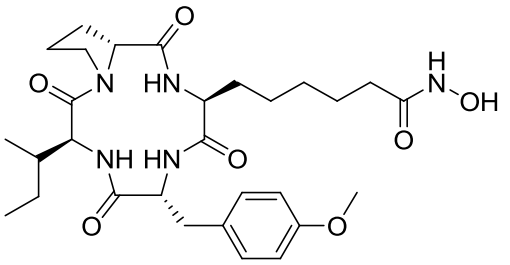

50r: CHAP31;
HDAC IC_{50} = 3.3 nM

Figure 18. Cyclic hydroxamic-acid-containing peptide (CHAP).

Table 15. SAR of CHAPs

No.	Compounds	Structures	HDAC, IC_{50} (nM)
50a	CHAP1	*cyclo*(-L-Asu(NHOH)-L-Phe-L-Phe-D-Pro-)	6.0
50b	CHAP19	*cyclo*(-L-Asu(NHOH)-L-Phe-L-Phe-D-Pro-)2	83.7
50c	CHAP27	*cyclo*(-L-Asu(NHOH)-D-Phe-L-Phe-D-Pro-)	3.4
50d	CHAP38	*cyclo*(-L-Asu(NHOH)-D-Phe-L-Phe-L-Pro-)	5.3
50e	CHAP39	*cyclo*(-L-Asu(NHOH)-L-Phe-D-Phe-L-Pro-)	226
50f	CHAP18	*cyclo*(-L-Api(NHOH)-L-Phe-L-Phe-D-Pro-)	150
50g	CHAP17	*cyclo*(-L-Aza(NHOH)-L-Phe-L-Phe-D-Pro-)	24.7
50h	CHAP131	*cyclo*(-L-Asu(NHOH)-D-Phe-L-Pro-D-Phe-)	91.6
50i	CHAP132	*cyclo*(-L-Asu(NHOH)-D-Pro-L-Phe-D-Phe-)	25.5
50j	CHAP80	*cyclo*(-L-Asu(NHOH)-L-Ala-L-Phe-D-Pro-)	2.0
50k	CHAP88	*cyclo*(-L-Asu(NHOH)-D-Ala-L-Phe-D-Pro-)	3.2
50l	CHAP45	*cyclo*(-L-Asu(NHOH)-D-Phe-L-Ala-D-Pro-)	1.7
50m	CHAP57	*cyclo*(-L-Asu(NHOH)-D-Phe-L-Phe-D-Pip-)	2.9
50n	CHAP56	*cyclo*(-L-Asu(NHOH)-L-Phe-L-Phe-D-Pip-)	4.8
50o	CHAP58	*cyclo*(-L-Asu(NHOH)-D-Phe-L-Phe-L-Pip-)	4.2
50p	CHAP30	*cyclo*(-L-Asu(NHOH)-D-Tyr(Me)-L-Ile-L-Pro-)	3.3
50q	CHAP14	*cyclo*(-L-Asu(NHOH)-D-Tyr(Me)-L-Ile-L-Pro-)2	85
50r	CHAP31	*cyclo*(-L-Asu(NHOH)-D-Tyr(Me)-L-Ile-D-Pro-)	3.3
50s	CHAP42	*cyclo*(-L-Api(NHOH)-D-Tyr(Me)-L-Ile-D-Pro-)	54
50t	CHAP43	*cyclo*(-L-Aaz(NHOH)-D-Tyr(Me)-L-Ile-D-Pro-)	34
50u	CHAP44	*cyclo*(-L-Asu(NHOH)-D-Tyr(Me)-L-Ala-D-Pro-)	3.4
50v	CHAP77	*cyclo*(-L-Asu(NHOH)-D-Tyr-L-Ile-D-Pro-)	3.4
50w	CHAP50	*cyclo*(-L-Asu(NHOH)-D-Tyr(Me)-L-Ile-D-Pip-)	4.0
50x	CHAP49	*cyclo*(-L-Asu(NHOH)-D-Tyr(Me)-L-Ile-L-Pip-)	5.3

Yoshida and coworkers synthesized hydroxamic acid analogues of all these natural products and found that they inhibit HDAC strongly and reversibly. They carried out a SAR study using several combinations of amino acids for the cyclic tetrapeptide scaffold. Details of the SAR studies on CHAPs are given in Table 15. During the optimization of the CHAP molecules, Nishino *et al.* found that out of many combinations of optically different amino acids, LDLD, LLLD and LDLL combinations have almost similar extents of activity.[83, 96]

Table 16. Chlamydocin hydroxamic acid analogues

No.	Compounds	IC_{50} (nM) HDAC1	MHC_{Cx2} (nM)
44	Chlamydocin	0.15	4.6
51a	*cyclo*(-L-Asu(NHOH)-Aib-L-Phe-D-Pro-)	5.2	33.2
51b	*cyclo*(-L-Asu(NHOH)-Acc5-L-Phe-D-Pro-)	3.02	5.67
51c	*cyclo*(-L-Asu(NHOH)-Acc6-L-Phe-D-Pro-)	2.19	5.38
51d	*cyclo*(-L-Asu(NHOH)-Acc7-L-Phe-D-Pro-)	2.14	2.76
51e	*cyclo*(-L-Asu(NHOH)-Acc8-L-Phe-D-Pro-)	3.99	1.88
51f	*cyclo*(-L-Asu(NHOH)-A2in-L-Phe-D-Pro-)	0.98	1.29
51g	*cyclo*(-L-Asu(NHOH)-L-Ala-L-Phe-D-Pro-)	1.95	325
51h	*cyclo*(-L-Asu(NHOH)-D-Ala-L-Phe-D-Pro-)	3.23	NT
51i	*cyclo*(-L-Asu(NHOH)-L-A1in-L-Phe-D-Pro-)	1.12	2.69
51j	*cyclo*(-L-Asu(NHOH)-D-A1in-L-Phe-D-Pro-)	1.95	2.29
51k	*cyclo*(-L-Asu(NHOH)-L-Pro-L-Phe-D-Pro-)	3303	
51l	*cyclo*(-L-Asu(NHOH)-Aib-L-Phe-D-Pip-)	2.98	
51m	*cyclo*(-L-Asu(NHOH)-Acc5-L-Phe-D-Pip-)	12.4	37.8
51n	*cyclo*(-L-Asu(NHOH)-Acc8-L-Phe-D-Pip-)	2.75	
51o	*cyclo*(-L-Asu(NHOH)-A2in-L-Phe-D-Pip-)	1.2	
51p	*cyclo*(-L-Asu(NHOH)-A2in-L-Ile-D-Pip-)	2.68	
51q	*cyclo*(-D-Asu(NHOH)-L-Pro-D-Phe-Aib-)	8.57	3950
51r	*cyclo*(-L-Asu(NHOH)-L-Pro-L-Phe-Aib-)	31.7	57,800
51s	*cyclo*(-L-Asu(NHOH)-Aib-L-Phe-L-Pro-)	45.7	717

However, the activity to induce MHC class-1 molecule expression and growth inhibition was high for LDLD configuration, that is, positions 2 and 3 are best occupied with hydrophobic L- and D-amino acids. Further, CHAPs with five methylene units spacer is the best for good inhibitory activity (Table 15). One of these compounds, CHAP31 (Figure 18) was extensively studied *in vivo* and it exhibits antitumor activity in mice bearing B16/BL6 tumor cells. CHAP31 inhibited the growth in four of five human tumor lines implanted in nude mice. Further, these cyclic tetrapeptide containing HDAC inhibitors are very useful in understanding the factors for the HDAC specificity and selectivity. These cyclic tetrapeptides will help in getting more details about the interaction between the enzyme and the inhibitor which will lead to the development of selective inhibitors with improved qualities.

Chlamydocin, a natural cyclic tetrapeptide, isolated from *Diheterospora chlamydosphoria*, has shown to exhibit potent anticancer activity *in vitro*.[99] It belongs to a small family of hydrophobic cyclic tetrapeptide containing the unusual amino acid, (S)-2-amino-8-oxo-9,10-epoxy decanoic acid (Aoe), which is essential for their biological activity. Recently, Nishino *et al.*[100] have synthesized chlamydocin hydroxamic acid analogues by replacing epoxy ketone moiety of Aoe by hydroxamic acid functional group. They have also introduced several aromatic analogues in cyclic framework to study hydrophobic interaction of capping group. The details of HDAC inhibitory data of chlamydocin hydroxamic acids are shown in Table 16.

Very recently, Islam *et al.*[101] reported a series of bicyclic tetrapeptide hydroxamic acids by changing the length of the aliphatic loop to explore the effect of the loop length on the activity of inhibitors. The sequence and configuration of amino acids in CHAP31 were considered as the basis of the designing these inhibitors. The activity toward HDAC1 slightly changes with the size of the aliphatic loop (Table 17). The changes in activity toward HDAC4 and HDAC6 are not so remarkable. All the compounds were specific toward HDAC4 compared to HDAC1 and HDAC6. With the exception of compound **52a**, all of the bicyclic tetrapeptides were excellent in p21 promoter-inducing activity. Compound **52b** showed better selectivity (the ratio of IC_{50} values: HDAC6/HDAC4 = 75).

Table 17. HDAC inhibitory activity and p21 promoter activity data for bicyclic tetrapeptide hydroxamic acids and reference compounds

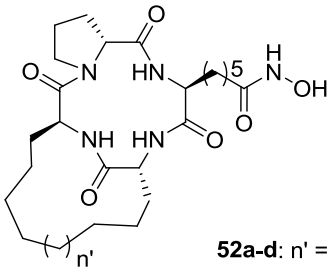

52a-d: n' = 2-5

Compounds	Loop size	IC_{50} (nM)			p21 promoter assay EC_{1000} (nM)
		HDAC1	HDAC4	HDAC6	
Tricostatin A	-	23	44	65	20
CHAP31[50r]	-	0.4	3	13	22
52a	$-(CH_2)_9-$	9.1	5.4	330	92
52b	$-(CH_2)_{10}-$	9.1	5.5	410	7.2
52c	$-(CH_2)_{11}-$	11	4.5	280	2.6
52d	$-(CH_2)_{12}-$	13	5.0	240	2.0

9.5.3. Cyclic tetrapeptide containing ketone functionality

Apicidin (**53a**, Table 18), a cyclic tetrapeptide, isolated from *Fusarium Pallodoroseum* which is an endophytic fungus collected from Costa Rica, as a potent and broad spectrum antiprotozoal agent that exerts its biological activity by reversibly inhibiting HDAC activity.[102] A group of scientists from Merck research laboratory extensively studied the HDAC inhibitory activity of apicidin and its synthetic derivatives.[103-109] Apicidin contains an ethyl ketone moiety in its side chain and so it is different from other natural cyclic peptides like trapoxin or HC-Toxin with epoxyketone side chain. The high potency of HDAC inhibitory activity of apicidin further confirmed the importance of the cyclic tetrapeptide scaffold for the inhibitor design.

The shift of keto group from position C-8 to C-9 decreases potency, confirming that the exact location of the C-8 keto group is critical for proper mimicking of acetylated histone lysine. In addition to that, reduction of the C-8 keto group to epimeric alcohols, formation of olefin or epoxide or conversion to CH_2 reduces activity. On the other hand, if the ethyl ketone moiety is changed to hydroxamic acid, epoxyketone or methyl ester

with a spacer of five methylene groups, the inhibitory activity is further enhanced.[110] Further, they found that the tryptophan moiety of apicidin is a key site and the replacement or modification of this moiety have great influence on the HDAC inhibitory activity which means that the amino acid present in the cyclic tetrapeptide inhibitor have some interactions with the rim of the HDACs active site pocket.[111]

Table 18. SAR of apicidin analogues

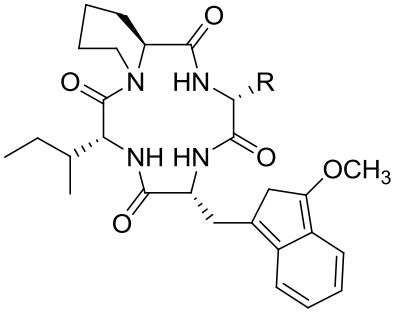

Compounds	R	HDAC Activity IC_{50} (nM)	Compounds	R	HDAC Activity IC_{50} (nM)
53a	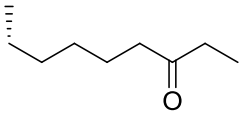	1	53f	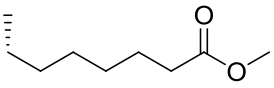	7
53b	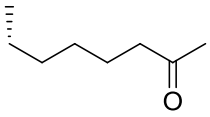	2	53g	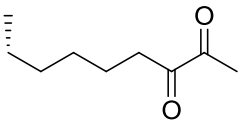	30
53c	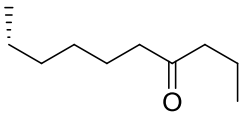	1	53h	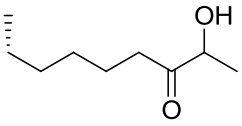	0.3
53d	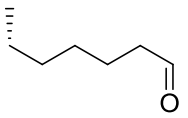	6	53i	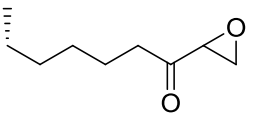	0.1
53e	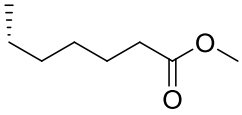	0.4	53j	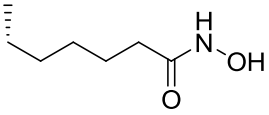	0.2

The introduction of a basic group at the tryptophan`s NH increases the HDAC activity and similar enhancement in activity is observed with the introduction of a bulky aryl substituent at the 2-position of tryptophan.

In light of above view that the apicidin contain an ethyl ketone moiety as zinc ligand, Nishino *et al.* [112] have replaced the epoxy ketone moiety in chlamydocin with several ketones and aldehyde to synthesize potent reversible and selective HDAC inhibitors. They found that most of them were potent inhibitors and some of these compounds have shown remarkable selectivity among HDAC paralogs (Table 19).

Table 19. HDAC inhibitory activity of chlamydocin analogues bearing carbonyl as functional group

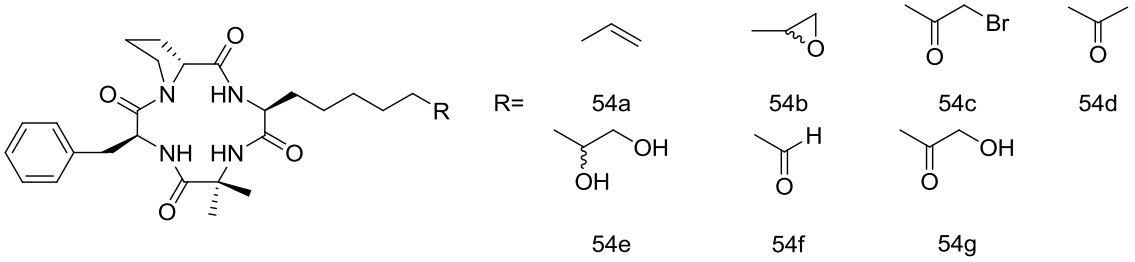

Compounds	IC_{50} (μM)			p21 promoterassay
	HDAC1	HDAC4	HDAC6	EC_{1000} (μM)
TSA	0.0190	0.0200	0.0280	0.190
54a	>100	>100	>100	>250
54b	4.69	4.05	>100	22.7
54c	0.0619	0.0595	0.621	0.344
54d	1.08	0.290	3.70	1.20
54e	>100	>100	>100	NT
54f	4.33	1.29	14.1	20.9
54g	0.223	0.0604	0.887	0.234

9.5.4. Retrohydroxamic acids

Retrohydroxamic acids (N-formyl hydroxylamine) are reported as potent, long lived orally bioavailable matrix metalloproteinase's (MMPs) inhibitors which are zinc proteases.[113,114] Based on the assumption that retrohydroxamates can also act as good inhibitors of HDACs, Nishino *et al.*[115] designed and synthesized HDAC inhibitors containing retrohydramate (**55**, Figure 19) as the zinc binding ligand with cyclic tetrapeptide cap group and with an optimum spacer length of five methylene units. Even though they have ten times lower inhibitory activity than the corresponding hydroxamic acids, these novel class of inhibitors have potential as anticancer agents. Recently,

researchers from Scripps Research Institute reported SAHA based retrohydroxamates (**56** and **57**) as HDAC inhibitors.[116] These compounds are 50 times weaker in activity than the parent compound SAHA. However, retrohydroxamic acids have potential as HDAC inhibitors due to their long half-life and possible oral bioavailability.

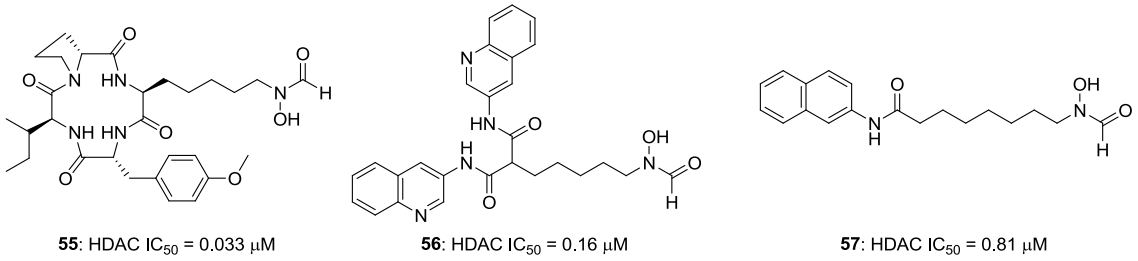

Figure 19. HDAC inhibitors with retrohydroxamic acid group.

9.5.5. Cyclic tetrapeptide containing electrophilic ketones

Jose *et al.*[117] have synthesized cyclic tetrapeptides containing trifluoromethyl ketone and pentafluoroethyl ketone (**58** and **59**) as the zinc binding functionality. Out of these compounds trifluoromethylketone is found to have excellent inhibitory activity (Figure 20). Changing from trifluoro to pentafluoro group did not increase the activity, probably because of the bulkiness of the pentafluromethyl group. Incorporation of a sulfur atom to the carbonyl (**60**) increased the activity that may provide different mode of ligation with Zn^{2+} ions using longer spacer length.

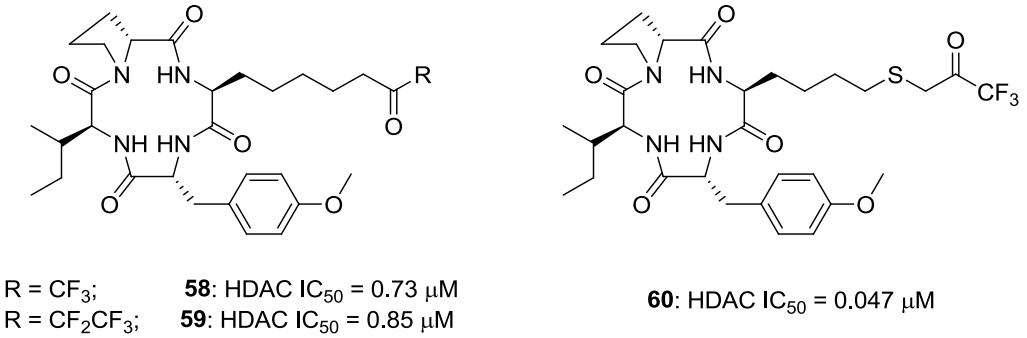

Figure 20. Cyclic tetrapeptide containing electrophilic ketone.

9.5.6. Cyclic tetrapeptide containing hydroxymethyl ketone

So far, several novel fungal metabolites have been characterized which lack the reactive epoxide which is assumed to be essential for significant biological activity. These new

compounds include a phytotoxin structurally related to chlamydocin: 9, 10-desepoxy-9(R)-hydroxy-chlamydocin (**61**) produced by *Verticillium coccosporum*[118] as well as the tumorigenic Tan-1746 (**62**) (Figure 21).[119]

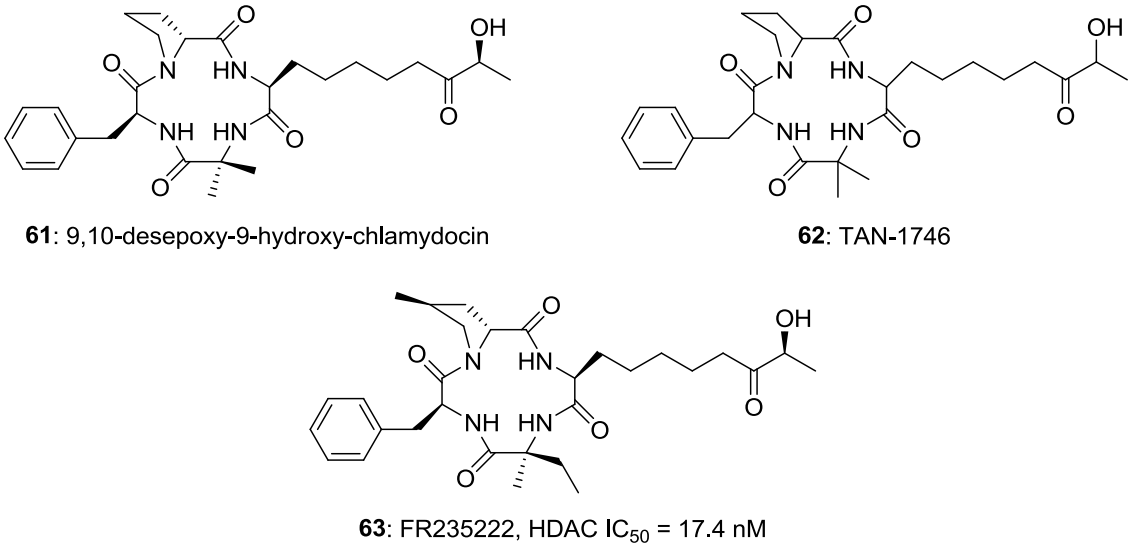

Figure 21. Cyclic tetrapeptides containing hydroxymethylketone functionality.

Both new analogues, as noted, lack the 9,10-epoxide and instead bear a 9-hydroxyl group. A published patent has described a desepoxy-trapoxin analogue (FR-225497, compound not shown) which had good activity against human tumor cell lines *in vitro* (IC_{50} = 152 and 158 ng/mL against Jurkat and HT-29 cells respectively).[120] Total synthesis of a potent immunosuppressant FR235222 (**63**), that inhibits mammalian HDACs has been reported.[121] It has a chlamydocin like cyclic tetrapeptide structure, inhibiting the HDACs with IC_{50} = 9.7 ng/mL.

9.5.7. Cyclic peptides with thiols

The natural product FK228 (**64**) (formerly named FR901228 and known as cyclic depsipeptide) produced by C*hhromobacterium violaceum* displayed potent *in vivo* antitumor activity. Ueda and co-workers reported that FK228 have HDAC inhibitory activity.[122-124] There is no visible functional group in FK228 that interacts with the zinc ion in the HDAC binding pocket. FK228 serves as a stable natural prodrug that inhibits class 1 HDAC enzymes. It is activated by the glutathione-mediated reduction of the

disulfide bond to sulfhydryl and this sulfhydryl group is coordinated to the zinc metal ion present in the HDAC binding pocket (Figure 22).[125]

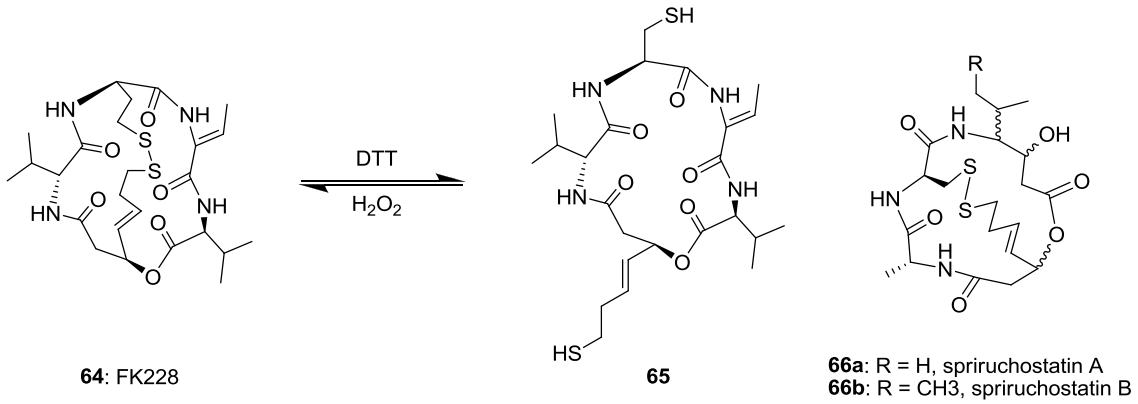

Figure 22. Cyclic peptides containing sulfur as zinc ligand.

In 2001, the structure of spiruchostatin A and B (**66**, Figure 22), isolated from a *Pseudomonas* extract were discovered with potent HDAC inhibitory activity and the total synthesis of spiruchostatins were reported.[126,127]

Table 20. Comparative activity study of SCOPs

Compounds	IC_{50} (μM)				EC_{1000} (μM)
	HDAC1	HDAC4	HDAC6	HDAC8	
TSA	0.022	0.02	0.028	0.04	0.062
64	0.0358	0.512	>500	NT	0.0031
65	0.0001	NT	0.624	NT	0.0157
67	0.142	0.145	>500	>500	0.0368
67 + DTT	0.0046	0.0021	1.4	1.69	0.0677
68	0.007	0.068	1.61	3.14	0.140
68 + DTT	0.00055	0.0011	2.01	0.494	0.0597

On the basis of the inhibitory activity of FK228, Nishino and coworkers[128] synthesized many potent inhibitors of HDAC containing a sulfhydryl moiety as the functional group for HDAC inhibition. These sulfur-containing cyclic tetrapeptides (SCOPs) contain L-2-

amino-7-mercaptoheptanoic acid (L-Am7) instead of L-Aoe (2S, 9S)-2-amino-8-oxo-9,10-epoxydecanoic acid of Cyl-1. The SCOPs were synthesized as stable disulfide dimers (**67**) and hybrids (**68**) (Figure 23) with several thiols. These compounds showed potent inhibitory activity as shown in Table 20.

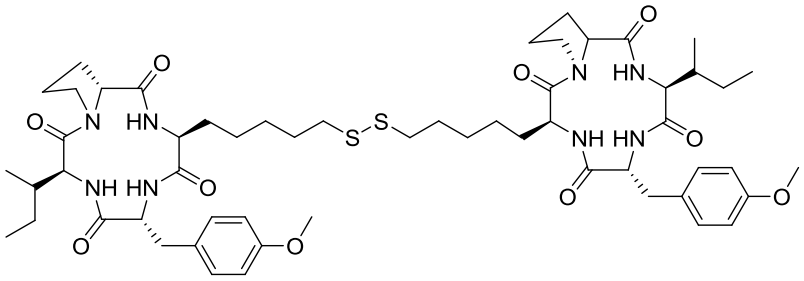

67: SS-Dimer+DTT; HDAC IC_{50} = 4.6 nM

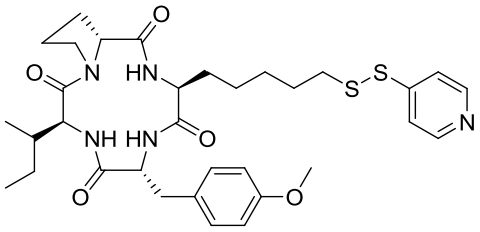

68: SS-Hybrid+DTT; HDAC IC_{50} = 0.5 nM

Figure 23. Sulfur containing cyclic tetrapeptides.

To know the interaction of aliphatic cap groups with HDACs, bicyclic peptide disulphide hybrid (Figure 24)[129] was also synthesized without aromatic ring in their macrocyclic framework by ring closing metathesis using Grubbs first generation catalyst.

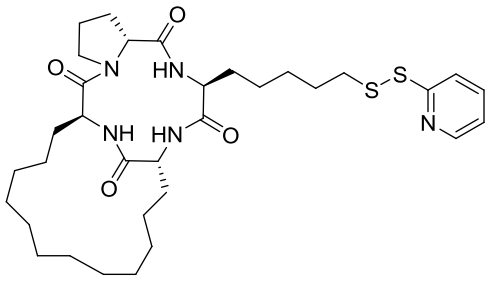

Figure 24. Bicyclic peptide disulphide hybrid.

The bicyclic peptide was found to be active in both cell free and cell based condition and it has some selectivity among HDAC1 and HDAC6.

To find out HDAC inhibitors with good selectivity and potency, Shivashimpi *et al.*[130] have synthesized compounds containing S-S disulphide by shifting benzene ring of L-Phe in chlamydocin framework and found some potent inhibitors as shown in Table 21.

Table 21. Comparative activity study of S-S disulphide cyclic tetrapeptides

Compound	No.	IC_{50} (nM)			HDAC1/ HDAC4[a]	EC_{1000} (nM)
		HDAC1	HDAC4	HDAC6		
cyclo(-L-Am7(S2Py)-A2in-L-Ala-D-Pro-)	70a	2.0	1.6	8.8	1.2	140
cyclo(-L-Am7(S2Py)-D-A1in-L-Ala-D-Pro-)	70b	2.7	2.4	12	1.1	55
cyclo(-L-Am7(S2Py)-L-A1in-L-Ala-D-Pro-)	70c	36	25	33	1.4	2000
cyclo(-L-Am7(S2Py)-D-2MePhe-L-Ala-D-Pro-)	70d	170	70	71	2.4	25600
cyclo(-L-Am7(S2Py)-L-2MePhe-L-Ala-D-Pro-)	70e	3.7	2.2	56	1.6	550
cyclo(-L-Am7(S2Py)-Aib-L-Ala-D-Tic-)	70f	4.7	4.2	29	1.1	200
cyclo(-L-Am7(S2Py)-Aib-L-Phg-D-Pro-)	70g	88	56	86	1.5	7400
cyclo(-L-Am7(S2Py)-Aib-L-Ph4-D-Pro-)	70h	6.2	3.2	36	1.9	320
cyclo(-L-Am7(S2Py)-Aib-L-Ph5-D-Pro-)	70i	5.3	2.7	43	1.9	110
cyclo(-L-Am7(S2Py)-Aib-L-Ser(Bzl)-D-Pro-)	70j	3.2	1.6	24	2.0	72
cyclo(-L-Am7(S2Py)-Aib-L-Ser-D-Pro-)	70k	6.4	4.0	26	1.6	580
cyclo(-L-Am7(S2Py)-Aib-L-Ala-D-Pro-)	70l	9.4	5.2	43	1.8	750

[a]Seletivity of the enzymes

Another group of natural products psammaplins isolated from the sponge *Pseudoceratina purpurea* are potent inhibitors of HDAC.[131]

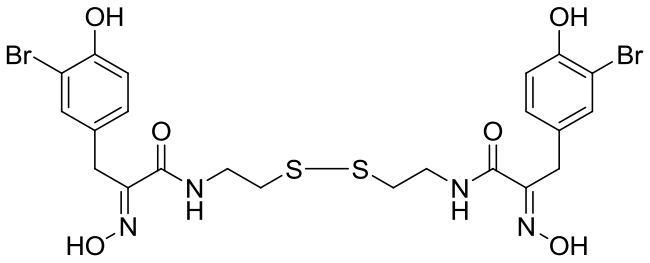

69: psammaplin A

Figure 25. Structure of psammaplin A.

These psammaplins contains a disulphide linkage and therefore the inhibitory activity may be due to the chelation of the zinc ion with sulfhydryl in the active-site pocket. The structure of psammaplin A (**69**) is shown in Figure 25. Studies on the mechanism of action of psammaplin and its synthetic derivatives also supported cellular disulphide cleavage type mechanism of inhibition.[132,133]

9.5.8. HDAC inhibitors with phosphonates

Etzkorn and coworkers synthesized several phosphorus based SAHA analogues **71** and related compounds as HDAC inhibitors.[134] However, these compounds also showed very weak inhibitory activity during HDAC assays. Further, the side chain modification of apicidins ketone moiety to phosphonate by Merck group also showed very low HDAC inhibitory activity.[111]

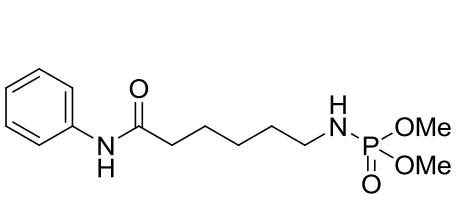

71

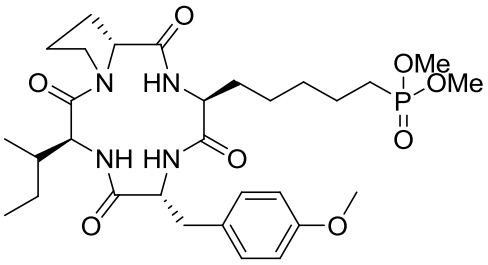

72

Figure 26. HDAC inhibitors containing phosphonate functional groups.

From all these phosphonate compounds studied for HDAC, it is clear that phosphonates are not good inhibitors for the HDAC inhibition, probably due to the highly acidic nature of phosphonate moiety, instead of the basic nature of the HDAC substrate. Jose *et al.*[135] synthesized a phosphonate with a cap group of cyclic tetrapeptide and a spacer of five methylene units. The HDAC inhibitory activity study showed that this phosphonate compound **72** is a very weak inhibitor of HDAC (Figure 26).

9.6. Miscellaneous

There are a number of HDAC inhibitors that cannot be classified as a structural class. Depudecin, a natural product (**73**, Figure 27) having an epoxide was shown to inhibit HDAC in 1998.[136] Rich *et al.*[137] synthesized a cytostatic chlamydocin derivative having

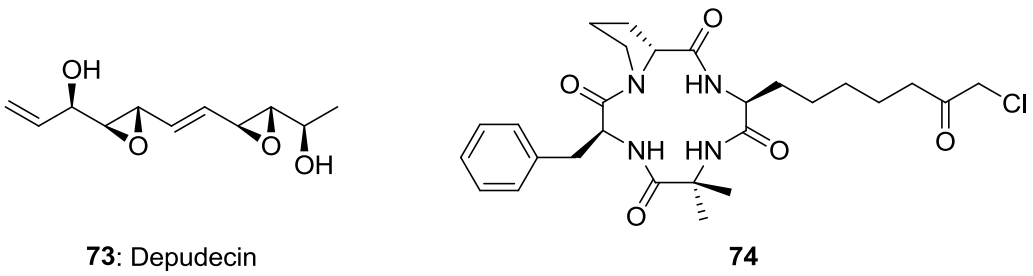

73: Depudecin **74**

Figure 27. Chloromethylketone and epoxy alcohol as zinc ligands.

α-chloroketone functional group as Zn^{2+} ligand. Though the new derivative exhibited somewhat decreased potencies in cell based antiproliferative assay (~3-4 fold) relative to the parent natural product, still it adds a new variation to the zinc ligand library.

10. Selectivity of HDAC inhibitors

In 2001, Yoshida *et al.*[98] reported the differential inhibitory activities of a series of CHAP compounds and a number of natural products for class I/II HDACs. This work demonstrated for the first time that the surface recognition domain of the pharmacophore (Figure 4) affects not only inhibitory potency but selectivity as well. For the characterization of individual members in the HDAC family, development of selective inhibitors of individual members of the HDAC family will be a valuable tool. Also specific drugs for different malignant diseases will be the possible from selective inhibitors. Few reports on the selective inhibitors of HDAC families are available so far and the current research on HDAC inhibitors is mainly directed towards this direction. A class I HDAC specific inhibitors named SCOPs were already reported.[128]

Another report on paralog selectivity was recently disclosed from Schreiber's laboratory.[78] They screened mainly two compounds from the library of several 1,3-dioxane based compounds. Out of the two compounds tubacin **75** inhibit HDAC6 and on the other hand, histacin **76** inhibit HDAC1. The main difference between these two compounds is the zinc binding ligand with some difference in the cap group (Figure 28). Tubacin has the hydroxamic acid as the zinc binding ligand and histacin has benzamide as the zinc binding ligand. Also the interactions at the rim of the binding channel are also important for the specific inhibitors. The cap group of histacin and tubacin were based on 1,3-dioxane but with different groups attached to the dioxane base.

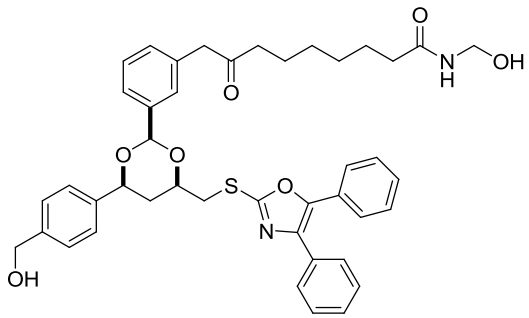

75: Tubacin

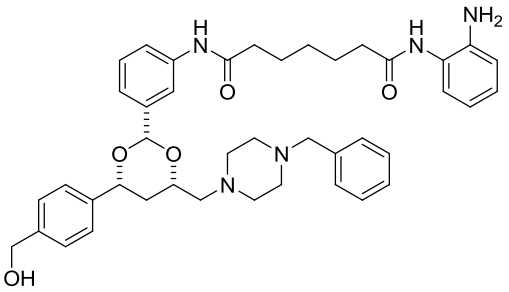

76: Histacin

Figure 28. Selective HDAC inhibitors.

Researchers are now concentrating their attention on the synthesis of selective inhibitors of HDAC. However, progress towards the design of selective inhibitors of HDAC is at the preliminary stages. The synthesis of selective inhibitors will help not only in therapeutic discovery but also to elucidate the biological functions of HDACs.

11. Purpose of this study

One of the three essential parts of a histone deacetylase inhibitor is its functional group which interferes the mechanism of catalysis by coordinating with zinc ion and engaging in multiple hydrogen bonds with the residues at the active site. Therefore, for the development of HDAC inhibitors, optimizations of functional group have been sought. To find optimal functional groups, a large number of HDAC inhibitors with a variety of functional groups, such as hydroxamic acid, retro-hydroxamic acid, o-aminoanilide, ketone, trifluoromethylketone, hydroxymethylketone, methoxymethylketone, carboxylate, mercaptan, disulfide, thioether, thioacetate, borate, phosphate and so on have been reported in literatures and patented. But every functional group suffers from some limitations.

The most potent hydroxamic acids often present metabolic and pharmacokinetic problems such as glucuronidation and sulfation that result in a short *in vivo* half life. Many hydroxamates are unstable *in vivo* and are prone to hydrolysis giving hydroxylamine which has potential mutagenic properties. On the other hand, drawback of chlamydocin and related other (2S,9S)-2-amino-9,10-epoxy-8-oxodecanoic acid (Aoe) containing cyclic tetrapeptides is that they irreversibly inhibits the HDACs by epoxyketone moiety. The trifluoromethylketones exhibit short half-lives both *in vivo*

and *in vitro* by rapid reduction to the corresponding alcohol which occurs *in vitro* in the presence of whole blood or cells. Aminobenzamides and fatty acids have limited potency. These aspects in HDAC inhibitors have thus still to be resolved.

Our aim was to find potent functional groups/zinc ligands which may have enhanced binding affinities for zinc in HDAC inhibition mechanism. For this purpose, we have introduced new and known functional groups to the chlamydocin framework and evaluated these functional groups in the same molecular condition as HDAC inhibitory activity against HDAC1, HDAC4 and HDAC6. We have then compared the potency of these functional groups with chlamydocin and the reported compounds CHAP15. We have next replaced the hydroxamic acid group from the monopeptide HDAC inhibitor SK-658 by new and known functional groups and evaluated these functional groups in the same molecular condition as HDAC inhibitory activity against the same HDAC enzymes as described for chlamydocin analogues and finally compared the potency of these functional groups with the reported compounds SK-658 and SAHA. Some functional groups wete potent and some are not potent HDAC inhibitors.The optimal functional groups or zinc ligands from our findings can be utilized as the preferred functional groups/zinc ligands for other HDAC inhibitors.

12. References

1. Butler, K. V.; Kozikowski, A. P. *Curr. Pharm. Des.* **2008**, *14*, 505-528.
2. Sengupta, N.; Seto, E. *J. Cell Biochem.* **2004**, *93*, 57-67.
3. Jenuwein, T.; Aillis, C. D. *Science* **2001**, *293*, 1074-1080.
4. Izuka, M.; Smith, M. M. *Curr. Opin. Genet. Dev* **2003**, *13*, 154-160.
5. Johnstone, R. W. *Nat. Rev. Drug Discov.* **2002**, *1*, 287-299.
6. Urnov, F. D.; Wolfeffe *Emerging Ther. Targets* **2000**, *4*, 665-685.
7. Mahlknecht, U.; Hoelzer, D. *Mol. Med.* **2000**, *6*, 623-644.
8. Timmerman, S.; et. al. *Cell. Mol. Life Sci.* **2001**, *58*, 728-736.
9. Crsee, W. D.; Seto, E. J. *Cell. Physiol.* **2000**, *184*, 1-16.
10. Kornberg, R. D.; Lorch, Y. *Cell* **1999**, *98*, 285-294.
11. Strahl, B. D.; Allis, C. D. *Nature (London)* **2000**, *403*, 41-45.
12. Gregory, P. D.; Wagner, K.; Horz, W. *Exp. Cell. Res.* **2001**, *265*, 195-202.

13. Davie, J. R. *Curr. Opin. Genet. Dev.* **1998**, *8*, 173-178.
14. Roth, S. Y.; Denu, J. M.; Allis, C. D. *Annu. Rev. Biochem.* **2001**, *70*, 81-120.
15. Deckert, J.; Struhl, K. *Mol. Cell. Biol*. **2001**, *8*, 2726-2735.
16. Kochbin, S.; Verdel, A.; Lemercier, C.; Seigneurin-Berny, D. *Curr. Opin. Genet. Dev.* **2001**, *11*, 162-166.
17. Gray, G. G.; Ekstrom, T. J. *Exp. Cell. Res.* **2001**, *262*, 75-83.
18. Gayther, S. A.; Batley, S. J.; Linger, L.; Bannister, A.; Thorpe, K.; Chin, S. F.; Daigo, Y.; Russell, P.; Wilson, A.; Sowter, H. M.; Delhanty, J. D.; Ponder, B. A.; Kouzarides, T.; Caldas, C. *Nat. Genet.* **2000,** *24*, 300. (b) Kouzarides, T. *Curr. Opin. Genet. Dev.* **1999**, *9*, 40.
19. Amann, J. M.; Nip, J.; Strom, D. K.; Lutterbach, B.; Harada, H.; Lenny, N.; Downing, J. R.; Meyers, S.; Hiebert, S. W. *Mol. Cell Biol*. **2001**, *21*, 6470. (b) Davind, G.; Alland, L; Hong, S. H.; Wong, C. W.; DePinho, R. A.; Dejean, A. *Oncogene* **1998**, *16*, 2549. (c) Dhordain, P.; Lin, R. J.; Quief, S.; Lantoine, D.; Kerckaert, J. P.; Evans, R. M.; Albagli, O. *Nucleic Acids Res*. **1998**, *26*, 4645.
20. Tauton, J.; Hassig, C. A.; Schreiber, S. L.; *Science*, **1996**, *272*, 408-411.
21. Rundlett, S. E.; Carmen, A. A.; Kobayashi, R.; Bavikin, S.; Turner, B. M.; Grunstein, M. *Proc. Natl. Acad. Sci. USA*, **1996**, *93*, 14503-14508.
22. de Ruijter, A. J.; van Gennip, A. H.; Caron, H. N.; Kemp, S.; van Kuilenburg, A. B. *Biochem. J*. **2003**, *370*, 737-749.
23. Gregoretti, I. V.; Lee, Y. M.; Goodson, H. V.; *J. Mol. Biol.* **2004**, *338*, 17-31.
24. Witt, O.; Hedgwig, E. D.; Milde, T.; Oehme, I. *Cancer Letters*, **2009**, *277*, 8-21.
25. Hubbert, C.; Guardiola, A.; Shao, R.; Kawaguchi, Y.; Ito, A.; Nixon, A.; Yoshida, M.;Wang, X. F.; Yao, T. P. *Nature*, **2002**, *417*, 455-458.
26. Hildmann, C.; Wegener, D.; Riester, D.; Hempel, R.; Schober, A.; Merana, J. et al. *J. Biotechnol.* **2006**, *124*, 258-270.
27. Wang D. F.; Helquist, P.; Wiech, N. L.; Wiest, O.; *J. Med. Chem.* **2005**, *48*, 6936-6947.
28. Grozinger C. M.; Schreiber S. L. *Proc. Natl. Acad. Sci. U.S.A.* **2000**, *97*, 7835-7840.
29. Verdin, E.; Dequiedt, F.; Kasler, H. G. *Trends Genet.* **2003**, *19*, 286-293.
30. Haggarty, S. J.; Koeller, K. M.; Wong, J. C.; Grozinger, C. M.; Schreiber, S. L. *Proc. Natl. Acad. Sci. U.S.A.* **2003**, *100*, 4389-4394.

31. Grozinger, C. M.; Hassig C. A.; Schreiber, S. L. *Proc. Natl. Acad. Sci. U.S.A.* **1999**, *96*, 4868-4873.
32. Somoza, J. R.; Skene, R. J.; Katz, B. A.; Mol, C.; Ho, J. D.; Jennings, A. J.; et al. *Structure* , **2004,** *12*, 1325-1334.
33. Schuetz, A.; Min, J.; Allali-Hassani A.; Schapira, M.; Shuen, M.; Loppnau, P. *J. Biol. Chem.*, **2008**, *283*, 11355-11363.
34. Finnin, M. S.; Donigian, J. R.; Cohen, A.; Richon, V. M.; Rifkind, R. A.; Marks, P. A.; Breslow, R.; Pavletich, N. P. *Nature* **1999**, *401*, 188-193.
35. Nielsen, T. K.; Hildmann, C.; Dickmanns, A.; Schwienhorst, A.; Ficner, R. *J. Mol. Biol.* **2005**, *354*, 107-120.
36. Yoshida, M.; Horinouchi, S.; Beppu, T. *BioEssays* **1995**, *17*, 423-430.
37. Yoshida, Y.; Matsuyama, A.; Komatsu, Y.; Nishino, N. *Curr. Med. Chem*. **2003**, *10*, 2351-2358.
38. Suzuki, T.; Miyata, N. *Curr. Med. Chem.* **2005**, 12, 2867-2880.
39. Suzuki, N.; Suzuki, T.; Ota, Y. et al. *J. Med. Chem.* **2009**, *52*, 2909-2922.
40. Suzuki, T.; Nagano, Y.; Matsuura, A.; Kohara, A.; Ninomiya, S.; Kohda, K. et al. *Bioorg. Med. Chem. Lett.* **2003**, *13*, 4321-4326.
41. Kijima, M.; Yoshida, M.; Sugita, K.; Horinouchi, S.; Beppu, T. *J. Biol. Chem.* **1993**, *268*, 22429-22435.
42. Wang, D. F.; Wiest, O.; Helquest, P.; Lan-Hargest, H. Y.; Wiech, N. L. *J. Med. Chem.* **2004**, *47*, 3409-3417.
43. Boffa, L. C.; Vidaldi, G.; Mann, R. S.; Allfrey, V. G. *J. Biol. Chem*. **1978,** *253*, 3364-3366.
44. Phiel, C. J.; Zhang, F.; Huang, E. Y.; Guenther, M. G.; Lazer, A. M.; Klein, P. S. *J. Biol. Chem.* **2001**, *276*, 36734-36741.
45. Tsuji, N.; Kobayashi, M.; Nagashima, K.; Wakisaka, Y.; Koizumi, K. *J. Antibiot*. **1976**, *29*, 1-6.
46. Yoshida, M.; Kijima, M.; Akita, M.; Beppu, T. *J. Biol. Chem*. **1990**, *265*, 17174-17179.
47. Yoshida, M.; Hoshikawa, Y.; Koseki, K.; Mori, K.; Beppu, T. *J. Antibiot.* **1990**, *43*, 1101-1106.
48. Mori, K.; Koseki, K. *Tetrahedron* **1998**, *44*, 6013-6020.

49. Breslow, R.; Belvedere, S.; Gershell, L. *Helv. Chim. Acta*. **2000**, *83*, 1685-1692.
50. Richon, V. M.; Webb, Y.; Merger, R.; Sheppard, T.; Jursic, B.; Ngo, L.; Civoli, F.; Breslow, R.; Rifkind, R. A.; Marks, P. A. *Proc. Natl. Acad. Sci. USA*. **1996**, *93*, 5705-5708.
51. Richon, V. M.; et al. *Proc. Natl. Acad. Sci. USA*. **1998**, *93*, 5705-5708.
52. Grant, S.; Easley, C.; Kirkpatrick, P. *Nat. Rev. Drug. Discov*. **2007**, *6*, 21-22.
53. Van Ommeslaeghe, K. E. G.; et al. *Bioorg. Med. Chem. Lett.* **2003**, *13*, 1861-1864.
54. Su, G. H.; Sohn, T. A.; Ryu, B.; Kern, S. E. *Cancer Res.* **2000**, 60, 3137-3142.
55. Wo02062773. *Expert Opin. Ther. Pat.* **2003**, 13, 387-391.
56. Jung, M.; Brosch, G.; Kölle, D.; Scherf, H.; Gerhäuser, C.; Loidl, P. *J. Med. Chem.* **1999**, *42*, 4669-4679.
57. Wittich, S.; Scherf, H.; Xie, C.; Brosch, G.; Loidl, P.; Gerhäuser, C.; Jung, M. *J. Med. Chem.*, **2002**, *45*, 3296-3309.
58. Woo, S. H.; Frechette, S.; Khalil, E. A.; Bouchain, G.; Vaisburg, A.; Bernstein, N.; Moradei, O.; Leit, S.; Allan, M.; Fournel, M.; Trachy-Bourget, M-C.; Li, Z.; Besterman, J. M.; Delorme, D. *J. Med. Chem*. **2002**, *45*, 2877-2885.
59. Glaser, K. B.; et al. *Mol. Cancer Ther*. **2002**, *1*, 759-768.
60. Curtin, M. L.; Garland, R. B.; Heyman, R.; Frey, R. R.; Michaelides, M. R.; Li, J.; Pease, L. J.; Glaser, K. B.; Marcotte, P. A.; Davidson, S. K. *Bioorg. Med. Chem. Lett*. **2002**, *12*, 2919-2923.
61. Dai, Y.; et al. *Bioorg. Med. Chem. Lett.* **2003**, 13, 1897-1901.
62. Kim, Y. B.; Lee, K-H.; Sugitha, K.; Yoshida, M.; Horinouchi, S. *Oncogene* **1999**, *18*, 2461-2470.
63. Lavoie, R.; Bouchain, G.; Frechette, S.; Woo, S. H.; Khalil, E. A.; Leit, S.; Fournel, M.; Yan, P. T.; Trachy-Bourget, M-C.; Beaulieu, C.; Li, Z., Besterman, J.; Delorme, D. *Bioorg. Med. Chem. Lett.* **2001**, 11, 2847-2850.
64. Bouchain, G.; Leit, S.; Frechette, S.; Khalil, E. A.; Lavoie, R.; Moradei, O.; Woo, S. H.; Fournel, M.; Yan, P. T.; Kalita, A.; Trachy-Bourget, M-C.; Beaulieu, C.; Li, Z.; Robert, M-F.; MacLeod, R.; Besterman, J.; Delorme, D. *Bioorg. Med. Chem. Lett.* **2003**, 46, 820-830.

65. Uesato, S.; Kitagawa, M.; Nagaoka, Y.; Maeda, T.; Kuwajima, H.; Yamori, T. *Bioorg. Med. Chem. Lett*. **2002**, *12*, 1347-1349.
66. Lu, Q.; Yang, Y-T.; Chen, C-S.; Davis, M.; Byrd, J. C.; Etherton, M. R.; Umar, A.; Chen, C-S. *J. Med. Chem*. **2004**, *47*, 467-474.
67. Massa, S.; Mai, A.; Sbardella, G.; Esposito, M.; Ragno, R.; Loidl, P.; Brosch, G., *J. Med. Chem*. **2001**, *44*, 2069-2072.
68. Mai, A.; Massa, S.; Ragno, R.; Esposito, M.; Sbardella, G.; Nocca, G.; Scatena, R.; Jesacher, F.; Loidl, P.; Brosch, G. *J. Med. Chem*. **2002**, *45*, 1778-1784.
69. Mai, A.; Massa, S.; Ragno, R.; Cerbara, I.; Jesacher, F.; Loidl, P.; Brosch, G. *J. Med. Chem*. **2003**, *46*, 512-524.
70. Sternson, S. M.; Wong, J. C.; Grozinger, C. M.; Schreiber, S. L. *Org. Lett*. **2001**, *3*, 4239-4242.
71. Marson, C. L.; Savy, P.; Rioja, A. S.; Mahadevan, T.; Mikol, C.; Veerupillai, A.; Nsubuga, E.; Chahwan, A.; Joel, S. P. *J. Med. Chem.* **2006**, *49*. 800-805.
72. Kahnberg, P.; Lucke, A. J.; Glenn, M. P.; Boyle, G. M.; Tyndall, J. D. A.; Parsons, P. G.; Fairlie, D. P. *J. Med. Chem*. **2006**, *49*, 7611-7622.
73. Glen, M. P.; Kahnberg, P.; Boyle, G. M.; Hansford, K. A.; Hans, D.; Martyn, A. C.; Parsons, P. G.; Fairlie, D. P. *J. Med. Chem*. **2004**, *47*, 2984-2994.
74. Suzuki, T.; Ando, T.; Tsuchiya, K.; Fukazawa, N. *J. Med. Chem*. **1999**, *42*, 3001-3003.
75. Saito, A.; Yamashita, T.; Mariko, Y.; Nosaka, Y.; Tsuchiya, K.; Ando, T.; Suzuki, T.; Tsuruo, T.; Nakanishi, O. *Proc. Natl. Acad. Sci. USA*. **1999**, *96*, 4592-4597.
76. Jaboin, J.; et al. *Cancer Res*. **2002**, *62*, 6108-6115.
77. Vaisburg, A.; Bernstein, N.; Frechette Allan, M.; Aboi-Khalil, E.; Leit, S.; Moradi, O.; Bouchain, G.; Wang, J.; Woo, S. H.; Fournel, M.; Yan, P. T.; Trachy-Bourget, M-C.; Kalita, A.; Beaulieu, C.; Li, Z.; MacLeod, R.; Besterman, J. M.; Delorme, D. *Bioorg. Med. Chem. Lett*. **2004**, *14*, 283-287.
78. Wong, J. C.; Hong, R.; Schreiber, S. L. *J. Am. Chem. Soc.* **2003**, 125, 5586-5587.
79. Christianson, D. W.; Lipscomb, W. N. *J. Am. Chem. Soc.* **1986**, *108*, 4998-5003.
80. Walter, M. W.; Felici, A.; Galleni, M.; Soto, R. P.; Adlington, R. M.; et al. *Bioorg. Med. Chem. Lett.* **1996**, *6*, 2455-2458.

81. Frey, R. R.; Wada, C. K.; Garland, R. B.; Curtin, M. L.; Michaelides, M. R.; Li, J.; Pease, L. J.; Glaser, K. B.; Marcotte, P. A.; Bouska, J. J.; Murphy, S. S.; Davidson, S. K. *Bioorg. Med. Chem. Lett*. **2002**, *12*, 3443-3447.
82. Wada, C. K.; Frey, R. R.; Ji, Z.; Curtin, M. L.; Garland, R. B.; Holms, J. H.; Li, J.; Pease, L. J.; Guo, J.; Glaser, K. B.; Marcotte, P. A.; Richardson, P. L.; Murphy, S. S.; Bouska, J. J.; Tapang, P.; Magoc. T. J.; Albert, D. H.; Davidson, S. K.; Michaelides, M. R. *Bioorg. Med. Chem. Lett*. **2003**, *13*, 3331-3335.
83. Komatsu, Y.; Tomizaki, K.; Tsukamoto, M.; Kato, T.; Nishino, N.; Sato, S.; Yamori, T.; Tsuruo, T.; Furumai, R.; Yoshida, Y.; Horinouchi, S.; Hayashi, H. *Cancer Res.* **2001**, *61*, 4459-4466.
84. Liesch, J. M.; Sweeley, C. C.; Staffeld, G. D.; Anderson, M. S.; Weber, D. J.; Scheffer, R. P. *Tetrahedron* **1982**, *38*, 45-48.
85. Pope, M. R.; Ciuffetti, L. M.; Knoche, H. W.; McCrery, D.; Daly, J. M.; Dunkle, L. D. *Biochemistry*, **1983**, *22*, 3502-3506.
86. Gross, M. L.; McCrery, D.; Crow, F.; Tomer, K. B.; Pope, M. R.; Ciuffetti, L. M.; Knoche, H. W.; Daly, J. M.; Dunkle, L. D. *Tetrahedron Lett*. **1982**, *23*, 5381-5384.
87. Tanis, S. P.; Horenstein, B. A.; Scheffer, R. P.; Rasmussen, J. B. *Heterocycles* **1986**, *24*, 3423-3431.
88. Kim, S-D.; Knoche, H. W.; Dunkle, L. D.; McCrery, D. A.; Tomer, K. B. *Tetrahedron Lett*. **1985**, *26*, 969-972.
89. Closse, A.; Huguenin, R. *Helv. Chim. Acta*. **1974**, *57*, 553-545.
90. Izakai, H.; Nagashima, K.; Sugita, K.; Yoshida, H.; Kawamura, Y.; Yasuda, Y.; Matsumoto, K.; Ishii, K.; Uotani, N.; Nakai, H.; Terui, A.; Yoshimatsu, S.; Ikenishi, Y.; Nakagawa, Y. *J. Antibiot*. **1990**, *63*, 1524-1532.
91. Umehara, K.; Nakahara, K.; Kiyoto, S.; Iwami, M.; Okamoto, M.; Tanaka, H.; Kohsaka, M.; Aoki, H.; Imanaka, H. *J. Antiobiot*. **1983**, *36*, 478-483.
92. Hirota, A.; Suzuki, A.; Suzuki, H.; Tamura, S. *Agr. Biol. Chem*. **1973**, *37*, 643-647.
93. Hirota, A.; Suzuki, A.; Aizawa, K.; Tamura, S. *Agr. Biol. Chem*. **1973**, *37*, 955-956.
94. Hirota, A.; Suzuki, A.; Tamura, S. *Agr. Biol. Chem*. **1973**, *37*, 1185-1189.
95. Kim, S-D. *J. Biochem. Mol. Biol*. **1995**, *28*, 227-231.
96. Walton, J. D.; Earle, E. D.; Staehelin, H.; Grieder, A.; Hiroda, A.; Suzuki, A. *Experientia* **1985**, *41*, 348-350.

97. Taunton, J.; Hassig, C. A.; Schreiber, S. L. *J. Am. Chem. Soc.* **1996**, *118*, 10412-10422.
98. Furumai, R.; Komatsu, Y.; Nishino, N.; Kochbin, S.; Yoshida, Y.; Horinouchi, S. *Proc. Natl. Acad. Sci. USA*. **2001**, *98*, 87-92.
99. Closse, A.; Hugenin, R. *Helv. Chim. Acta*. **1974**, *57*, 533-545.
100. Nishino, N.; Jose, B.; Shinta, R.; Kato, T.; Komatsu, Y.; Yoshida, M. *Bioorg. Med. Chem*. **2004**, *12*, 5777-5784.
101. Islam, N. M.; Kato, T.; Nishino, N.; Kim, H. J.; Ito, A.; Yoshida, M. *Bioorg. Med. Chem. Lett*. **2010**, *20*, 997-999.
102. Singh, S. B.; Zink, D. L.; Polishook, J. D.; Dombrowski, A. W.; Darkin-Rattray, S. J.; Schmatz, D. M.; Goetz, M. A. *Tetrahedron Lett*. **1996**, *37*, 8077-8080.
103. Darkin-Rattray, S. J.; Gurnett, A. M.; Myers, R. W.; Dulski, P. M.; Crumley, T. M.; Allocco, J. J.; Cannova, C.; Meinke, P. T.; Colletti, S. L.; Bednarek, M. A.; Singh, S. B.; Goetz, M. A.; Dombrowski, A. W.; Polishook, J. D.; Schmatz, D. M. *Proc. Natl. Acad. Sci. USA*. **1996**, *93*, 13143-13147.
104. Singh, S. B.; Zink, D. L.; Liesch, J. M.; Dombrowski, A. W.; Darkin-Rattray, S. J.; Schmatz, D. M.; Goetz, M. A. *Org. Lett*. **2001**, *3*, 2815-2818.
105. Singh, S. B.; Zink, D. L.; Liesch, J. M.; Mosley, R. T.; Dombrowski, A. W.; Bills, G. F.; Darkin-Rattray, S. J.; Schmatz, D. M.; Goetz, M. A. *J. Org. Chem*. **2002**, *67*, 815-825.
106. Colletti, S. L.; Li, C.; Fisher, M. H.; Wyvratt, M. J.; Meinke, P. T., *Tetrahedron Lett*. **2000**, *41*, 7825-7829.
107. Meinke, P. T.; Colletti, S. L.; Ayer, M. B.; Darkin-Rattray, S. J.; Myers, R. W.; Schmatz, D. M.; Wyvratt, M. J.; Fisher, M. H. *Tetrahedron Lett.* **2000**, *41*, 7831-7835.
108. Colletti, S. L.; Myers, R. W.; Darkin-Rattray, S, J.; Schmatz, D. M.; Fisher, M.; Wyvratt, M. J.; H., Meinke, P. T. *Tetrahedron Lett.* **2000**, *41*, 7837-7841.
109. Meinke, P. T.; Liberator P. *Curr. Med. Chem.* **2001**, *8*, 211-235.
110. Colletti, S. L.; Myers, R. W.; Darkin-Rattray, S. J.; Gurnett, A. M.; Dulski, P. M.; Galuska, S.; Allocco, J. J.; Ayer, M. B.; Li, C.; Lim, J.; Crumley, T. M.; Cannova, C.; Schmatz, D. M.; Wyvratt, M. J.; Fisher, M. H.; Meinke, P. T. *Bioorg. Med. Chem. Lett*. **2001**, *11*, 107-111.

111. Colletti, S. L.; Myers, R. W.; Darkin-Rattray, S. J.; Gurnett, A. M.; Dulski, P. M.; Galuska, S.; Allocco, J. J.; Ayer, M. B.; Li, C.; Lim, J.; Crumley, T. M.; Cannova, C.; Schmatz, D. M.; Wyvratt, M. J.; Fisher, M. H.; Meinke, P. T. *Bioorg. Med. Chem. Lett.* **2001,** *11*, 113-117.

112. Bhuiyan, M. P. I.; Kato, T.; Okauchi, T.; Nishino, N.; Maeda, S.; Nishino, T. G.; Yoshida, M. *Bioorg. Med. Chem*. **2006**, *14*, 3438-3446.

113. Michaelides, M. R.; Dellaria, J. F.; Gong, J.; Holms, J. H.; Bouska, J. J.; Stacey, J.; Wada, C. K.; Heyman, H. R.; Curtin, M. L.; Guo, Y.; Goodfellow, C. L.; Elmore, I. B.; Albert, D. H.; Magoc, T. J.; Marcotte, P. A.; Morgan, D. W.; Davidsen, S. K. *Bioorg. Med. Chem. Lett.* **2001**, *11*, 1553-1556.

114. Wada, C. K.; Holms, J. H.; Curtin, M. L.; Dai, Y.; Florjancic, A. S.; Garland, R. B.; Guo, Y.; Heyman, H. R.; Stacey, J. R.; Steinman, D. H.; Albert, D. H.; Bouska, J. J.; Elmore, I. N.; Goodfellow, C. L.; Marcotte, P. A.; Tapang, P.; Morgan, D. W.; Michaelides, M. R.; Davidsen, S. K. *J. Med. Chem*. **2002**, *45*, 219-232.

115. Nishino, N.; Yoshikawa, D.; Watanabe, L. A.; Kato, T.; Jose, B.; Komatsu, Y.; Sumida, Y.; Yoshida, M. *Bioorg. Med. Chem. Lett.* **2004**, *14*, 2427-2431.

116. Wu, T. Y. H.; Hassig, C.; Wu, Y.; Ding, S.; Schultz, P. G. *Bioorg. Med. Chem. Lett*. **2004**, *14*, 449-453.

117. Jose, B.; Oniki, Y.; Kato, T.; Nishino, N.; Sumida, Y.; Yoshida, M. *Bioorg. Med. Chem. Lett.* **2004**, *14*, 5343-5346.

118. Gupta, S.; Peiser, G.; Nakajima, T.; Hwang, Y-S. *Tetrahedron Lett*. **1994**, *35*, 6009-6012.

119. Yoshimura, K.; Tsubotani, S.; Okazaki, K. *JP 7196686* **1995**.

120. Mori, H.; Abe, F.; Yoshimura, S.; Takase, S.; Hino, M. WO200008048-A2 **2000**.

121. Xie, W.; Zou, B.; Pei, D.; Ma, D. *Org. Lett*. **2005**, *7*, 2775-2777.

122. Ueda, H.; Nakajima, H.; Hori, Y.; Fujita, T.; Nishimura, M.; Goto, T.; Okuhara, M. *J. Antibiot.* **1994**, *47*, 301-310.

123. Ueda, H.; Manda, T.; Matsumoto, S.; Mukumoto, S.; Nishigaki, F.; Kawamura, I.; Shimomura, K. *J. Antibiot.* **1994**, *47*, 315-323.

124. Nakajima, H.; Kim, Y. B.; Terano, H.; Yoshida, M.; Horinouchi, S. *Exp. Cell. Res*. **1998**, *241*, 126-133.

125. Furumai, R.; Matsuyama, A.; Kobashi, M.; Lee, K-H.; Nishiyama, M.; Nakajima, H.; Tanaka, A.; Komatsu, Y.; Nishino, N.; Yoshida, M.; Horinouchi S. *Cancer Res*. **2002**, *62*, 4916-4921.
126. Shin-ya, K.; Masuoka, Y.; Ngai, A.; Furihata, K.; Nagai, K.; Suzuki, K.; Hayakawa, Y.; Seto, Y. *Tetrahedron Lett*. **2001**, *42*, 41-44.
127. Yurek-George, A.; Habens, F.; Birmmell, M.; Packham, G.; Ganesan, A. *J. Am. Chem. Soc*. **2004**, *126*, 1030-1031.
128. Nishino, N.; Jose, B.; Okamura, S.; Ebisusaki, S.; Kato, T.; Sumida, Y.; Yoshida, M. *Org. Lett*. **2003**, *5*, 5079-5082.
129. Nishino,N.; Shivashimpi, G. M.; Soni, P. B.; Bhuiyan, M. P. I.; Kato, T.; Maeda, S.; Tomonori G. Nishino; Yoshida, M. *Bioorg. Med. Chem.* **2008**, *16*, 437-445.
130. Shivashimpi, G. M.; Amagai, S.; Kato, T.; Nishino,N.; Maeda, S.; Nishino, T, G.; Yoshida, M. *Bioorg. Med. Chem.* **2007**, *15*, 7830-7839.
131. Pina, I. C.; Gautschi, J. T.; Wang, G-Y-S.; Sanders, M. L.; Schmitz, F. J.; France, D.; Cornell-Kennon, S.; Sambucetti, L. C.; Remiszewski, S. W.; Perez, L. B.; Bair, K. W.; Crews, P. *J. Org. Chem*. **2003**, *68*, 3866-3873.
132. Nicolaou, K. C.; Hughes, R.; Pfefferkorn, J. A.; Barluenga, S.; Roecker, A. J. *Chem. Eur. J.* **2001**, *7*, 4280-4295.
133. Nicolaou, K. C.; Hughes, R.; Pfefferkorn, J. A.; Barluenga, S. *Chem. Eur. J.* **2001**, *7*, 4296-4310.
134. Kapustin, G. V.; Fejer, G.; Grounlund, J. L.; McCafferty, D. G.; Seto, E.; Etzkorn, F. A. *Org. Lett.* **2003**, *5*, 3053-3056.
135. Jose, B.; Kato, T.; Sumida, Y.; Yoshida, M.; Nishino, N. *American peptide symposium*, **2003**.
136. Kwon, H. J.; Owa, T.; Hassig, C. A.; Shimada, J.; Schreiber, S. L. *Proc. Natl. Acad. Sci. USA.* **1998**, *95*, 3356-3361.
137. Shute, R. E.; Dunlap, B.; Rich, D. H. *J. Med. Chem*. **1986**, *30*, 71-78.

Chapter 2

Synthesis of various amino acids

1. Introduction

Naturally occurring proteinogenic amino acids have been extensively applied to the area of synthetic organic chemistry.[1] They can serve as cheap, commercially available and enantiomerically pure starting materials for synthetic purposes,[2] as key building blocks for the synthesis of ligands for homogeneous catalysis[3] and as a result of their diversity, be incorporated in libraries of compounds that are built from amino acids.[4] But, opportunities for the use of proteinogenic amino acids for synthetic purposes are rather limited because of the narrow range of functional groups present in the side chains. So, in recent years, the use of optically active non-proteinogenic amino acids in different areas of chemistry, biology and material science provides an additional means for structural modification using the non-natural functionality in the amino acid side chain. To meet the demand for α-amino acids with specific non-proteinogenic functional groups, over the years, a large number of methods have been developed to synthesize such amino acids in enantiomerically pure form.[5] Compared to the amino acids with fixed non-natural functionality, optically pure amino acids having easily modifiable functional groups at the ω-positions in the side chain will be more interesting synthetic targets. The functional groups at the ω-position can be modified to the required groups which provide a series of non-natural amino acids.

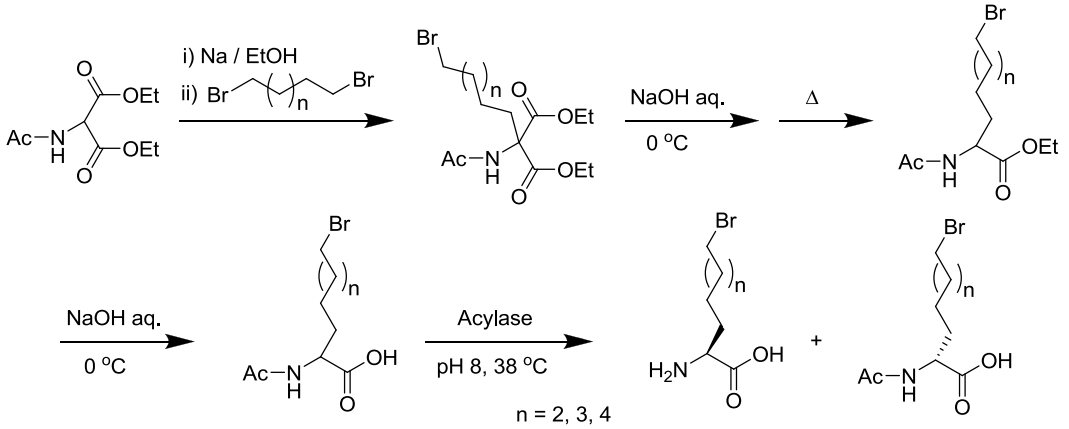

Scheme 1. Synthesis of α-amino-ω-bromo alkanoic aids from diethyl 2-acetamidomalonate.

Several modifiable terminal functionality e.g., carboxyl, hydroxyl, amino, halides and alkenes are possible in the side chain of α-amino acid. Among these modifiable moieties, halides, carboxyl, alkenes and hydroxyl groups are particularly important because they are easily replaceable and/or modifiable and serve as precursors of many non-natural amino acids. As an example, in 2004 Nishino *et al.*[6] reported a convenient and efficient method for the synthesis of a series of chiral 2-amino-n-bromoalkanoic acids (Abn; n = 6-12) starting from diethyl 2-acetamidomalonate and the corresponding dibromoalkane (Scheme 1).

They also demonstrated the versatility of the Abns by converting the terminal ω–bromo group into different functionality. For instance, the terminal bromo group of fully protected Ab7 was converted into phosphonate,[6] thiol[7] and retrohydroxamate[8] by the treatment of trimethyl phosphite, potassium thioacetate and *N*-benzyloxyformamide respepctively (Scheme 2 and 3).

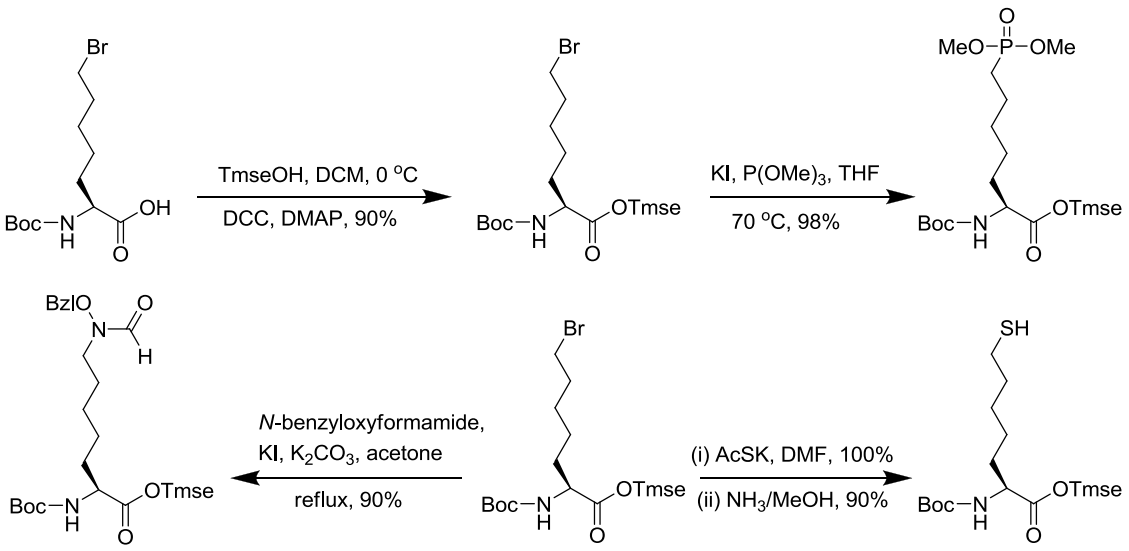

Watanabe, L. A.; Jose, B.; Kato, T.; Nishino, N.; Yoshida, M. *Tetrahedron Lett.* **2004**, *45*, 491-494.

Scheme 2. Replacement of bromide by various functional groups for the synthesis of biologically active peptides.

These groups were subsequently used as zinc binding ligand of cyclic tetrapeptide based histone deacetylase inhibitors. Nishino and coworkers[9] have also synthesized a series of fullerene containing amino acids from Abns. The side chain alkyl bromide was converted to amino group of lysine homologues by Gabriel phthalimide reaction. The

primary amine was mono-protected by *p*-nitrobenzenesulfonyl chloride and then reacted with benzyl 2-bromoacetate to get the corresponding glycine derivative.

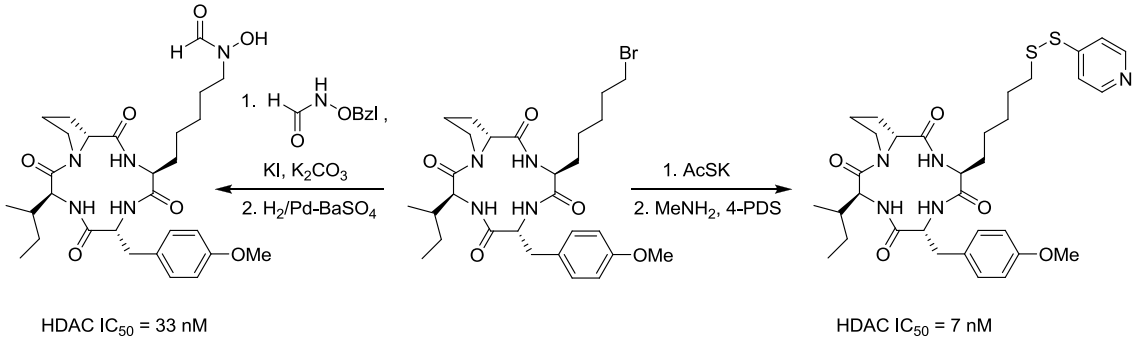

Scheme 3. Cyclic tetrapeptide based HDAC inhibitors from Ab7.

By attaching a carboxymethyl group to the amino group, they reacted with C_{60} according to the literature[10] to yield 2-amino-n-fulleropyrrolidinoalkanoic acid (Afn) in reasonable yield (Scheme 4).

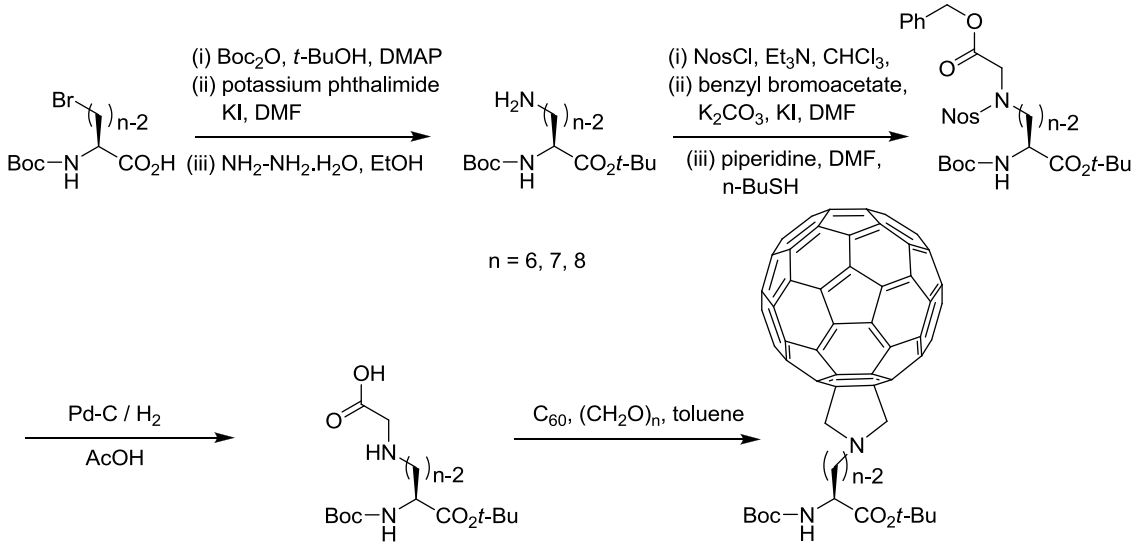

Scheme 4. Synthesis of fulleroamino acids from Abns.

Collet *et al.*[11] in 1998 synthesized chiral ω-borono-α-amino acids from the corresponding ω-unsaturated α-amino acids. α-Aminoboronic acids and related peptides are the most potent inhibitors of serine proteases Rutjes and coworkers[12] synthesized pipecolic acid derivatives from allylglycine using alkene metathesis reaction (Scheme 5). They developed a practical and concise transition metal-catalyzed route to a variety of substituted pipecolic acid derivatives including the natural product baikiain.

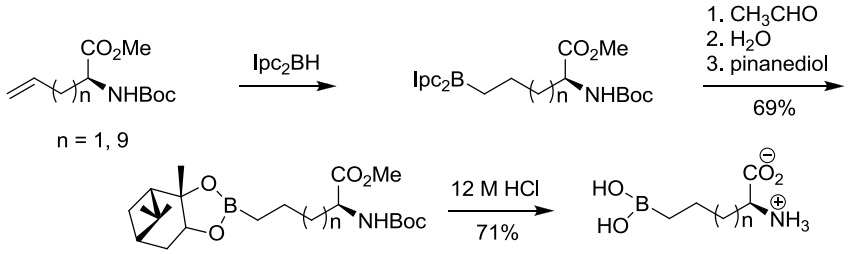

Collet, S.; Bauchat, P.; Danion-Bougot, R.; Danion, D. *Tetrahedron: Asymmetry* **1998**, 9, 2121-2131

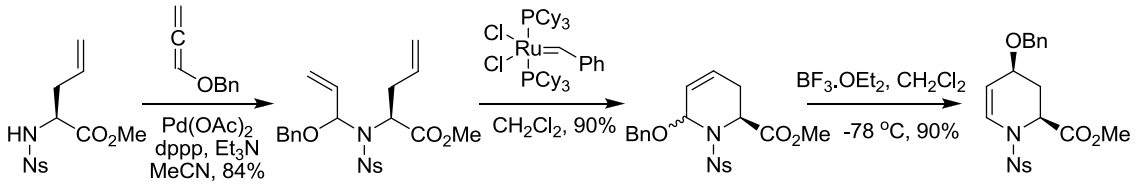

Tjen, K. C. M. F.; Kinderman, S. S.; Schoemaker, H. E.; Hiemstra, H.; Rutjes, F. P. J. T. *Chem. Commun.* **2000**, 699-700.

Scheme 5. Application of ω-unsaturated α-amino acid.

Li Yan-Mei and coworkers[13] described a facile, mild and efficient synthesis of N^{α}-Fmoc-N^{ε}-(benzyl, methyl)-lysine, a building block for monomethylated peptide synthesis (Scheme 6).

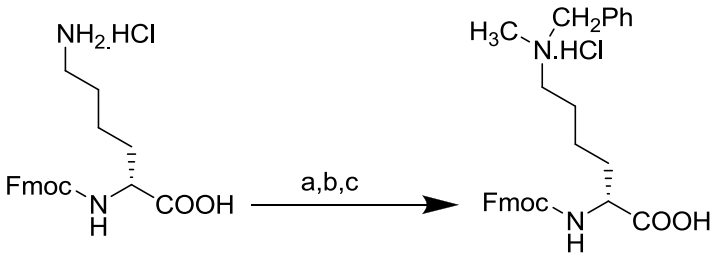

Scheme 6. Synthesis of Fmoc-L-Lys(Bzl, Me)-OH. Reagents and conditions: (a) PhCHO, 3 Å molecular sieve, $NaBH_3CN$, ethanol; (b) HCHO, $NaBH_3CN$, ethanol; (c) HCl.

This building block was proved to be efficient for the synthesis of site-specifically monomethylated peptide. Benzyl group which was incorporated by reductive benzylation and removed via catalytic hydrogenolysis served as an excellent protecting group.

From the above discussion it is clear that α-amino acids with an easily modifiable terminal functional group in the side chain of α-carbon atom can act as a versatile

intermediate for the synthesis of various biologically interesting peptides and related compounds. So the author intended to design and synthesize α-amino acids having terminal modifiable moieties in their side chains.

2. Results and discussion

In this study, we concentrated to synthesize several types of α-amino acids containing modifiable moieties in the side chain. These amino acids were conveniently incorporated to the synthesis of peptides and subsequent transformation of the modifiable moieties yielded various biologically active compounds. The synthesis was designed according to the procedure demonstrated by Watanabe *et al.* [6]

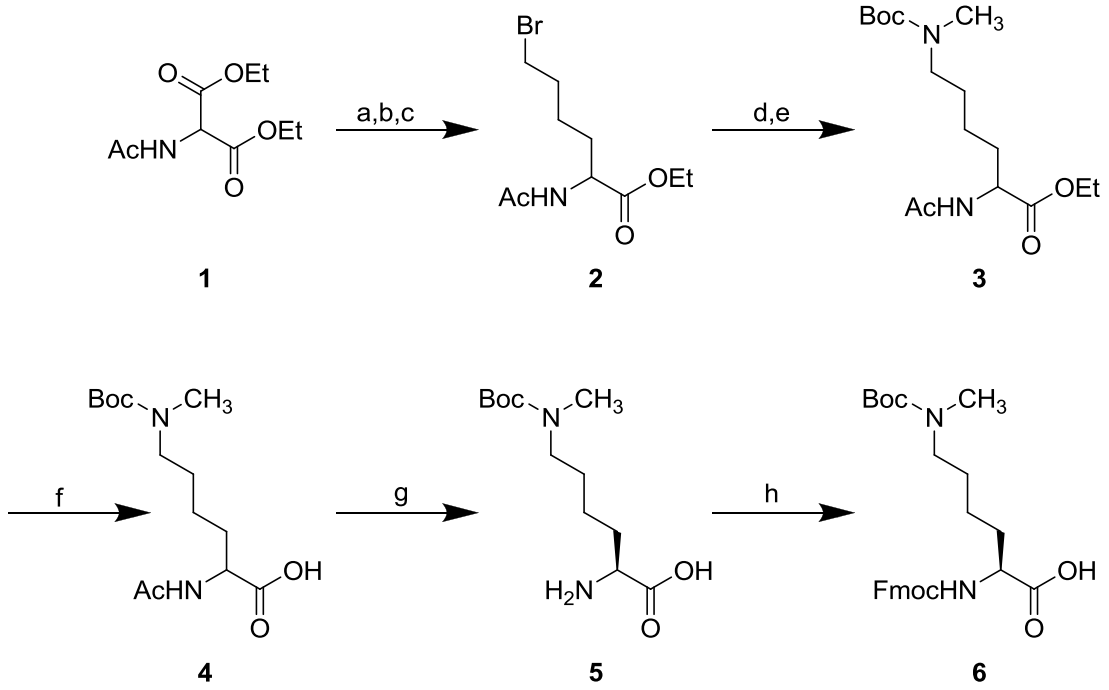

Scheme 7. Synthesis of Fmoc-L-Lys(Boc, Me)-OH (**6**). Reagents and conditions: (a) (i) dehydrated EtOH, Na, reflux, 30 min; (ii) 1,4-dibromobutane, reflux, 6 h; (b) NaOH aq, 0^0C, 4 h, 61%; (c) toluene, reflux, 4 h, 91%; (d) DMF, KI, $MeNH_2$/MeOH, 30 min; (e) dioxane, Boc_2O, DIEA, 86%; (f) NaOH aq, 2 h, 100%; (g) L-aminoacylase, $CoCl_2.6H_2O$, pH 7-8, 38^0C, 20 h; (h) Na_2CO_3 aq, dioxane, Fmoc-OSu, pH 10, 60%.

The synthesis started with the commercially available diethyl 2-acetamidomalonate **(1)** (Scheme 7). 1,4-dibromobutane was coupled with **1** in the presence of sodium ethoxide in dehydrated ethanol. The adduct product was partially hydrolyzed with one equivalent of 1 M NaOH in an ice-bath to obtain the corresponding monoacid monoester as a white

solid after work-up. It was then subjected to decarboxylation by refluxing in toluene. After evaporation of toluene, the residue was purified by silica gel chromatography to yield ethyl 2-acetamido-6-bromohexanoate, Ac-DL-Ab6-OEt **(2)** as oil in quantitative yield. The oil was then reacted with 40% $MeNH_2$/MeOH in DMF in the presence of potassium iodide. Removal of DMF left a residue which was treated without further purification with Boc_2O in dioxane in the presence of DIEA. This reaction yielded Ac-DL-Lys(Boc, Me)-OEt **(3)** which was converted to Ac-DL-Lys(Boc, Me)-OH **(4)** by the action of NaOH in ethanol. *Aspergillus* genus L-aminoacylase (TCI, Tokyo, Japan) was applied to resolve the racemic mixture. The reaction mixture was concentrated and then acidified with 1 M HCl at pH 3-4. The unreacted Ac-D-Lys(Boc, Me)-OEt was extracted with ether. To the aqueous solution containing L-Lys(Boc, Me) **(5)**, dioxane was added and the mixture was treated with Fmoc-OSu in the presence of Na_2CO_3. After completion of the reaction, the desired Fmoc-L-Lys(Boc, Me)-OH **(6)** was extracted in ethyl acetate after evaporation of dioxane and acid treatment. The residue obtained after evaporation of ethyl acetate was purified by silica gel chromatography.

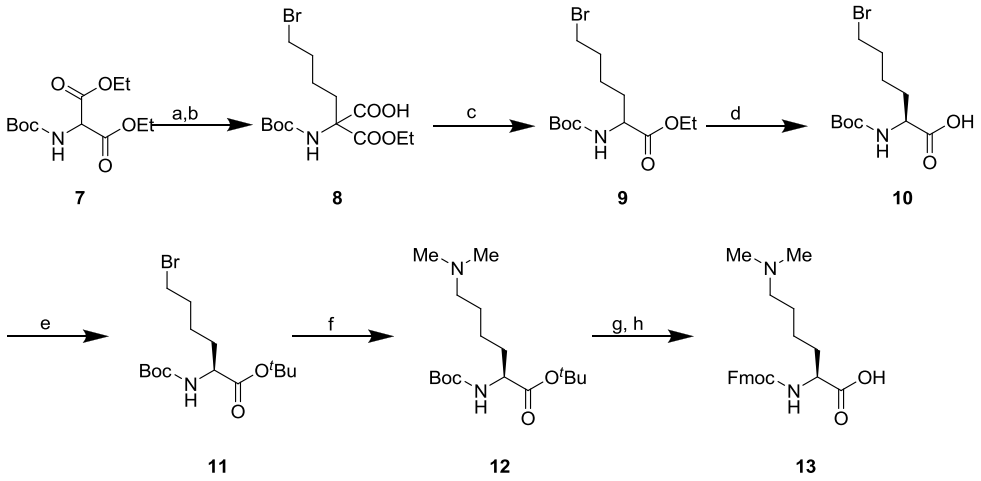

Scheme 8. Synthesis of Fmoc-L-Lys(Me)$_2$-OH (**13**). Reagents and conditions: (a) (i) dehydrated EtOH, Na, reflux, 30 min; (ii) 1,4-dibromobutane, reflux, 6 h; (b) NaOH aq, 0^0C, 4 h, 55%; (c) toluene, reflux, 6 h, 70%; (d)) subtilisin, H_2O/DMF = 3/1, pH 7-8, 38^0C, 3 h; (e) ^{t}BuOH, Boc_2O, DMAP, 66%; (f) DMF, KI, Me_2NH.HCl, 80%; (g) TFA; (h) Na_2CO_3 aq, dioxane, Fmoc-OSu, pH 10, 60%.

In a similar manner, Fmoc-L-Lys(Me)$_2$-OH **(13)** was synthesized starting with diethyl (Boc-amino)malonate and using dimethyl ammonium chloride, $(Me)_2NH$.HCl as methylating agent as depicted in Scheme 8.

The method for the preparation of Boc-L-Ah5(Bzl)-OH, a new unusual amino acid containing hydroxyl group in the side chain, starting from diethyl (Boc-amino)malonate with 3-bromopropan-1-ol is illustrated in Scheme 9. One equivalent of 3-bromopropan-1-ol coupled with diethyl (Boc-amino)malonate preceded by the treatment of sodium ethoxide in ethanol. The adduct product **14** was completely hydrolyzed with three equivalents of 2 M NaOH at room temperature to obtained the oily diacid **15** after work-up which was then subjected to the decarboxylation by refluxing in toluene. After evaporation of toluene, the residue was purified by silica gel chromatography to yield the crystalline solid tert-butyl-2-oxotetrahydro-2*H*-pyran-3-ylcarbamate (δ-lactone) (**16**). The lactone was hydrolyzed with 1 M NaOH at room temperature to obtain the oily hydroxy acid, Boc-DL-Ah5-OH (**17**) after work-up which was subjected to benzylation by reacting with two equivalents of NaH and one equivalent of benzyl bromide in DMF to yield the oily Boc-DL-Ah5(Bzl)-OH (**18**). Esterification of this acid with ethanol in DCM in the presence of DCC and DMAP gave an oily Boc-DL-Ah5(Bzl)-OEt (**19**).

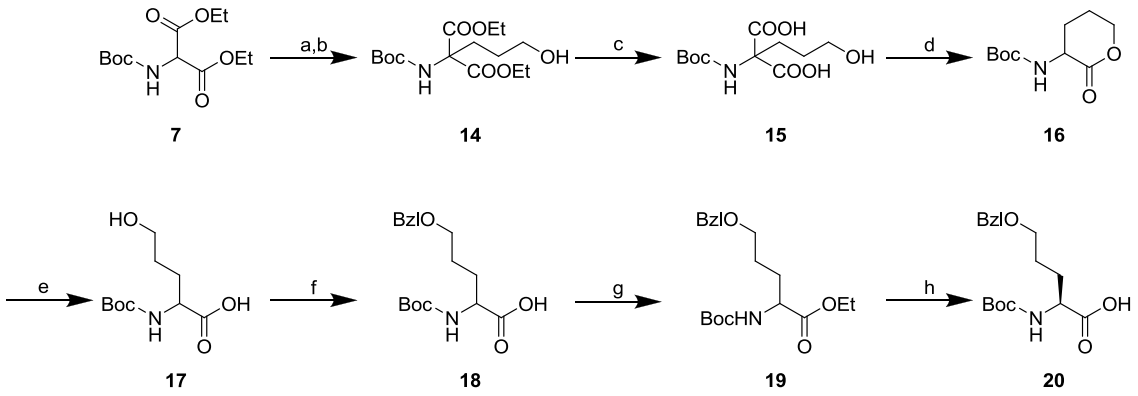

Scheme 9. Synthesis of Boc-L-Ah5(Bzl)-OH (**20**). Reagents and conditions: (a) dehydrated EtOH, Na, reflux, 30 min; (b) 3-bromopropan-1-ol, reflux, 6 h; (c) NaOH aq, EtOH, 2 h, 87%; (d) toluene, reflux, 4 h, 41%; (e) NaOH aq, EtOH, 1 h, 86%; (f) NaH, benzyl bromide, DMF, 5 h, 98%; (g) EtOH, DCC, DMAP, DCM, 12 h, 55%; (h) subtilisin, H_2O/DMF = 1/1, pH 7-8, 38^0C, 4 h, 34%.

After purification by silica gel chromatography, the racemic amino acid ethyl ester was resolved to L-amino acid using subtilisin Carlsberg from *Bacillus licheniformis* (Sigma) in a mixture of water and DMF (1/1, v/v) at pH 7-8. The pH was maintained by the addition of 1 M aqueous ammonia and the reaction was completed in 3 h. Then the

unreacted ethyl ester was removed by ether extraction. The L-amino acid was extracted to ethyl acetate at pH 3-4 using 1 M HCl. Evaporation of ethyl acetate gave the desired oily compound, Boc-L-Ah5(Bzl)-OH (**20**).

The free hydroxyl group of Boc-DL-Ah5-OH **(17)** was again modified by treating with first sodium hydride and then allyl bromide (Scheme 10) and benzyl 2-bromoacetate (Scheme-11) to get more two desired amino acids Boc-DL-Ah5(allyl)-OH **(21)** and Boc-DL-Ah5($AcOCH_2Ph$)-OH **(22)** respectively.

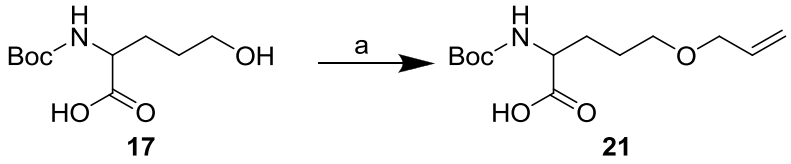

17 **21**

Scheme 10. Synthesis of Boc-DL-Ah5(allyl)-OH (**21**). Reagents and conditions: (a) NaH, allyl bromide, DMF, 12 h, 75%.

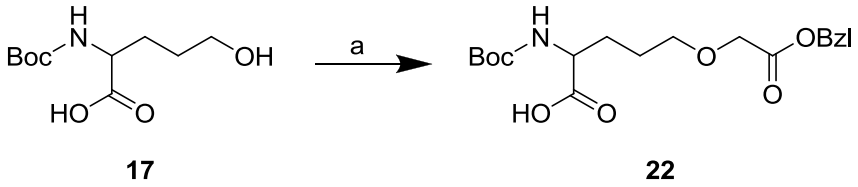

17 **22**

Scheme 11. Synthesis of Boc-DL-Ah5($AcOCH_2Ph$)-OH (**22**). Reagents and conditions: (a) NaH, benzyl 2-bromoacetate, DMF, 12 h, 79%.

3. Summary

In summary, the author developed a convenient route for the synthesis of Fmoc-L-Lys(Boc, Me)-OH and Fmoc-Lys$(Me)_n$-OH to be used as building block for the preparation of methylated peptides. The methylated lysines produced have been incorporated efficiently at specific site to prepare methylated H3 peptide using both manual and automated solid phase syntheses. The author also designed and synthesized amino acid containing hydroxyl group in the side chain which could be transformed into several other functionalities to synthesize a wide variety of biologically interesting non-proteinogenic amino acids.

4. Experimental

4.1. General

Unless otherwise noted, all solvents and reagents were reagent grade and used without purification. Flash chromatography was performed using silica gel 60 (230–400 mesh) eluting with solvents as indicated. All compounds were routinely checked by thin layer chromatography (TLC) and/or high performance liquid chromatography (HPLC). TLC was performed on aluminum-backed silica gel plates (Merck DC-Alufolien Kieselgel 60 F_{254}) with spots visualized by UV light or charring. Analytical HPLC was performed on a Hitachi instrument equipped with a chromolith performance RP-18e column (4.6 × 100 mm, Merck). The mobile phases used were A: H_2O with 0.1% TFA, B: CH_3CN with 0.1% TFA using a solvent gradient of A-B over 15 min with a flow rate of 2 mL/min, with detection at 220 nm. HR FAB-mass spectra were measured on a JEOL JMS-SX 102A instrument.

4.2. Synthesis of Ac-DL-Ab6-OEt (2)

In a 500 mL round-bottomed flask equipped with a sodium hydroxide guard tube, 100 mL of dehydrated ethanol was taken to which 0.95 equivalent (2.23 g, 95 mmol) of metallic sodium was added and completely dissolved with stirring. After 30 minutes, one equivalent of diethyl 2-acetamidomalonate **(1)** (21.7 g, 100 mmol) was added to the sodium ethoxide solution and the reaction mixture was refluxed at 100-110°C for 30 min. The reaction mixture was then allowed to cool to room temperature. Three equivalents (64.2 g, 300 mmol) of 1,4-dibromobutane was added and the reaction mixture was refluxed for an additional 6 h. Sodium bromide salt formation was observed during reflux. After evaporating ethanol and 1,4-dibromobutane, water (100 mL) was added and extracted with ether. The ether was washed with brine, dried over anhydrous $MgSO_4$ and filtered. Finally evaporation of ether gave the oily diester 2-acetamido-6-bromo-2-ethoxycarbonylethylhexanoate, (35.2 g, 100 mmol, 100%).

The malonate synthesis product (35.2 g, 100 mmol) was dissolved in 100 mL of ethanol and the solution was stirred in an ice bath, when 1 M aqueous sodium hydroxide solution (100 mmol, 100 mL) was added. Stirring was continued for 4 h. TLC and

HPLC showed the complete conversion of the starting diester into the monoacid mono ester. After completion of the reaction, ethanol was evaporated and the aqueous solution was washed with ether while pH of the aqueous layer was maintained in the basic region. The acid was extracted into ethyl acetate at pH 3-4 by using solid citric acid which was dried with anhydrous magnesium sulfate, filtered and evaporated to get the solid 2-acetamido-6-bromo-2-ethoxycarbonylhexanoic acid (19.6 g, 61 mmol, 61%). Analytical RP HPLC, R_t: 4.88 min.

The monoacid monoester (19.6 g, 61.0 mmol) was dissolved in 120 mL of toluene and refluxed at 135^{o}C for 4 h. Completion of the reaction was detected by TLC in which appearance of a faster moving product was observed at the expense of the slower moving acid. Toluene was evaporated and the concentrated oily mass was purified by silica gel column chromatography using a mixture of hexane and ethyl acetate (2/1-1/3) solvent system to obtain the oily Ac-DL-Ab6-OEt **(2)** (15.5 g, 55 mmol, 91%). Analytical RP HPLC, R_t: 5.39 min, TLC: R_f, 0.65 (chloroform/MeOH, 9/1, v/v).

4.3. Synthesis of Ac-DL-Lys(Me, Boc)-OEt (3)

To a solution of Ac-DL-Ab6-OEt **(2)** (14.1 g, 50 mmol) in DMF (50 mL), KI (8.30 g, 50 mmol) was dissolved and then added $MeNH_2$/MeOH (9 M, 55.6 mL, 500 mmol) and the mixture was allowed to stand for 30 min at room temperature. Solvents and excess $MeNH_2$ were removed by evaporation in vacuo to remain syrup which was dissolved in dioxane (50 mL) and added diisopropyl ethyl amine (DIEA) (17.5 mL, 100 mmol). The removal of $MeNH_2$ during the concentration of the solution was thus carried out. The compound, AC-DL-Lys(Me)-OEt in the remaining syrup was again dissolve in dioxane (100 mL) and reacted with boc anhydride (Boc_2O) (13.1 g, 60 mmol) at room temperature in the presence of one equivalent of DIEA (8.75 mL, 50 mmol) overnight. The product was extracted into ethyl acetate (150 mL), the solution being washed with 10% citric acid, 4% $NaHCO_3$ and brine respectively and dried over anhydrous $MgSO_4$. Filtration and concentration of the oily Ac-DL-Lys(Me, Boc)-OEt **(3)** which was passed through a silica gel column using a mixture of hexane and ethyl acetate (1:4) gave 15.8 g (48 mmol, 86%) of product. Analytical RP HPLC, R_t: 5.88 min, TLC: R_f, 0.66 (chloroform/MeOH, 9/1, v/v).

4.4. Synthesis of Ac-DL-Lys(Me, Boc)-OH (4)

The ethyl ester **(3)** (15.8 g, 48 mmol) was dissolved in ethanol (50 mL) and flashed once to remove ethyl acetate from the oily starting material. To the solution of the ester in ethanol (100 mL), 2 M aqueous sodium hydroxide solution (72 mmol, 36 mL) was added. Stirring was continued for 2 h. TLC and HPLC showed the completion of the reaction. The reaction mixture was then acidified with acetic acid (100 mmol, 5.72 mL) and ethanol was evaporated. The acid was extracted into ethyl acetate at pH 3-4 by using solid citric acid which was dried with anhydrous magnesium sulfate, filtered and evaporated to get the solid Ac-DL-Lys(Me, Boc)-OH **(4)** (14.5 g, 48 mmol, 100%). Analytical RP HPLC, R_t: 5.14 min.

4.5. Enzymatic resolution of Ac-DL-Lys(Me, Boc)-OH (4)

The racemic acid Ac-DL-Lys(Me, Boc)-OH (14.5 g, 48 mmol) was dissolved in water (240 mL) and the pH of the solution adjusted to 7 by the addition of 1 M aqueous sodium hydroxide solution at 38^0C. To this neutral solution, aqueous solution of $CoCl_2.6H_2O$ (57 mg) and *aspergillus* genus (amino acylase 1, 1.20 g) obtained from TCI, Tokyo, Japan were added and incubated. The pH of the solution was maintained at 7-8 by the addition of 1 M aqueous sodium hydroxide. After 20 h, the reaction mixture was concentrated to 100 mL but precipitation of L-Lys(Me, Boc) **(5)** was not observed.

4.6. Recovery of Ac-D-Lys(Me, Boc)-OH

The reaction mixture was then acidified with 1 M hydrochloric acid to make pH around 2 and the unreacted Ac-D-Lys(Me, Boc)-OH was extracted with ethyl acetate (100 mL), washed with brine and dried over $MgSO_4$. After filtration and evaporation of ethyl acetate, the compound was crystallized in ether/petroleum ether (1:4) to get a crystalline solid Ac-D-Lys(Me, Boc)-OH (5.14 g, 17.0 mmol, 70%). Analytical RP HPLC, R_t: 5.33 min.

4.7. Synthesis of Fmoc-L-Lys(Me, Boc)-OH (6)

To the aqueous solution (pH around 2) containing Lys(Me, Boc), 10% Na_2CO_3 (6 equiv,144 mmol, 15.3 g) and dioxane (200 mL) were added and allowed to react with

Fmoc-OSu at pH around 10 with stirring at room temperature overnight. TLC and HPLC showed the completion of the reaction. After evaporation of dioxane, the reaction mixture was washed with ether (100 mL) and acidified with 1 M hydrochloric acid to make pH 2-3. The compound Fmoc-L-Lys(Me, Boc)-OH was extracted with ethyl acetate (100 mL), washed with brine and dried over $MgSO_4$. Filtration and evaporation of ethyl acetate gave an oil which was passed through a silica gel column using a mixture of chloroform and methanol (49:1) to give the product Fmoc-L-Lys(Me, Boc)-OH **(6)** (6.95 g, 14.4 mmol, 60%). Analytical RP HPLC, R_t: 8.82 min, LC-MS (*m/z*): 483.3 $(M+H)^+$ (calcd for $C_{27}H_{35}N_2O_6$: 483.57).

4.8. Synthesis of Boc-DL-Ab6-OEt (9)

The compound Boc-DL-Ab6-OEt **(9)** was synthesized from diethyl (Boc-amino)malonate **(7)** (27.5 g, 100 mmol) and 1,4-dibromobutane (64.2 g, 300 mmol) following the procedure described for compound **2**. Yield = 12.8 g (38.0 mmol, 70%). Analytical RP HPLC, R_t: 7.86 min.

4. 9. Synthesis of Boc-L-Ab6-OH (10)

The oily mass of compound Boc-DL-Ab6-OEt **(9)** (4.39 g, 13 mmol) was suspended into a mixture of DMF (39 mL) and water (13 mL) (3/1, v/v) solvent system at 38^0C using a mechanical stirrer and pH was adjusted at about 7–8 by adding 1 M aqueous ammonia solution. Then subtilisin Carlsberg from *Bacillus licheniformis* (13 mg, 1 mg enzyme per mmol of substrate) was added and pH was maintained at 7–8 by continuous addition of 1 M aqueous ammonia solution. The reaction was completed within 3 h and then the mixture concentrated. The unreacted Boc-D-Ab6-OEt was extracted with diethyl ether under basic condition. The acid was extracted into ethyl acetate at pH 3-4 by using solid citric acid which was washed with brine, dried with anhydrous magnesium sulfate, filtered and evaporated to get the oily Boc-L-Ab6-OH **(10)** (1.95 g, 6.30 mmol, 96%). Analytical RP HPLC, R_t: 6.29 min.

4.10. Synthesis of Boc-L-Ab6-O^{t}Bu (11)

Boc-L-Ab6-OH **(10)** (1.12 g, 3.62 mmol) was dissolved in 10 mL of *t*-butyl alcohol. To the solution, Boc_2O (1.11 g, 5.10 mmol) and 4-methylaminopyridine (DMAP) (0.14 g,

1.10 mmol) were added. After 1 h reaction at room temperature, the solution was concentrated and the residues were applied to a silica gel column using a mixture of ethyl acetate and hexane (1:6) to get the oily Boc-L-Ab6-O^{t}Bu **(11)** (0.10 g, 2.40 mmol, 66%). Analytical RP HPLC, R_t: 8.82 min.

4.11. Synthesis of Boc-L-Lys(Me)$_2$-O^{t}Bu (12)

Boc-L-Ab6-O^{t}Bu **(11)** (0.10 g, 2.40 mmol) was dissolved in 5 mL of DMF. To the solution, KI (0.40 g, 2.40 mmol), $(CH_3)_2$NH.HCl (0.59 g, 7.20 mmol) and triethylamine (1 mL, 7.14 mmol) were added and stirred overnight. After completion of the reaction, DMF was evaporated and the residue was dissolved in ethyl acetate, washed with saturated sodium carbonate and then dried over anhydrous Na_2CO_3, filtered and evaporated to get the oily Boc-L-Lys(Me)$_2$-O^{t}Bu **(12)** (0.64 g, 1.92 mmol, 80%).

4.12. Synthesis of TFA.H-L-Lys(Me)$_2$-OH

Boc-L-Lys(Me)$_2$-O^{t}Bu **(12)** (0.64 g, 1.92 mmol) was dissolved in TFA (6 mL) at 0^0C and kept for 3 h at room temperature. After evaporation of TFA, the residue was crystallized with a mixture of ether and petroleum ether (1:4) to yield TFA.H-L-Lys(Me)$_2$-OH as TFA salt (0.52 g, 1.90 mmol, 99%).

4.13. Synthesis of Fmoc-L-Lys(Me)$_2$-OH (13)

To the aqueous solution containing TFA.H-L-Lys(Me)$_2$-OH (0.520 g, 1.90 mmol), 10% aqueous Na_2CO_3 (6 equiv, 11.4 mmol, 1.21 g) and dioxane (12 mL) were added and allowed to react with Fmoc-OSu at pH around 10 with stirring at room temperature overnight. TLC and HPLC showed the completion of the reaction. After evaporation of dioxane, the reaction mixture was washed with ether (10 mL) and acidified with 1 M hydrochloric acid to make pH 2-3. The compound Fmoc-L-Lys(Me)$_2$-OH was extracted with ethyl acetate (100 mL), washed with brine and dried over $MgSO_4$. Filtration and evaporation of ethyl acetate gave an oil which was passed through a silica gel column using a mixture of chloroform and methanol (19:1) to give the desired product Fmoc-L-Lys(Me)$_2$-OH (**13**) (0.45 g, 1.15 mmol, 60%). Analytical RP HPLC, R_t: 5.18 min, LC-MS (*m/z*): 397.5 $(M+H)^+$ (calcd for $C_{22}H_{29}N_2O_4$: 397.21).

4.14. Synthesis of diethyl 2-(Boc-amino)-2-(3-hydroxypropyl)malonate (14)

The compound diethyl 2-(Boc-amino)-2-(3-hydroxypropyl)malonate **(14)** was synthesized from diethyl (Boc-amino)malonate **(7)** (23.4 g, 85 mmol) and 3-bromopropan-1-ol (11.9 g, 85 mmol) following the procedure described in section 4.2. Yield = 11.0 g (33 mmol, 39%).

4.15. Synthesis of 2-(Boc-amino)-2-(3-hydroxypropyl)malonic acid (15)

The alkylated diethyl ester **14** (11.0 g, 33 mmol) was dissolved in 50 mL of ethanol and the solution was stirred at room temperature, when 2 M aqueous sodium hydroxide solution (49.5 mL, 99 mmol) was added. Stirring was continued for 2 h. TLC and HPLC showed the complete conversion of the starting diethyl ester into the corresponding diacid. After completion of the reaction, ethanol was evaporated and the aqueous phase was washed with ether while pH of the aqueous layer was maintained in the basic region. The acid was extracted into ethyl acetate at pH 3-4 by using 1 M HCl. The organic phase was dried with anhydrous magnesium sulfate, filtered and evaporated to get the oily 2-(Boc-amino)-2-(3-hydroxypropyl)malonic acid, **(15)** (7.96 g, 28.7 mmol, 87%).

4.16. Decarboxylation of 2-(Boc-amino)-2-(3-hydroxypropyl)malonic acid (15)

The diacid **15** was then dissolved in toluene (60 mL) and refluxed for 4 h. After evaporation of toluene, the residue was purified by silica gel chromatography using a mixture of chloroform and methanol (99:1) to yield the solid tert-butyl-2-oxotetrahydro-2*H*-pyran-3-ylcarbamate (δ-lactone) **(16)** (2.50 g, 11.6 mmol, 41%).

4.17. Synthesis of Boc-DL-Ah5-OH (17)

The solid compound **16** (2.50 g, 11.6 mmol) was dissolved in 14 mL of ethanol and the solution was stirred at room temperature, when 1 M aqueous sodium hydroxide solution (14 mL, 13.9 mmol) was added. Stirring was continued for 1 h. TLC and HPLC showed the complete conversion of the starting material into the corresponding hydroxy acid. After completion of the reaction, ethanol was evaporated and the aqueous phase was washed with ether while pH of the aqueous layer was maintained in the basic region.

The acid was extracted into ethyl acetate at pH 3-4 by using 1 M HCl. The organic phase was dried with anhydrous magnesium sulfate, filtered and evaporated to get the oily Boc-DL-Ah5-OH **(17)** (2.34 g, 10 mmol, 86%).

4.18. Synthesis of Boc-DL-Ah5(Bzl)-OH (18)

To a cooled solution of Boc-DL-Ah5-OH **(17)** (2.34 g, 10 mmol) in DMF (25 mL), 60% NaH (0.88 g, 22 mmol) was added and stirred until the evolution of hydrogen gas was finished. Benzyl bromide (1.32 mL, 11 mmol) was added and the reaction mixture was stirred for 5 h. The reaction was monitored by TLC. After completion of the reaction, it was quenched by acetic acid and water and DMF was evaporated. The residue was dissolved in 4% sodium bicarbonate and washed with ether. The acid was extracted into ethyl acetate at pH 3-4 by using 1 M HCl. The organic phase was dried with anhydrous magnesium sulfate, filtered and evaporated to get the oily Boc-DL-Ah5(Bzl)-OH (**18**) (3.18 g, 9.8 mmol, 98%). Analytical RP HPLC, R_t: 6.70 min.

4.19. Synthesis of Boc-DL-Ah5(Bzl)-OEt (19)

To a cooled solution of Boc-DL-Ah5(Bzl)-OH **(18)** (3.08 g, 9.5 mmol) in DCM (20 mL), ethanol (0.85 mL, 14.3 mmol), DCC (2.95 g, 14.3 mmol) and DMAP (0.12 g, 0.95 mmol) were added and the mixture was stirred at room temperature for 12 h. After completion of the reaction, DCM was evaporated and the residue was dissolved in ethyl acetate and washed with 10% citric acid, 4% sodium bicarbonate and brine respectively and then dried over anhydrous $MgSO_4$. After evaporation of the ethyl acetate, the residue was purified by silica gel chromatography using a mixture of chloroform and methanol (99:1) to yield oily Boc-DL-Ah5(Bzl)-OEt **(19)** (1.83 g, 5.2 mmol, 55%). Analytical RP HPLC, R_t: 7.92 min.

4.20. Synthesis of Boc-L-Ah5(Bzl)-OH (20)

The oily mass of compound **19** (3.96 g, 11.2 mmol) was suspended into a mixture of DMF (35 mL) and water (35 mL) (1/1, v/v) solvent system at 38^0C using a mechanical stirrer and pH was adjusted at about 7–8 by adding 1 M aqueous ammonia solution. Then subtilisin Carlsberg from *Bacillus licheniformis* (12 mg, 1 mg enzyme per mmol of substrate) was added and pH was maintained at 7–8 by continuous addition of 1 M

aqueous ammonia solution. The reaction was completed within 4 h and then the mixture concentrated. The unreacted Boc-D-Ah5(Bzl)-OEt was extracted with diethyl ether under basic condition. Then the aqueous solution was extracted with ethyl acetate as described above to get Boc-L-Ah5(Bzl)-OH as colorless oil (1.20 g, 3.7 mmol, 66%). Analytical RP HPLC, R_t: 6.71 min. LC-MS (*m/z*): 324.5 $(M+H)^+$ (calcd for $C_{17}H_{26}NO_5$: 324.18).

4.21. Synthesis of Boc-L-Ah5(allyl)-OH (21)

To a cooled solution of Boc-DL-Ah5-OH **(17)** (1.60 g, 6.80 mmol) in DMF (20 mL), 60% NaH (0.598 g, 14.9 mmol) was added and stirred until the evolution of hydrogen gas was finished. Allyl bromide (0.578 mL, 6.80 mmol) was added and the reaction mixture was stirred for 12 h. The reaction was monitored by TLC. After completion of the reaction, it was quenched by acetic acid and water and DMF was evaporated. The residue was dissolved in 4% sodium bicarbonate and washed with ether. The acid was extracted into ethyl acetate at pH 3-4 by using solid citric acid. The organic phase was dried with anhydrous magnesium sulfate, filtered and evaporated to get the oily Boc-DL-Ah5(allyl)-OH **(21)** (1.41 g, 5.13 mmol, 75%). Analytical RP HPLC, R_t: 5.64 min. LC-MS (*m/z*): 274.5 $(M+H)^+$ (calcd for $C_{13}H_{24}NO_5$: 274.2).

4.22. Synthesis of Boc-L-Ah5($AcOCH_2Ph$)-OH (22)

To a cooled solution of Boc-DL-Ah5-OH **(17)** (1.17 g, 5 mmol) in DMF (10 mL), 60% NaH (0.43 g, 11 mmol) was added and stirred until the evolution of hydrogen gas was finished. Benzyl 2-bromoacetate (0.87 mL, 5.5 mmol) was added and the reaction mixture was stirred for 12 h. The reaction was monitored by TLC. After completion of the reaction, it was quenched by acetic acid and water and DMF was evaporated. The residue was dissolved in 4% sodium bicarbonate and washed with ether. The acid was extracted into ethyl acetate at pH 3-4 by using solid citric acid. The organic phase was dried with anhydrous magnesium sulfate, filtered and evaporated to get the oily Boc-DL-Ah5($AcOCH_2Ph$)-OH **(22)** (1.5 g, 3.93 mmol, 79%). Analytical RP- HPLC, R_t: 6.78 min. LC-MS (*m/z*): 382.5 $(M+H)^+$ (calcd for $C_{19}H_{28}NO_7$: 382.2).

5. References

1. For recent reviews, see *e.g.*, (*a*) F. J. Sardina and H. Rapoport, *Chem. Rev.*, **1996**, *96*, 1825; (*b*) S. Hanessian, G. McNaughton- Smith, H. G. Lombart and W. D. Lubell, *Tetrahedron*, **1997**, *53*, 12789.
2. G. M. Coppola and H. F. Schuster, *Asymmetric synthesis: construction of chiral molecules using amino acids*, Wiley, New York, **1987**.
3. For various applications of amino acid-derived ligands in asymmetric catalysis, see *e.g., Comprehensive Asymmetric Catalysis*, eds. E. N. Jacobsen, A. Pfaltz and H. Yamamoto, Springer, Berlin, **2000**.
4. For entries into combinatorial chemistry applications, see e.g., (a) D. Obrecht and J. M. Villalgordo, *Solid-Supported Combinatorial and Parallel Synthesis of Small-Molecular-Weight Compound Libraries*, Pergamon, Oxford, **1998**; (b) *Combinatorial peptide and non-peptide libraries: a handbook*, ed. G. Jung, Wiley–VCH, **Scheme 60** Weinheim, **1996**; (c) *Combinatorial chemistry: synthesis, analysis,screening*, ed. G. Jung, Wiley–VCH, Weinheim, **1999**.
5. For general reviews on the synthesis of (non-proteinogenic) amino acids, see *e.g.*, (*a*) R. M. Williams, *Synthesis of Optically Active α-Amino Acids*, Pergamon, Oxford, **1989**; (*b*) *α-Amino Acid Synthesis (Tetrahedron Symposium-in-Print)*, ed. M. J. O'Donnell, *Tetrahedon*, **1988**, *44*, 5253; (*c*) R. M. Williams and J. A. Hendrix, *Chem. Rev.*, **1992**, *92*, 889.
6. Watanabe, L. A.; Jose, B.; Kato, T.; Nishino, N.; Yoshida, M. *Tetrahedron Lett.* **2004**, *45*, 491-494.
7. Nishino, N.; Jose, B.; Okamura, S.; Ebisusaki, S.; Kato, T.; Sumida, Y.; Yoshida, M. *Org. Lett.* **2003**, *5*, 5079-5082.
8. Nishino, N.; Yoshikawa, D.; Watanabe, L. A.; Kato, Jose, B.; Komatsu, Y.; T.; Sumida, Y.; Yoshida, M. *Bioorg. Med. Chem. Lett.* **2004**, *14*, 2427-2431.
9. Watanabe, L. A.; Bhuiyan M. P. I.; Jose, B.; Kato, T.; Nishino, N.; Yoshida, M. *Tetrahedron Lett.* **2004**, *45*, 7137-7140.
10. (a) Pellarini, F.; Pantarotto, D.; Da Ros, T.; Giangaspero, A.; Tossi, A.; Prato, M. *Org. Lett.* **2001**, *3*, 1845-1848; (b) Giangaspero, A.; Zelensky, I.; Briand, J.-P.; Prato, M. *J. Am. Chem. Soc.* **2002**, *124*, 12543-12549.

11. Collet, S.; Bauchat, P.; Danion-Bougot, R.; Danion, D. *Tetrahedron: Asymmetry* **1998**, *9*, 2121-2131.
12. Tjen, K. C. M. F.; Kinderman, S. S.; Schoemaker, H. E.; Hiemstra, H.; Rutjes, F. P. J. T. *Chem. Commun.* **2000**, 699-700.
13. Huang, Z. P.; Su, X. Y.; Du, J. T.; Zhao, Y. F.; Li, Y. M. *Tetrahedron Lett.* **2006**, *47*, 5997-5999.

Chapter 3

Design, synthesis and evaluation of various functional groups as HDAC inhibitors on chlamydocin analogues

1. Introduction

Histone deacetylases (HDACs) have attracted considerable interest as targets in the treatment of cell proliferative diseases such as cancer.[1] Therefore, the detailed knowledge of their catalytic mechanism is of high impotance for the development of anti-tumor drugs.[2,3]

1.1. Mechanistic aspects

Finnin *et al.*[4] from their crystallographic study of HDLP complexed with TSA, proposed a first explanation of the catalytic activity of these enzyme that is widely used as a model for zinc-dependant HDACs (Scheme 1).

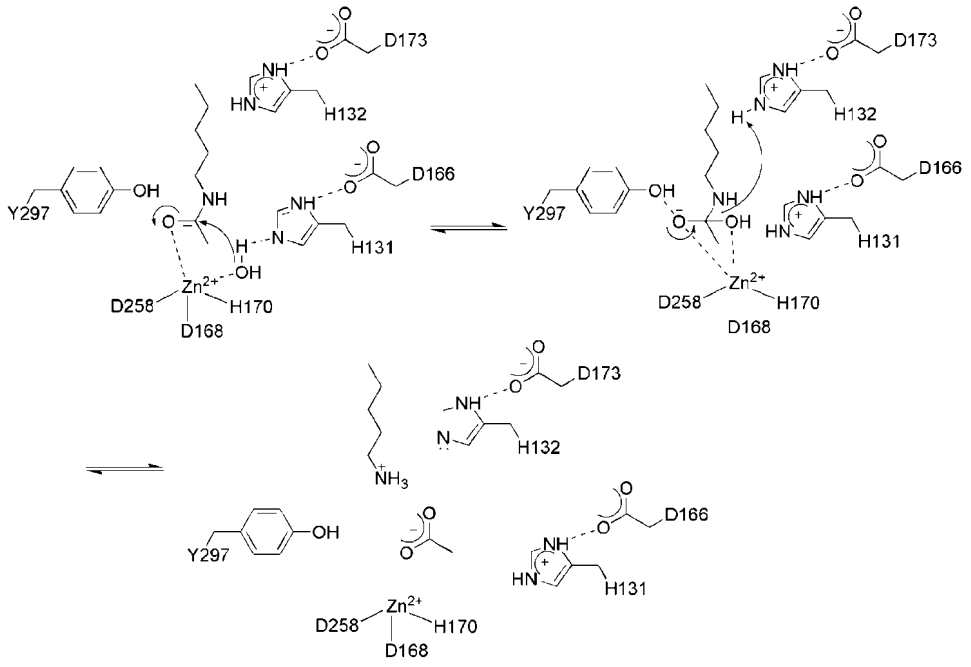

Scheme 1. Mechanism proposed by Finnin *et al.* in 1999.

For HDLP, the zinc atom is surrounded by two histidine-aspartic acid dyads (His131-Asp166 and His132-Asp173), a tyrosine (Tyr297) for proton assistance and is stably coordinated to two aspartic acids (Asp258 and Asp168) and one histidine (His170). This

environment is common to all zinc dependant HDACs with some possible residue changes. Both HDLP and HDACs have a highly conserved catalytic domain and are generally assumed to share a common mechanism. The mechanism leading to the lysine deacetylation proposed starts with intermediate chelating of the necessary water molecule and the carbonyl group of the acetyl lysine to the zinc atom. His132 is assumed to be protonated at this stage. The water is deprotonated under the action of His131, leading to protonation of His131 and the production of a hydroxide ion that can attack the carbonyl of the acetyl group to form a tetrahedral intermediate. The resulting oxy-anion intermeadiate is stabilized by interaction with the hydroxyl group of Tyr297. The rearrangement of the oxy-anion led to the production of an acetate ion and the formation of a terminal ammonium on the lysine side chain. At the end of the mechanism, His131 is protonated while His132 is not.

K.Vanommeslaeghe *et al.*[1] in 2005 proposed a new mechanism based on the investigation of the coordination states in the catalytic site (Scheme 2).

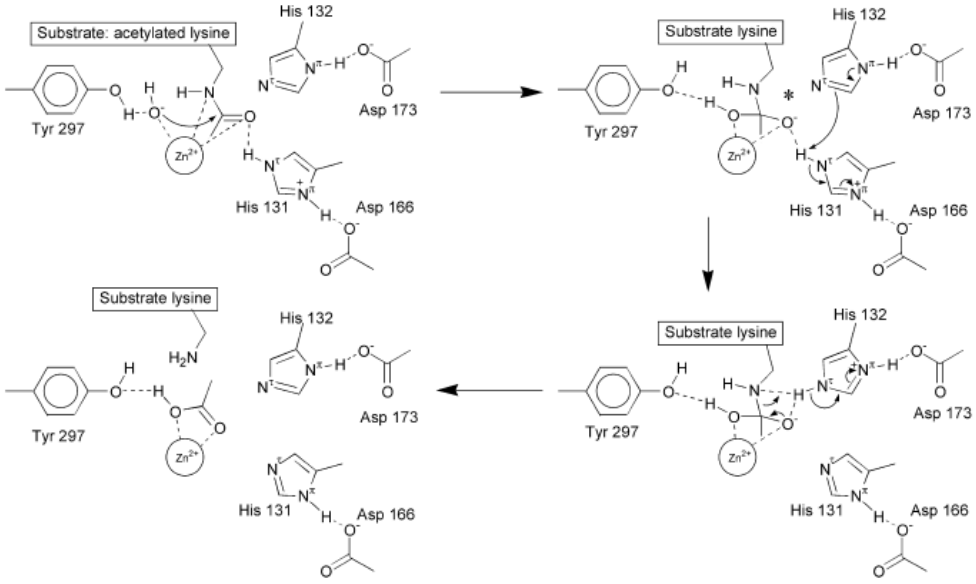

Scheme 2. Mechanism proposed by Vanommeslaeghe *et al*. in 2005.

They carried out a DFT (density functional theory) studies, the result of which was summarized as follows: (a) His131 has pronounced basic characteristics, whilst His132 is more acidic; (b) simultaneous protonation of His131 and His132 is unlikely because protonation of the one strongly inhibits protonation of the other; (c) a low potential

channel between His131 N^{τ} and His132 N^{τ} should facilitate proton transfer; (d) the native state of the active site was identified. In this mechanism, His131 will preferably be protonated by an active site-bound water molecule; this is not the case for His132. This suggests that in the catalytic mechanism, His131 could function as "general base" and His132 as "general acid". Upon binding of an acetylated lysine side chain, the zinc-bound hydroxide ion would attack the amide carbon, in analogy with the mechanism of carbonic anhydrase.[5] The result is a tetrahedral transition state in which an excess of negative charge is expected between His132 N^{τ} and the amide nitrogen, indicated by the symbol * in Scheme 2. This energetically unfavourable situation could be resolved by transferring His131`s N^{τ} proton to His132, via the low potential channel that exists between these two residues. From there, taking into account the higher acidity of His132, protonation of the amide nitrogen is evident, resulting in the cleavage of the amide bond. Finally, after a proton transfer from acetic acid to the histone`s lysine and the subsequent release of the products (not shown in the scheme), a new water molecule may bind the Zn^{2+} ion and protonate the basic His131 to complete the catalytic cycle.

The concept of hydroxyl mediated mechanism for zinc proteases was challenged by Corminboeuf *et al.*[6] based on the differences in the total negative charges.

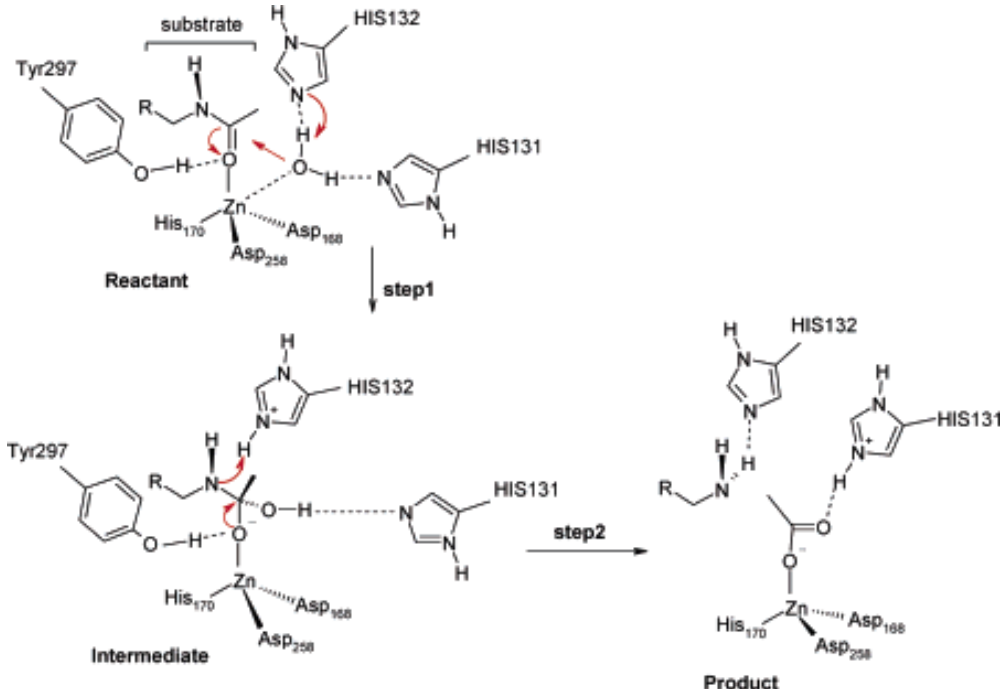

Scheme 3. Mechanism proposed by Corminboeuf *et al*. in 2006.

They explained that the liagand environment is quite different between these two families of enzymes. In zinc protease, such as carboxypeptidase and thermolysin, Zn^{2+} is bound to one Glu/Asp and two His residues[7] which have a total of -1 charge, rather than one His and two Asp residues in HDACs with a total charge of -2. They proposed a mechanism where the two histidine residues are singly coordinated (Scheme 3). The nucleophilic water oxygen attack of the carbonyl carbon to form the tetrahedral intermediate is the rate-determining step and is facilitated by His132, which accepts one proton from the water. The transition state is strongly stabilized by Tyr297, Asp166, and Asp173. In the second step of the reaction, His132 serves as a general acid to transfer one proton to the amide nitrogen which assists the rupture of the amide bond and leads to the lysine and acetic acid product. Meanwhile, the proton spontaneously transfers from acetic acid to His131.

After refinement of the catalytic mechanism of the zinc assisted deacetylation by HDAC, Vanommeslaeghe *et al*.[8] detailed how framework for bidendate chelating group should be handled considering five structural elements (Figure 1) where (**i**) A should be a soft nonbonding electron pair donor in order to coordinate the zinc ion and a H-bond acceptor in order to accept a hydrogen bond from tyrosine OH (**ii**) B should link the zinc-chelating moiety to the spacer and hence be at least trivalent (**iii**) C should be a H-bond donor in order to donate a H-bond to His132 (HDLP). Consequently, C also needs to be trivalent or higher (**iv**) D should be a proton donor in order to protonate His131 (HDLP) and subsequently accept an ionic H-bond from it and form a strong interaction with the zinc ion and (**v**) L links the zinc-chelating group to the spacer. Considering this framework, it can be easily seen why hydroxamates are such good HDAC inhibitotrs. However, the conditions for having a bidentate binding mode like the hydroxamate are very stringent. Indeed, the current results suggest that this goal cannot be accomplished if either centre A or D is a sulfur

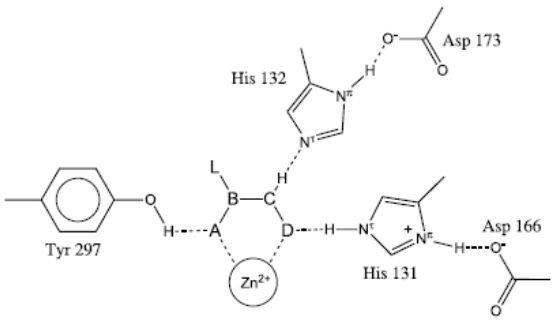

Figure 1. Common framework for bidendate zinc binding group as HDAC inhibitors.

atom. Having a good hydrogen bond donor at C seems to be important for the binding affinity. Lastly, groups with a high chemical hardness interact best with the catalytic core which is a drawback for strategies involving heavier atoms such as sulfur and phosphorus.

1.2. Functional groups/zinc ligands

The essential part of an HDAC inhibitor is its functional group which interferes the mechanism of catalysis by coordinating with zinc ion and engaging in multiple hydrogen bonds with the residues at the active site. Class I and II HDACs involve zinc atom at the active site to employ metalloprotease-like mechanism in cleavage of acetyl group. As natural inhibitors of these HDAC enzymes, two different types of metabolites have been known. One group includes tricostatin A which bears hydroxamic acid functional moiety at the end of the molecule. Cyclic tetrapeptides constitute another group which have typically epoxyketone moiety as a part of quite unusual amino acid in their structures. Having epoxyketone is not necessary as the natural inhibitors. Simple ketone and hydroxymethylketones are also found as HDAC inhibitors so far. Till date, naturally occurring HDAC inhibitors have been reported are trichostatin A (TSA),[9] depsipeptide FK228,[10] sodium butyrate[11] and the cyclic tetrapeptide family including trapoxin (TPX),[12] chlamydocin,[13] TAN-1746,[14] FR-235222,[15] HC toxin,[16] Cyl-1 and Cyl-2,[17] WF-3161[18] and apicidin[19] etc. (Figure 2).

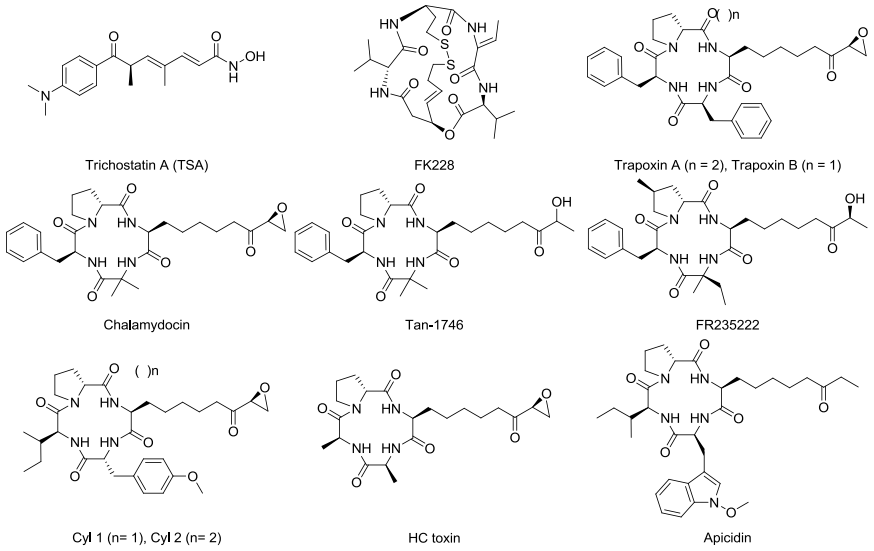

Figure 2. Naturally occurring HDAC inhibitors with different functional groups.

In the past years, a number of HDAC inhibitors containing different functional groups have been reported in literatures and patented as the possible candidate for cancer drugs. However, they have randomly different type of so-called zinc ligand which is expected to bind to the enzyme strongly at the active site. The functional groups are, for instance, hydroxamic acid, retro-hydroxamic acid, ketone, trifluoromethylketone, hydroxymethylketone, methoxymethylketone, o-aminoanilide, mercaptan, disulfide, thioether, thioacetate, borate, phosphate and so on. Examples of these synthetic HDAC inhibitors are sodium phenylbutyrate,[20] sodium valproate,[21] suberoylanilide hydroxamic acid (SAHA),[22] straight chain TSA and SAHA analogues,[23] scriptaid,[24] oxamflatin,[25] electrophilic ketones,[26] cyclic hydroxamic-acid-containing peptides (CHAPs),[27] sulfer-containing cyclic tetrapeptides (SCOPs)[28] and the benzamide (MS-275)[29] (Figure 3). The epoxyketone moiety of chlamydocin was also replaced with several ketones and aldehyde to develop ketone-based HDAC inhibitors.[30] Very recently, bicyclic tetrapeptide based HDAC inhibitors have also been reported.[31]

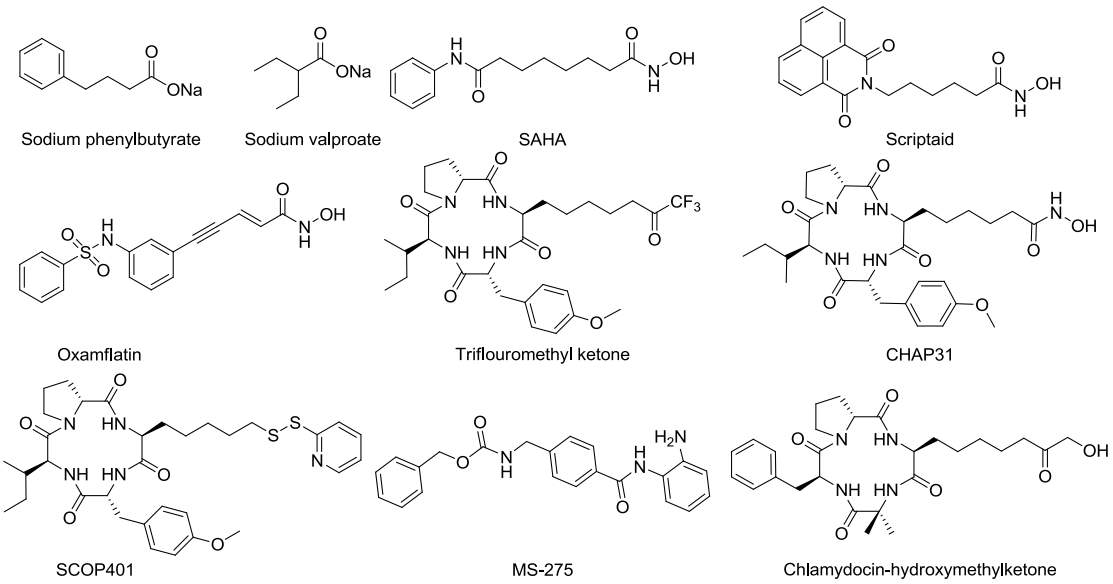

Figure 3. Synthetic HDAC inhibitors with different functional groups.

Most of the currently available functional groups have some limitations. For instance, Hydroxamates have been found to exhibit unfavorable pharmacokinetic behavior resulting from glucuronidation and sulfation[32] and from metabolic hydrolysis,[33] all of which result in short *in vivo* half-lives of the hydroxamic acid group. The trifluoromethyketones studied exhibit short half-lives both *in vivo* and *in vitro* by rapid

reduction to the corresponding alcohol, which occurs *in vitro* in the presence of whole blood or cells.[34] Aminobenzamides and fatty acids have limite potency. These aspects in HDAC inhibitor field have thus still to be resolved. Of various approaches to achieve optimal functional group, one was to introduce new and known functional group to the chlamydocin framework.

2. Results and discussion

2.1. Design

Chlamydocin was originally isolated from the fungus *Diheterospora chlamydosporia.* This naturally occurring cyclic tetrapeptide is a very potent inhibitor of cell proliferation. It is a highly potent HDAC inhibitor, inhibiting HDAC activity *in vitro* with an IC_{50} value of 1.3 nM.[35] In our designing, we focused on the deacetylation mechanism proposed by Finnin *et al*.[4] We selected chlamydocin scaffold as the carrier of functional groups and several functional groups/zinc ligands. In order to evaluate the functional groups in the same molecular condition as HDAC inhibitory activity and elucidate the role of them in the mechanism of HDAC enzymes, we introduced new and known functional groups to the chlamydocin framework, cyclo(-L-AA-Aib-L-Phe-D-Pro-), (where AA stands for different possible zinc ligands at the end of side chain) as standard of comparison. The functional groups or zinc ligands are azide, triazole, borate, acrylamide, chloroacetamide, oxyacetic hydroxamate and dioxyacetone. The structures of the designed HDAC inhibitors, chlamydocin and CHAP15 (a synthesized chlamydocin-hydroxamate) are shown in Figure 4.

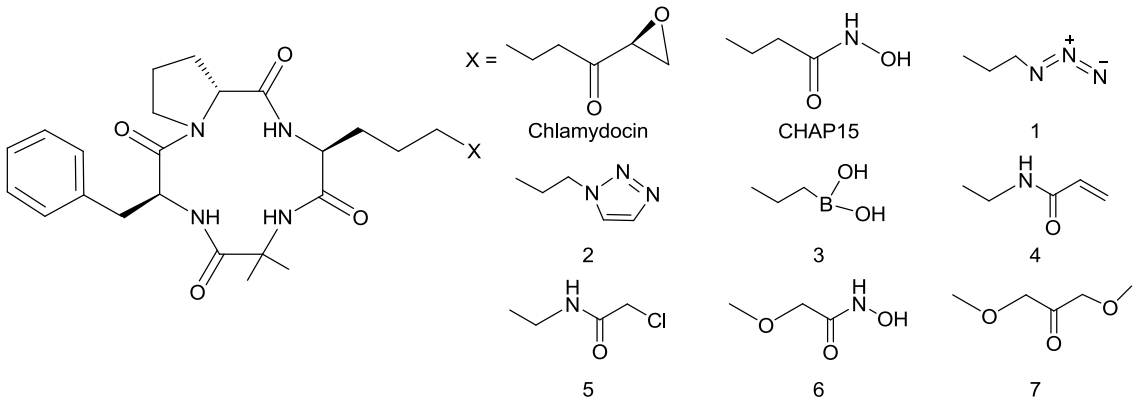

Figure 4. Structures of the designed and reported compounds.

The possible mode of interaction of the zinc ion of HDLP with the functional groups of these designed HDAC inhibitors and with acetylated lysine in the mechanism of inhibition are shown in Figure 5.

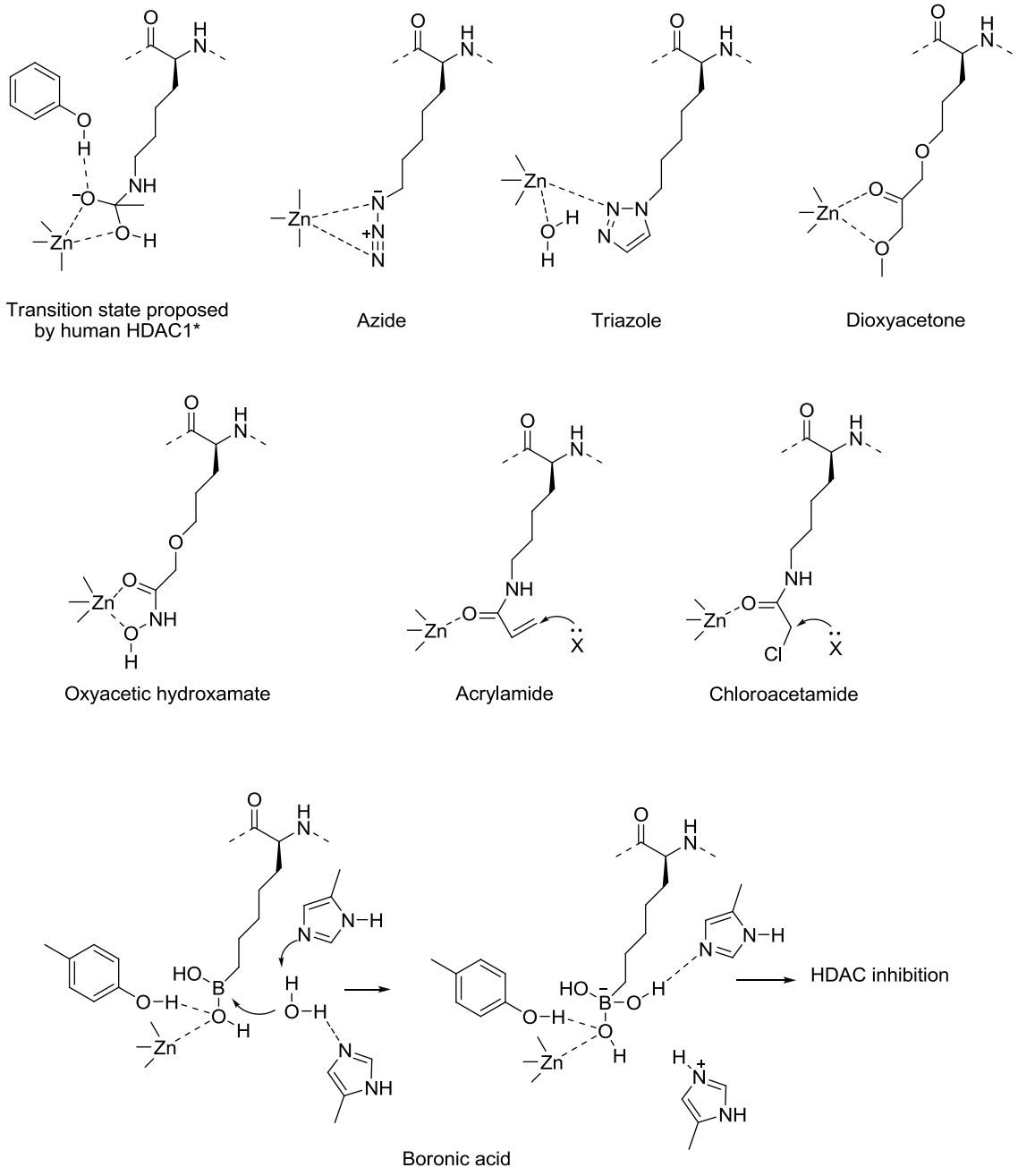

*Nature, **1999**, *401*, 188-193.

Figure 5. Proposed HDAC hydrolysis mechanism of acetylated lysine moiety of histone and mode of interaction of the designed HDAC inhibitors.

2.2. Synthesis

Synthesis of cyclic tetrapeptides was carried out according to the general Scheme 4 by the conventional solution phase method starting from the Z-imino acid tert-butylester. After the removal of Z-protection by catalytic hydrogenation, free amine was extracted and used for condensation with Z-amino acid using DCC/HOBt. The *N*-terminal of the tripeptide was deprotected and coupled with Boc-protected different amino acids to yield linear tetrapeptides. After removal of both side protections by treating with trifluoroacetic acid, cyclization was carried out by the aid of HATU in DMF (2 mM) with minimum amount of DIEA (2.5 equivalent). The yield of cyclic tetrapeptides was 22-82% after purification by silica gel chromatography. When cyclic tetrapeptides were obtained as diastereomers (compounds **6** and **7**), they were successfully separated by silica gel column chromatography. Terminal moieties of the synthesized cyclic tetrapeptides were converted into several functional groups/zinc ligands (Scheme 5, 6, 7, 8 and 9).

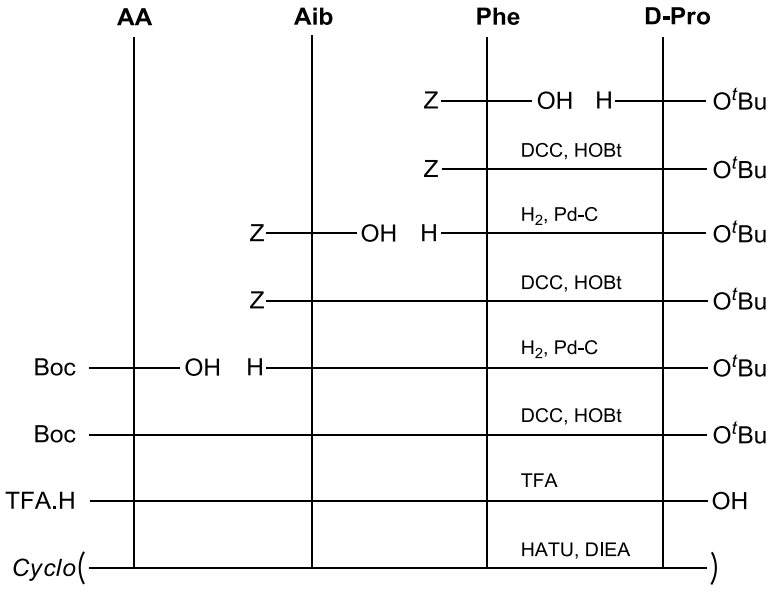

Scheme 4. Synthesis of cyclic tetrapeptides

AA: L-Ab7: (*S*)-2-amino-7-bromoheptanoic acid, L-Ae7: (*S*)-2-aminohept-6-enoic acid, L-Lys(Z), DL-Ah5(allyl): 5-(allyloxy)-2-aminopentanoic acid, DL-Ah5(AcOCH$_2$Ph): 2-amino-5-(2-(benzyloxy)-2-oxoethoxy)pentanoic acid

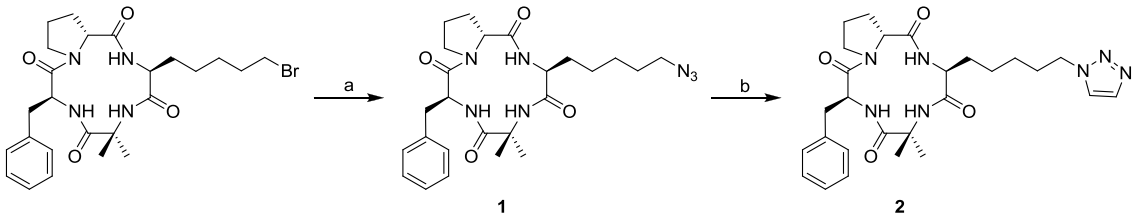

Scheme 5. Reagents and conditions: (a) NaN_3, DMF, 0^0C, 4 h, 100%; (b) CuI, TEA, acetylene, DMF, 120 h, 55%.

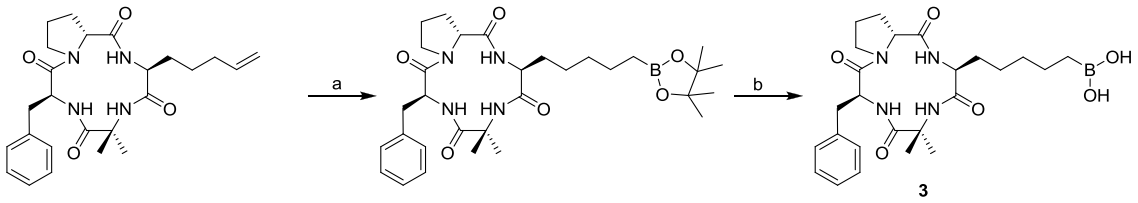

Scheme 6. Reagents and conditions: (a) $[Ir(cod)Cl]_2$: bis(1,5-cyclooctadiene)diiridium(I) dichloride, DPPM: 1,1-bis(diphenylphosphino)methane, pinacolborane, DCM, 48 h, 90%; (b) NH_4OAc, $NaIO_4$, Acetone, H_2O, 20 h, 42%.

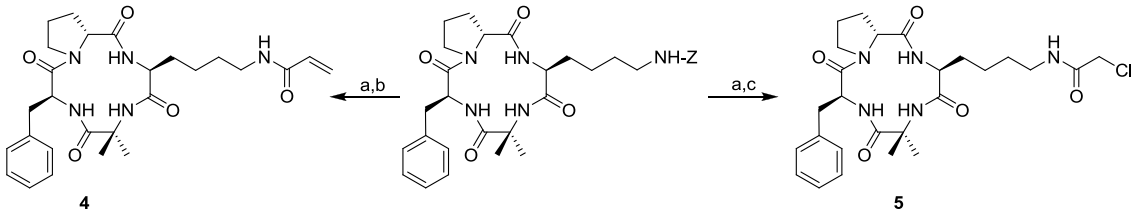

Scheme 7. Reagents and conditions: (a) AcOH, Pd-C, H_2, 12 h, 72%; (b) acryloyl chloride, TEA, DCM, 66%; (c)) 2-chloroacetic acid, DCC, DCM, 67%.

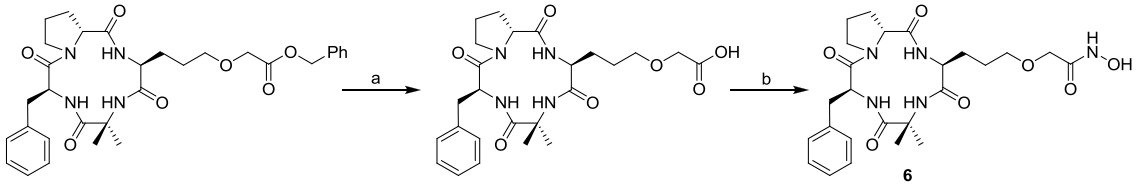

Scheme 8. Reagents and conditions: (a) AcOH, Pd-C, H_2, 12 h, (b) $HCl.H_2N$-OH, BOP: benzotriazole-1-yl-oxy-tris-(dimethylamino)-phosphonium hexafluorophosphate, DIEA, DMF, 23%.

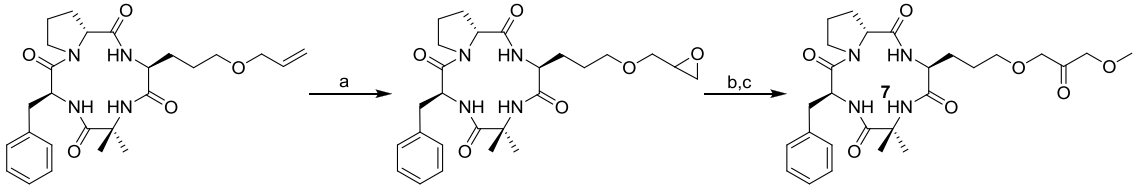

Scheme 9. Reagents and conditions: (a) m-CPBA: meta-chloroperoxybenzoic acid, DCM, 15 h, 76%; (b) NaOMe/MeOH, 18 h, 50%; (c) DMP: Dess-Martin periodinane, DCM, 8 h, 40%.

All the synthesized compounds were characterized by high resolution FAB-MS. The purity of compounds was determined by HPLC analysis and all the synthesized cyclic tetrapeptides showed purity above 97%.

2.3. Evaluation of functional groups as HDAC inhibitors

The synthesized compounds were assayed for HDAC inhibitory activity using HDAC1, HDAC4 and HDAC6 enzymes prepared by 293T cells.[36] In addition, to know the inhibitory activity of these compounds in cell based condition, we carried out p21 promoter assay according to the literature (Figure 6).[30] Detailed experimental procedure for the preparation and assay performed are being explained in experimental section. The results of HDAC inhibitory activity and the p21 promoter assay of the compounds are shown in Table 1.

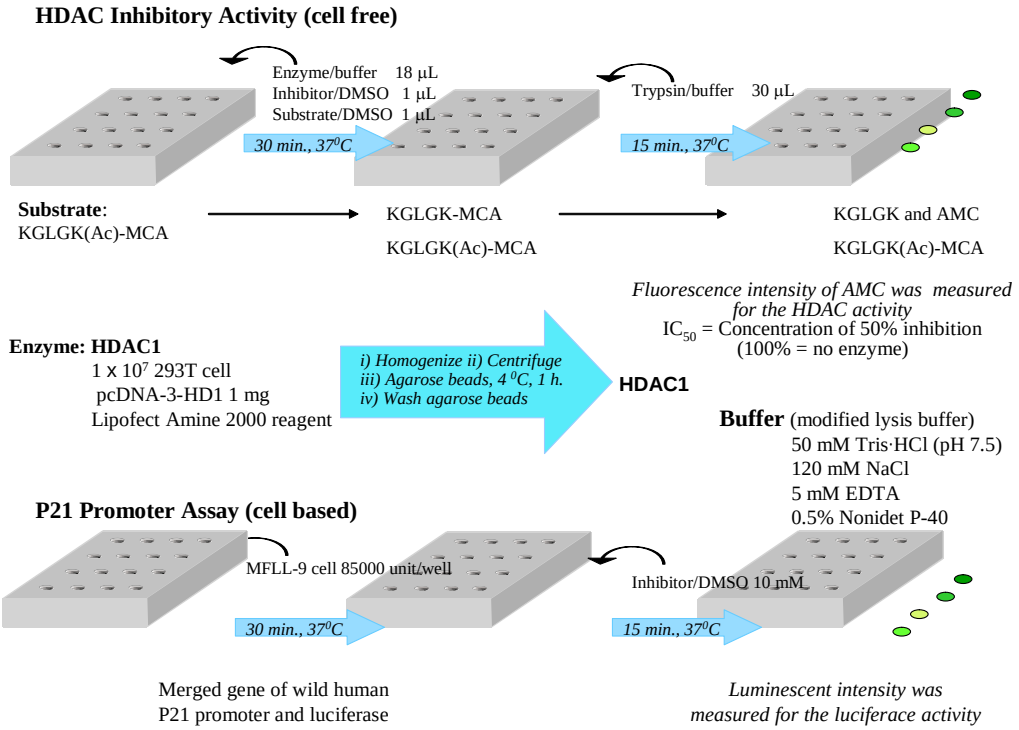

Figure 6. Assay method for HDAC inhibitory activity measurements.

It is apparent from Table 1 that compound **1** bearing azide functional group is quite inactive which might be due to the presence of a positive charge on one of the nitrogen atom developed by resonance. The repulsive force produced between zinc ion and positively charged nitrogen atom inhibits zinc coordination. Compound **2** having triazole zinc binding group is very less active. This might be due to the delocalization of the lone pair of electrons on nitrogen atom into the triazole ring which disfavored zinc chelation. Compounds **4** and **5** are moderate active. Acrylamide functional group

(compound **4** which contains α, β-unsaturated carbonyl group) has conjugated double bonds in which Michael addition is expected by the nucleophiles present in the active site-pocket. In case of chloroacetamide (compound **5**), α-hydrogen (hydrogen attached to α-carbon) is active due to –I inductive effect of the chlorine atom. Nucleophilic attack to α-hydrogen could occur resulting in HDAC inhibition. On the other hand, compounds **3, 6** and **7** having boronic acid, oxyacetic hydroxamate and dioxyacetone functional groups respectively are potent HDAC inhibitors. These functional groups have somewhat enhanced binding affinities for zinc compared to other functional groups in HDAC inhibition mechanism.

Table 1. HDAC inhibitory activity and p21 promoter assay data of the synthesized and reported compounds

Compounds	HPLC R_t (min)	IC_{50} (μM)			p21 promoter assay EC_{1000} (μM)
		HDAC1	HDAC4	HDAC6	
Chlamydocin	-	0.00015	-	1.100	-
[a]CHAP15	-	0.00044	-	0.038	-
1	6.09	>100	>100	>100	>250
2	5.67	65	52	>100	86
3	6.10	2.1	0.15	21	3.6
4	5.96	15	19	>100	>25
5	6.07	13	18	>100	>25
6	6.10	0.65	0.77	14	6.6
7	6.24	0.31	0.20	>100	0.47

[a]CHAP, cyclic hydroxamic-acid-containing peptide

The comparative studies showed that all the compounds were less potent than both chlamydocin and the reported compound chlamydocin-hydroxamate, CHAP15 which demonstrates that the extent of zinc binding affinities for these functional groups/zinc ligands in mechanism of HDAC inhibition is less than that of both chlamydocin (epoxyketone moiety) and CHAP15 (hydroxamic acid).

3. Summary

In summary, we attempted to find potent zinc ligands/functional groups, which may have enhanced binding affinities for zinc in HDAC inhibition mechanism. For this purpose, we have introduced new and known functional groups to the chlamydocin scaffold and evaluate these functional groups in the same molecular condition as HDAC

inhibitory activity and finally compared with chlamydocin and the reported compound CHAP15. Some of the compounds were potent and some were not potent HDAC inhibitors. The optimal functional groups or zinc ligands from these findings can be utilized as the preferred functional groups/zinc ligands for other HDAC inhibitors.

4. Experimental

4.1. General

Unless otherwise noted, all solvents and reagents were reagent grade and used without purification. Flash chromatography was performed using silica gel 60 (230–400 mesh) eluting with solvents as indicated. All compounds were routinely checked by thin-layer chromatography (TLC) and/or high-performance liquid chromatography (HPLC). TLC was performed on aluminum-backed silica gel plates (Merck DC-Alufolien Kieselgel 60 F_{254}) with spots visualized by UV light or charring. Analytical HPLC was performed on a Hitachi instrument equipped with a chromolith performance RP-18e column (4.6 × 50 mm, Merck). The mobile phases used were A: H_2O with 0.1% TFA, B: CH_3CN with 0.1% TFA using a solvent gradient of A to B over 15 min with a flow rate of 2 mL/min, with detection at 220 nm. FAB-mass spectra and high-resolution mass spectra (HRMS) were measured on a JEOL JMS-SX102A instrument. In positive-mode MS analysis using 3-nitrobenzyl alcohol (NBA) as a matrix, boronic acids are esterified with NBA and the molecular weight detected corresponds to $(M+2NBA-2H_2O+H)^+$ or $(M+2NBA-2H_2O)^+$. In negative mode analysis using glycerol as a matrix, the molecular weight detected corresponds to $(M+Glycerol-2H_2O-H)^-$. Coupling reactions were performed by standard solution-phase chemistry using dicyclohexylcarbodiimide (DCC) and 1-hydroxybenzotriazole (HOBt). Peptide cyclization was mediated by O-(7-azabenzotriazoyl-1-yl)-1,1,3,3-tetramethyluronium hexafluorophosphate (HATU) and benzotriazole-1-yl-oxy-tris-(dimethylamino)-phosphonium hexafluorophosphate (BOP).

4.2. Synthesis of the tripeptide intermediate Z-Aib-L-Phe-D-Pro-O^{t}Bu

To a cooled solution of H-D-Pro-O^{t}Bu (3.10 g, 18.1 mmol) and Z-L-Phe-OH (5.41 g, 18.1 mmol) in dimethylformamide (DMF) (36 mL), HOBt. H_2O (2.77 g, 18.1 mmol) and DCC (4.48 g, 21.7 mmol) were added and the mixture was stirred at room

temperature for 12 h. After completion of the reaction, DMF was evaporated and the residue was dissolved in ethyl acetate and washed with 10% citric acid, 4% sodium bicarbonate and brine respectively and then dried over anhydrous $MgSO_4$. After evaporation of the ethyl acetate, the residue was purified by silica gel chromatography using a mixture of chloroform and methanol (99:1) to yield Z-L-Phe-D-Pro-O^{t}Bu (7.52 g, 16.6 mmol, 92%, HPLC, R_t: 6.55 min) as a colorless oil. The protected dipeptide (7.52 g, 16.6 mmol) was dissolved in acetic acid (85 mL, 5 mL/mmol). Pd-C (0.85 g, 50 mg/mmol) was added and the mixture was stirred under hydrogen atmosphere for 12 h. The reaction was monitored by TLC and HPLC. After completion of the reaction, Pd-C was filtered off and the acetic acid was evaporated. The residue was dissolved in ethyl acetate and the organic phase was washed with saturated sodium carbonate solution and dried over anhydrous Na_2CO_3. Evaporation of ethyl acetate gave H-L-Phe-D-Pro-O^{t}Bu (5.53 g, 13.7 mmol, 83%, HPLC, R_t: 5.43 min), which was coupled with Z-Aib-OH (3.25 g, 13.7 mmol) following the same procedure described above and purified by silica gel chromatography using a mixture of chloroform and methanol (99:1) to get Z-Aib-L-Phe-D-Pro-O^{t}Bu (7.01 g, 13 mmol, 95%, HPLC, R_t: 8.03 min) as a white foam.

4.3. Synthesis of *cyclo*(-L-Ab7-Aib-L-Phe-D-Pro-)

The tripeptide Z-Aib-L-Phe-D-Pro-O^{t}Bu (1.06 g, 2 mmol) was dissolved in acetic acid (10 mL) and Pd-C (0.10 g) was added. The mixture was stirred under hydrogen for 12 h. After completion of the reaction, Pd-C was filtered off and the acetic acid was evaporated. The residue was dissolved in ethyl acetate, washed with saturated sodium carbonate and dried over anhydrous Na_2CO_3. Evaporation of ethyl acetate gave H-Aib-L-Phe-D-Pro-O^{t}Bu (0.88 g, 2 mmol, 100%, HPLC, R_t: 4.56 min). The N-terminal free tripeptide H-Aib-L-Phe-D-Pro-O^{t}Bu (0.88 g, 2 mmol) was coupled with Boc-L-Ab7-OH (0.648 g , 2 mmol), according to the method described earlier and the fully protected crude linear tetrapeptide was purified by silica gel chromatography using a mixture of chloroform and methanol (99:1) to yield Boc-L-Ab7-Aib-L-Phe-D-Pro-OtBu (0.99 g, 1.4 mmol, 70%) as a white foam. Boc-L-Ab7-Aib-L-Phe-D-Pro-OtBu (0.99 g, 1.40 mmol) was dissolved in trifluoroacetic acid (TFA) (7 mL) at 0ºC and kept for 3 h at room temperature. After evaporation of TFA, the residue was crystallized with a mixture of ether and petroleum ether (1:4) to yield H-L-Ab7-Aib-L-Phe-D-Pro-OH as TFA salt

(0.898 g, 1.32 mmol, 94%). To a volume of DMF (660 mL), TFA.H-L-Ab7-Aib-L-Phe-D-Pro-OH (0.898 g, 1.32 mmol), HATU (0.752 g, 1.98 mmol), *N*,*N*-diisopropylethylamine (DIEA) (0.577 mL, 3.3 mmol) were added in five aliquots with 20 min time interval while the solution was stirred vigorously. After the final addition, the reaction mixture was allowed to stir for an additional hour. Completion of the cyclization reaction was monitored by HPLC and then DMF was evaporated under reduced pressure. The crude cyclic tetrapeptide was dissolved in ethyl acetate and the solution was washed successively by 10% citric acid, 4% sodium bicarbonate and brine. Finally the ethyl acetate solution was dried over anhydrous $MgSO_4$ and filtered. After evaporation of ethyl acetate, the residue was purified by silica gel chromatography using a mixture of chloroform and methanol (99:1) to yield *cyclo*(-L-Ab7-Aib-L-Phe-D-Pro-) (0.423 g, 0.79 mmol, 60%) as a white foam. Analytical RP HPLC, R_t: 6.19 min, LC-MS (*m/z*): 535.3 $(M+H)^+$ (calcd for $C_{25}H_{36}BrN_4O_4$: 535.2).

4.4. Synthesis of *cyclo*(-L-Aa7-Aib-L-Phe-D-Pro-) (1)

To a cooled solution of *cyclo*(-L-Ab7-Aib-L-Phe-D-Pro-) (0.107 g, 0.20 mmol) in DMF (1 mL), NaN_3 (0.016 g, 0.25 mmol) was added and the mixture was stirred gently for 4 h at room temperature. After completion of the reaction, DMF was evaporated and the residue was dissolved in ethyl acetate and washed with brine and then dried over anhydrous $MgSO_4$. After evaporation of the ethyl acetate, the residue was crystallized with ether to yield *cyclo*(-L-Aa7-Aib-L-Phe-D-Pro-) (0.10 g, 0.20 mmol, 100%). Analytical RP HPLC, R_t: 6.09 min, HR-FAB MS $[M+H]^+$ 498.2822 for $C_{25}H_{36}N_7O_4$ (calcd 498.2829).

4.5. Synthesis of *cyclo*(-L-Aa7(CL)-Aib-L-Phe-D-Pro-) (2)

To a solution of *cyclo*(-L-Aa7-Aib-L-Phe-D-Pro-) (0.10 g, 0.20 mmol) in DMF (2 mL),

CuI (0.8 mg, 4 µmol) and TEA (0.22 mmol, 31 µL) were added. Acetylene gas was passed through the mixture for 120 h. DMF was evaporated and the residue was dissolved in ethyl acetate and washed with brine and then dried over anhydrous $MgSO_4$. After evaporation of the ethyl acetate, the residue was purified by HPLC (30-55%

CH_3CN, 50 mm column) to yield *cyclo*(-L-Aa7(CL)-Aib-L-Phe-D-Pro-) (0.029 g, 55%, HPLC, R_t: 5.67 min, HR-FAB MS $[M+H]^+$ 524.3020 for $C_{27}H_{38}N_7O_4$ (calcd 524.2985).

4.6. Synthesis of *cyclo*(-L-Ae7-Aib-L-Phe-D-Pro-)

The tripeptide Z-Aib-L-Phe-D-Pro-O^{t}Bu (1.32 g, 2.4 mmol) was dissolved in acetic acid (12 mL) and Pd-C (0.120 g) was added. The mixture was stirred under hydrogen for 12 h. After completion of the reaction, Pd-C was filtered off and the acetic acid was evaporated. The residue was dissolved in ethyl acetate, washed with saturated sodium carbonate and dried over anhydrous Na_2CO_3. Evaporation of ethyl acetate gave H-Aib-L-Phe-D-Pro-O^{t}Bu (0.950 g, 98%, HPLC, R_t: 6.8 min). The N-terminal free tripeptide H-Aib-L-Phe-D-Pro-O^{t}Bu (0.95 g, 2.35 mmol) was coupled with Boc-L-Ae7-OH (0.685 g, 2.82 mmol) according to the method described earlier and the fully protected crude linear tetrapeptide was purified by silica gel chromatography using a mixture of chloroform and methanol (99:1) to yield Boc-L-Ae7-Aib-L-Phe-D-Pro-O^{t}Bu (1.31 g, 2.09 mmol, 88%) as a white foam. Boc-L-Ae7-Aib-L-Phe-D-Pro-O^{t}Bu (1.31 g, 2.09 mmol) was dissolved in TFA (6 mL) at 0ºC and kept for 3 h at room temperature. After evaporation of TFA, the residue was crystallized with a mixture of ether and petroleum ether (1:4) to yield H-L-Ae7-Aib-L-Phe-D-Pro-OH as TFA salt (1.17 g, 2.06 mmol, 99.8%). HPLC, R_t: 5.83 min. To a volume of DMF (200 mL), TFA.H-L-Ae7-Aib-L-Phe-D-Pro-OH (1.17 g, 2.06 mmol), HATU (1.14 g, 3 mmol), and DIEA (870 µL, 5.0 mmol) were added in five aliquots with 30 min time interval while the solution was stirred vigorously. After the final addition, the reaction mixture was allowed to stir for an additional hour. Completion of the cyclization reaction was monitored by HPLC and then DMF was evaporated under reduced pressure. The crude cyclic tetrapeptide was dissolved in ethyl acetate and the solution was washed successively by 10% citric acid, 4% sodium bicarbonate and brine. Finally the ethyl acetate solution was dried over anhydrous $MgSO_4$ and filtered. After evaporation of ethyl acetate, the residue was purified by silica gel chromatography using a mixture of chloroform and methanol (99:1) to yield cyclo(-L-Ae7-Aib-L-Phe-D-Pro-) (0.768 g, 82%) as a white foam. HPLC, R_t: 7.91 min, LC-MS $[M+Na]^+$ 477.5 for $C_{25}H_{34}N_4NaO_4$ (calcd 477.3).

4.7. Synthesis of *cyclo*(-L-Ax7(Bpin)-Aib-L-Phe-D-Pro-)

A solution of $[Ir(cod)Cl]_2$ (bis(1,5-cyclooctadiene)diiridium(I) dichloride) (0.034 g, 0.05 mmol) and DPPM (bis(diphenylphosphino)methane) (0.038 g, 0.10 mmol) in anhydrous and degassed dichloromethane (DCM) (5 mL) was flashed with Ar for 5 minutes and stirred for 10 minutes at room temperature. After that, to the solution, *cyclo*(-L-Ae7-Aib-L-Phe-D-Pro-) (0.227 g, 0.50 mmol) and HBpin (pinacolborane) (113 μL, 0.75 mmol) were added and the mixture was flashed with Ar for 5 minutes, then stirred at room temperature for 2 days. The reaction mixture was concentrated by evaporating DCM and purified by silica gel flash column chromatography using a mixture of chloroform and methanol (99:1) to give *cyclo*(-L-Ax7(Bpin)-Aib-L-Phe-D-Pro-) (0.26 g, 90%) as a white solid. HPLC, R_t: 8.94 min, LC-MS $[M+H]^+$ 583.5 (calcd 583.4).

4.8. Synthesis of *cyclo*(-L-Ax7($B(OH)_2$)-Aib-L-Phe-D-Pro-) (3)

To a solution of *cyclo*(-L-Ax7(Bpin)-Aib-L-Phe-D-Pro-) (0.20 g, 0.34 mmol) in acetone/H_2O (4 mL/2 mL), $NaIO_4$ (0.215 g, 1 mmol) and NH_4OAc (0.77 g, 1 mmol) were added and the suspension was stirred at room temperature for 20 h. Then acetone was evaporated and the reaction mixture was poured into water and extracted with ethyl acetate. Finally the ethyl acetate solution was dried over anhydrous $MgSO_4$ and filtered. After evaporation of ethyl acetate, the residue was purified by silica gel chromatography using a mixture of chloroform and methanol (98:2) to yield *cyclo*(-L-Ax7($B(OH)_2$)-Aib-L-Phe-D-Pro-) (0.07 g, 42%) as a white solid. HPLC, R_t: 6.10 min, LC-MS $[M+Na]^+$ 523.5 (calcd 523.3). HR-FAB MS $(M + 2NBA - 2H_2O + H)^+$ 771.3587 for $C_{39}H_{48}O_{10}N_6B$ (calcd 771.3525, $(M+ Glycerol - 2H_2O - H)^-$ 555.

4.9. Synthesis of *cyclo*(-L-Lys-Aib-L-Phe-D-Pro-)

The protected tripeptide (2.03 g, 3.80 mmol) was dissolved in acetic acid (20 mL). Pd–C (0.20 g) was added and the mixture was stirred under hydrogen atmosphere for 12 h. After filtration, acetic acid was evaporated. The residue was dissolved in ethyl acetate and washed with saturated sodium carbonate solution and dried over sodium carbonate. Evaporation of ethyl acetate gave H-Aib-L-Phe-D-Pro-OtBu (1.44 g, 3.60 mmol, 95%)

which was coupled with Boc-L-Lys(Z)-OH (1.64 mg, 4.30 mmol) according to the method described above to yield Boc-L-Lys(Z)-D-Aib-L-Phe-D-Pro-OtBu (2.21 g, 80%). Boc-L-Lys(Z)-Aib-L-Phe-D-Pro-OtBu (2.21 g, 2.88 mmol) was dissolved in TFA (9 mL) and the mixture was cooled in ice bath for 3 h. After evaporation of TFA, the residue was solidified by treating with ether and dried under vacuum to yield H-L-Lys(Z)-Aib-L-Phe-D-Pro-OH as TFA salt (2.10 g, 100%). HPLC, R_t: 6.48 min. TFA.H-L-Lys(Z)-Aib-L-Phe-D-Pro-OH (2.10 g, 100%) was dissolved in DMF (400 mL) solvent and DIEA (1.3 mL, 7.25 mmol) and HATU (1.65 g, 4.35 mmol) were added in separate five portions in every 30 min with stirring, for the cyclization reaction. After the reaction, DMF was evaporated under vacuum, the residue dissolved in ethyl acetate and washed with 10% citric acid solution, 4% sodium bicarbonate solution and brine respectively. The ethyl acetate solution was then dried over anhydrous $MgSO_4$ and filtered. After evaporation of ethyl acetate, the residue was purified by column chromatography using a mixture of chloroform and methanol (99:1) to yield *cyclo*(-L-Lys(Z)-Aib-L-Phe-D-Pro-) (1.20 g, 71%). HPLC, R_t: 7.68 min. *Cyclo*(-L-Lys(Z)-Aib-L-Phe-D-Pro-) (0.30 g, 0.50 mmol) was dissolved in acetic acid (3 mL) and Pd–C (0.025 g) was added. The solution was stirred under hydrogen overnight. After the filtration of Pd–C, acetic acid was evaporated and the residue dissolved in ethyl acetate. The solution was washed with saturated sodium carbonate solution and dried over Na_2CO_3. Evaporation ethyl acetate yielded *cyclo*(-L-Lys-Aib-L-Phe-D-Pro-) (0.16 g, 72%). HPLC, R_t: 4.85 min.

4.10. Synthesis of *cyclo*(-L-Lys(Pe)-Aib-L-Phe-D-Pro-) (4)

To a cooled solution of *cyclo*(-L-Lys-Aib-L-Phe-D-Pro-) (0.08 g, 0.17 mmol) in dry DCM (1 mL), triethylamine (0.04 mL, 0.25 mmol) and acryloyl chloride (0.05 mL, 0.25 mmol) were added and stirred for 12 h at room temperature. After completion of the reaction, DCM was evaporated and the residue was dissolved in ethyl acetate and washed with 10% citric acid, 4% sodium bicarbonate and brine respectively and then dried over anhydrous $MgSO_4$. After evaporation of the ethyl acetate, the residue was purified by silica gel chromatography using a mixture of chloroform and methanol (99:1) to yield *cyclo*(-L-Lys(Pe)-Aib-L-Phe-D-Pro-) (0.059 g, 66%, HPLC R_t: 5.96 min, HR-FAB MS $[M+H]^+$ 512.2780 for $C_{27}H_{38}N_5O_5$ (calcd 512.2873).

4.11. Synthesis of *cyclo*(-L-Lys(Ca)-Aib-L-Phe-D-Pro-) (5)

To a cooled solution of 2-chloroacetic acid (0.048 g, 0.50 mmol) in DCM (1 mL), DCC (0.052 g, 0.25 mmol) was added and the mixture was stirred gently. After 2 h, *cyclo*(-L-Lys-Aib-L-Phe-D-Pro-) (0.080 g, 0.17 mmol) was added and the mixture was stirred for 12 h at room temperature. After completion of the reaction, DCM was evaporated and the residue was dissolved in ethyl acetate and washed with 10% citric acid, 4% sodium bicarbonate and brine respectively and then dried over anhydrous $MgSO_4$. After evaporation of the ethyl acetate, the residue was purified by silica gel chromatography using a mixture of chloroform and methanol (99:1) to yield *cyclo*(-L-Lys(Ca)-Aib-L-Phe-D-Pro-) (0.063 g, 67%, HPLC R_t: 6.07 min, HR-FABMS $[M+H]^+$ 534.2532 for $C_{26}H_{37}ClN_5O_5$ (calcd 534.2483).

4.12. Synthesis of *cyclo*(-L-Ah5(NHOH)-Aib-L-Phe-D-Pro-) (6)

The tripeptide Z-Aib-L-Phe-D-Pro-O^{t}Bu (2.69 g, 5 mmol) was dissolved in acetic acid (25 mL) and Pd-C (0.25 g) was added. The mixture was stirred under hydrogen for 12 h. After completion of the reaction, Pd-C was filtered off and the acetic acid was evaporated. The residue was dissolved in ethyl acetate, washed with saturated sodium carbonate and dried over anhydrous Na_2CO_3. Evaporation of ethyl acetate gave H-Aib-L-Phe-D-Pro-O^{t}Bu (1.90 g, 4.7 mmol, 94%). HPLC, R_t: 4.56 min. The N-terminal free tripeptide H-Aib-L-Phe-D-Pro-O^{t}Bu (1.90 g, 4.7 mmol) was coupled with Boc-DL-Ah5(AcOCH$_2$Ph)-OH (1.50 g , 3.9 mmol), according to the method described earlier and the fully protected crude linear tetrapeptide was purified by silica gel chromatography using a mixture of chloroform and methanol (99:1) to yield Boc-DL-Ah5(AcOCH$_2$Ph)-Aib-L-Phe-D-Pro-OtBu (1.60 g, 2.1 mmol, 63%) as a white foam. HPLC, R_t: 9.33 min. Boc-DL-Ah5(AcOCH$_2$Ph)-Aib-L-Phe-D-Pro-OtBu (1.60 g, 2.1 mmol) was dissolved in TFA (7 mL) at 0ºC and kept for 3 h at room temperature. After evaporation of TFA, the residue was crystallized with mixture of ether and petroleum ether (1:4) to yield H-DL-Ah5(AcOCH$_2$Ph)-Aib-L-Phe-D-Pro-OH as TFA salt (0.92 g, 1.3 mmol, 62%). HPLC, R_t: 6.46 min. To a volume of DMF (130 mL), TFA.H-DL-Ah5(AcOCH$_2$Ph)-Aib-L-Phe-D-Pro-OH (0.92 g, 1.3 mmol) HATU (0.60 g, 1.56 mmol), DIEA (0.742 mL, 4.42 mmol) were added in five aliquots with 20 min time interval

while the solution was stirred vigorously. After the final addition, the reaction mixture was allowed to stir for an additional hour. Completion of the cyclization reaction was monitored by HPLC and then DMF was evaporated under reduced pressure. The crude cyclic tetrapeptide was dissolved in ethyl acetate and the solution was washed successively by 10% citric acid, 4% sodium bicarbonate and brine respectively. Finally the ethyl acetate solution was dried over anhydrous $MgSO_4$ and filtered. After evaporation of ethyl acetate, the residue was purified by silica gel chromatography using a mixture of chloroform and methanol (99:1) to yield *cyclo*(-L-Ah5($AcOCH_2Ph$)-Aib-L-Phe-D-Pro-) (0.27 g, 0.45 mmol, 34%) as a white foam. HPLC, R_t: 9.33 min, LC-MS $[M+Na]^+$ 593.5 (calcd 593.3). The compound *cyclo*(-L-Ah5($AcOCH_2Ph$)-Aib-L-Phe-D-Pro-) (0.27 g, 0.45 mmol) was dissolved in methanol (2.5 mL) and Pd-C (0.025 g) was added. The solution was stirred under hydrogen overnight. After the filtration of Pd-C, methanol was evaporated to get *cyclo*(-L-Ah5(AcOH)-Aib-L-Phe-D-Pro-) (0.13 g, 0.26 mmol). The cyclic tetrapeptide carboxylic acid (0.13 g, 0.26 mmol) was dissolved in DMF (2 mL) and hydroxylamine hydrochloride (0.036 g, 0.52 mmol), benzotriazole-1-yl-oxy-tris-(dimethylamino)-phosphonium hexafluorophosphate (BOP reagent) (0.17 g, 0.39 mmol), DIEA (1.17 mmol, 0.20 mL) were added. The reaction mixture was stirred for 30 min. After work up, the compound was crystallized to yield *cyclo*(-L-Ah5(NHOH)-Aib-L-Phe-D-Pro-) (0.034 g, 0.07 mmol, 23%). HR-FAB MS $[M+H]^+$ 518.2620 for $C_{25}H_{36}N_5O_7$ (calcd 518.2615).

4.13. Synthesis of *cyclo*(-L-Ah5(Mmk)-Aib-L-Phe-D-Pro-) (7)

The tripeptide Z-Aib-L-Phe-D-Pro-O^{t}Bu (1.06 g, 2 mmol) was dissolved in acetic acid (8 mL) and Pd-C (0.10 g) was added. The mixture was stirred under hydrogen for 12 h. After completion of the reaction, Pd-C was filtered off and the acetic acid was evaporated. The residue was dissolved in ethyl acetate, washed with saturated sodium carbonate and dried over anhydrous Na_2CO_3. Evaporation of ethyl acetate gave H-Aib-L-Phe-D-Pro-O^{t}Bu (0.88 g, 2 mmol, 100%, HPLC, R_t: 4.56 min). The N-terminal free tripeptide H-Aib-L-Phe-D-Pro-O^{t}Bu (0.88 g, 2 mmol) was coupled with Boc-DL-Ah5(allyl)-OH (0.70 g , 2.5 mmol), according to the method described earlier and the fully protected crude linear tetrapeptide was purified by silica gel chromatography using a mixture of chloroform and methanol (99:1) to yield Boc-DL-Ah5(allyl)-Aib-L-Phe-D-

Pro-OtBu (0.83 g, 1.26 mmol, 63%) as a white foam. Boc-DL-Ah5(allyl)-Aib-L-Phe-D-Pro-OtBu (0.82 g, 1.24 mmol) was dissolved in TFA (7 mL) at 0ºC and kept for 3 h at room temperature. After evaporation of TFA, the residue was crystallized with a mixture of ether and petroleum ether (1:4) to yield H-DL-Ah5(allyl)-Aib-L-Phe-D-Pro-OH as TFA salt (0.73 g, 1.18 mmol, 95%). HPLC, R_t: 5.54 min. To a volume of DMF (120 mL), TFA.H-DL-A-Aib-L-Phe-D-Pro-OH (0.73 g, 1.18 mmol,), HATU (0.67 g, 1.77 mmol), DIEA (0.52 mL, 2.95 mmol) were added in five aliquots with 20 min time interval while the solution was stirred vigorously. After the final addition, the reaction mixture was allowed to stir for an additional hour. Completion of the cyclization reaction was monitored by HPLC and then DMF was evaporated under reduced pressure. The crude cyclic tetrapeptide was dissolved in ethyl acetate and the solution was washed successively by 10% citric acid, 4% sodium bicarbonate and brine respectively. Finally the ethyl acetate solution was dried over anhydrous $MgSO_4$ and filtered. After evaporation of ethyl acetate, the residue was purified by silica gel chromatography using a mixture of chloroform and methanol (99:1) to yield *cyclo*(-L-Ah5(allyl)-Aib-L-Phe-D-Pro-) (0.15 g, 0.31 mmol, 26%) as a white foam. HPLC, R_t: 6.73 min, LC-MS $[M+H]^+$ 485.5 for $C_{26}H_{37}N_4O_5$ (calcd 485.28).

To a cooled solution of *cyclo*(-L-Ah5(allyl)-Aib-L-Phe-D-Pro-) (0.14 g, 0.29 mmol) in anhydrous DCM (4 mL), *m*-chloroperoxybenzoic acid (*m*-CPBA) (0.10 g, 0.58 mmol) was added in aliquots over 30 min with stirring. The reaction mixture was allowed to stir for 18 h at room temperature. TLC and HPLC showed almost complete conversion of the olefin into epoxide. The solution was then washed with 4% aqueous sodium bicarbonate solution and brine followed by drying over anhydrous magnesium sulfate and filtration. After evaporation of dichloromethane, the residue was purified by silica gel chromatography using a mixture of chloroform and methanol (99:1) to yield *cyclo*(-L-Ah5(epoxide)-Aib-L-Phe-D-Pro-) (0.11 g, 0.22 mmol, 76%). HPLC, R_t: 5.99 min, LC-MS $[M+H]^+$ 501.5 for $C_{26}H_{37}N_4O_6$ (calcd 501.27).

Cyclo(-L-Ah5(epoxide)-Aib-L-Phe-D-Pro-) (0.10 g, 0.20 mmol) was dissolved in 0.5 M sodium methoxide solution (0.40 mL, 0.20 mmol) in methanol. The reaction mixture was stirred at room temperature for 16 h and then quenched by adding acetic acid. Ethyl acetate was added to the reaction solution and the organic phase washed with 10% citric

acid, 4% sodium bicarbonate solution and brine respectively and then dried over anhydrous $MgSO_4$. After evaporation of the ethyl acetate the residue was purified by silica gel chromatography using a mixture of chloroform and methanol (99:1) to yield the corresponding ether (0.065 g, 0.12 mmol, 61%). HPLC, R_t: 5.48 min. LC-MS $[M+H]^+$ 533.5 for $C_{27}H_{41}O_4N_7$ (calcd 533.29).

To a solution of vicinal alkoxy ether (0.05 g, 0.10 mmol) in anhydrous dichloromethane (2 mL) Dess-Martin periodinane (0.26 g, 0.60 mmol) was added. The reaction mixture was stirred at 25 ˚C for 7 h. TLC and HPLC showed complete conversion of the starting alcohol. The reaction solution was then diluted by adding diethyl ether (5 mL) followed by careful addition of a saturated solution of sodium bicarbonate containing 0.45 g (1.8 mmol) of sodium thiosulfate pentahydrate ($Na_2S_2O_3 \cdot 5H_2O$). After stirring for 10 min, the suspension became a clear solution. The organic layer was separated from the aqueous layer and was washed with brine, dried over anhydrous $MgSO_4$. The filtered organic phase was evaporated to get a crude methoxymethylketone which was then purified by silica gel chromatography using a mixture of chloroform and methanol (99:1) to yield *cyclo*(-L-Ah5(Mmk)-Aib-L-Phe-D-Pro-) (0.032 g, 0.06 mmol, 60%). HPLC, R_t: 6.24 min, HR-FAB MS $[M+H]^+$ 531.2835 for $C_{28}H_{41}O_6N_4$ (calcd 531.2819).

4.14. HDACs preparation and enzyme activity assay

In a 100-mm dish, 293T cells (1-2 × 10^6) were grown for 24 h and transiently transfected with 10 μg each of the vector pcDNA3-HDAC1 for human HDAC1, pcDNA3-HDAC4 for human HDAC4, or pcDNA3-mHDA2/HDAC6 for mouse HDAC6, using the LipofectAMINE2000 reagent (Invitrogen). After successive cultivation in DMEM for 24 h, the cells were washed with PBS and lysed by sonication in lysis buffer containing 50 mM Tris-HCl (pH 7.5), 120 mM NaCl, 5 mM EDTA, and 0.5% NP40. The soluble fraction collected by micro centrifugation was precleared by incubation with protein A/G plus agarose beads (Santa Cruz Biotechnologies, Inc.). After the cleared supernatant had been incubated for 1 h at 4˚C with 4 g of an anti-FLAG M2 antibody (Sigma-Aldrich Inc.) for HDAC1, HDAC4 and HDAC6, the agarose beads were washed three times with lysis buffer and once with histone deacetylase buffer consisting of 20 mM Tris-HCl (pH 8.0), 150 mM NaCl, and 10%

glycerol. The bound proteins were released from the immune complex by incubation for 1 h at 4˚C with 40 μg of the FLAG peptide (Sigma-Aldrich Inc.) in histone deacetylase buffer (200 mL). The supernatant was collected by centrifugation. For the enzyme assay, 10 μL of the enzyme fraction was added to 1 μL of fluorescent substrate (2 mM Ac-KGLGK(Ac)-MCA) and 9 μL of histone deacetylase buffer and the mixture was incubated at 37˚C for 30 min. The reaction was stopped by the addition of 30 μL of tripsin (20 mg/mL) and incubated at 37 ˚C for 15 min. The released amino methyl coumarin (AMC) was measured using a fluorescence plate reader. The 50% inhibitory concentrations (IC_{50}) were determined as the means with SD calculated from at least three independent dose response curves.

4.15. The p21 promoter assay

A luciferase reporter plasmid (pGW-FL) was constructed by cloning the 2.4 kb genomic fragment containing the transcription start site into *Hin*dIII and *Sm*aI sites of the pGL3-Basic plasmid (Promega Co., Madison, WI). Mv1Lu (mink lung epitherial cell line) cells were transfected with the pGW-FL and a phagemid expressing neomycin/kanamycin resistance gene (pBK-CMV, Stratagene, La Jolla, CA) with the Lipofectamine reagent (Life Technology, Rockville, MD USA). After the transfected cells had been selected by 400 μg/mL Geneticin (G418, Life Technology), colonies formed were isolated. One of the clones was selected and named MFLL-9. MFLL-9 expressed a low level of luciferase of which activity was enhanced by TSA in a dose-dependent manner. MFLL-9 cells (1 × 105) cultured in a 96-well multi-well plate for 6 h were incubated for 18 h in the medium containing various concentrations of drugs. The luciferase activity of each cell lysate was measured with a LucLite luciferase Reporter Gene Assay Kit (Packard Instrument Co., Meriden, CT) and recorded with a Luminescencer-JNR luminometer (ATTO, Tokyo, Japan). Data were normalized to the protein concentration in cell lysates. Concentrations at which a drug induces the luciferase activity 10-fold higher than the basal level are presented as the 1000% effective concentration 1000% (EC_{1000}). The human wild-type p21 promoter luciferase fusion plasmid, WWP-Luc, was a kind gift from Dr. B. Vogelstein.

5. Reference

1. Vanommeslaeghe, K.; De Proft, F.; Loverix, S.; Tourwe´, D.; Geerlings, P. *Bioorg. Med. Chem.* **2005**, *13*, 3987-3992.
2. Johnstone, R. W. *Nat.Re*V. *Drug Disco*V*ery* **2002**, *1*, 287-299.
3. Monneret, C. *Eur. J. Med. Chem.***2005**, *40*, 1-13.
4. Finnin, M. S.; Donigian, J. R.; Cohen, A.; Richon, V. M.; Rifkind, R. A.; Marks, P. A.; Breslow, R.; Pavletich, N. P. *Nature* **1999**, *401*, 188-193.
5. Woolley, P. Nature **1975**, *258*, 677–682.
6. Corminboeuf, C.; Hu, P.; Tuckerman, M. E.; Zhang, Y. *J. Am. Chem. Soc.* **2006**, *128*, 4530-4531.
7. Parkin, G. *Chem. Rev.* **2004**, *104*, 699-768.
8. Vanommeslaeghe, K.; Loverix, S.; Geerlings, P.; Tourwe, D. *Bioorg. Med. Chem.* **2005**, *13*, 6070-6082.
9. Yoshida, M.; Kijima, M.; Akita, M.; Beppu, T. *J. Biol. Chem.* **1990**, *265*, 17174-17179.
10. (a) Ueda, H.; Nakajima, H.; Hori, Y.; Fujita, T.; Nishimura, M.; Goto, T.; Okuhara, M. *J. Antibiot.* **1994**, *47*, 301-310. (b) Ueda, H.; Manda, T.; Matsumoto, S.; Mukumoto, S.; Nishigaki, F.; Kawamura, I.; Shimomura, K. *J. Antibiot.* **1994**, *47*, 315-323.
11. Kruh, J. *Mol. Cell. Biochem.* **1982**, *42*, 65-82.
12. Kijima, M.; Yoshida M.; Suguta, K.; Horinouchi, S.; Beppu, T. *J. Biol. Chem.* **1993**, *268*, 22249-22435.
13. Closse, A.; Hugenin, R. *Helv. Chim. Acta* **1974**, *57*, 533-545.
14. Yoshimura, K.; Tsubotani, S.; Okazaki, K. TAN1746 compounds, their production and use thereof. JP 7196686,**1995**.
15. Xie, W.; Zou, B.; Pei, D.; Ma, D. *Org. Lett.* **2005**, *7*, 2775-2777.
16. Shute, R. E.; Dunlap. B.; Rich, D. H. *J. Med. Chem.* **1987**, *30*, 71-78.
17. (a) Hirota, A.; Suzuki, A.; Suzuki, H.; Tamura, S. *Agr. Biol. Chem.*, **1973**, *37*, 643–647. (b) Hirota, A.; Suzuki, A.; Aizawa, K.; Tamura, *S. Agr. Biol. Chem.*, **1973**, *37*, 955–956. (c) Hirota, A.; Suzuki, A.; Tamura, S. *Agr. Biol. Chem.*, **1973**, *37*, 1185–1189.

18. Umehara, K.; Nahahara, K.; Kiyota, S.; Iwami, M.; Okamoto, M.; Tanaka, H.; Kohsaka, M.; Aoki, H.; Imanaka, H. *J. Antibiot.* **1983**, *36*, 478-483.
19. (a) Darkin-Rattray, S. J.; Gurnett, A. M.; Myers, R. W.; Dulski, P. M.; Crumley, T. M.; Allocco, J. J.; Cannova, C.; Meinke, P. T.; Colletti, S. L.; Bednarek, M. A.; Singh, S. B.; Goetz, M. A.; Dombrowski, A. W.; Polishook, J. D.; Schmatz, D. M. *Proc. Natl. Acad. Sci. U. S. A.* **1996**, *93*, 13143-13147. (b) Meinke, P. T.; Liberator, P. *Curr. Med. Chem.* **2001**, *8*, 211-235. (c) Han, J. W.; Ahn, S. H.; Park. S. H.; Wang, S. Y.; Bae, G. U.; Seo, D. W.; Known, H. K.; Hong, S.; Lee, Y. W.; Lee, H. W. *Cancer Res.* **2000**, *60*, 6068-6074.
20. Gore, S. D.; Carducci, M. A. *Exp. Opin. Invest. Drugs* **2000**, *9*, 2923-2934.
21. Phiel, C. J.; Zhang, F.; Huang, E. Y.; Guenther, M. G.; Lazar, M. A.; Klein, P. S. *J. Biol. Chem.* **2001**, *76*, 36734-36741.
22. Richon, V. M.; Emiliani, S.; Verdin, E.; Webb, Y.; Breslow, R.; Rifkind, R. A.; Marks, P. A. *Proc. Natl. Acad. Sci. U. S. A.* **1998**, *95*, 3003-3007.
23. (a) Jung, M.; Brosch, G.; Ko¨lle, D.; Scherf, H.; Gerha¨user, C.; Loidi P. *J. Med. Chem.* **1999**, *42*, 4669-4679. (b) Remiszewski, S. W.; Sambucetti, L. C.; Atadja, P.; Bair, K. W.; Cornell, W. D.; Green, M. A.; Howell, K. L.; Jung, M.; Known, P.; Trogani, N.; Walker, H. *J. Med. Chem.* **2002**, *45*, 753-757. (c) Woo, S. H.; Frechette, S.; Khalil, E. A.; Bouchain, G.; Vaisburg, A.; Bernstein, N.; Moradei, O.; Leit, S.; Allan, M.; Fournel, M.; Trachy-Bourget, M. C.; Li, Z.; Bestman, J. M.; Delorme, D. *J. Med. Chem.* **2002**, *45*, 2877-2885.
24. Su, G. H.; Sohn, T. A.; Ryu, B.; Kern, S. E. *Cancer Res.* **2000**, *60*, 3137-3142.
25. Kim, Y. B.; Lee, K. H.; Sugita, K.; Yoshida, M.; Horinouchi, S. *Oncogene* **1999**, *18*, 2461-2470.
26. Jose, B.; Oniki, Y.; Kato, T.; Nishino, N.; Sumida, Y.; Yoshida, *M. Bioorg. Med. Chem. Lett.* **2004**, *14*, 5343-5346.
27. (a) Furumai, R.; Komatsu, Y.; Nishino, N.; Khochbin, S.; Yoshida, M.; Horinouchi, S. *Proc. Natl. Acad. Sci. U. S. A.* **2001**, *98*, 87-92. (b) Komatsu, Y.; Tomizaki, K.; Tsukamoto, M.; Kato, T.; Nishino, N.; Sato, S.; Yamori, T.; Tsuruo, T.; Furumai, R.; Yoshida, M.; Horinouchi S.; Hayashi, H. *Cancer Res.* **2001**, *61*, 4459.

28. Nishino, N.; Jose, B.; Okamura, S.; Ebisusaki, S.; Kato, T.; Sumida, Y.; Yoshida, M. *Org. Lett.* **2003**, *5*, 5079-5082.
29. (a) Suzuki, T.; Ando, T.; Tsuchiya, K.; Fukazawa, N.; Saito, A.; Mariko, Y.; Nakanishi, O. *J. Med. Chem.* **1999**, *42*, 3001-3003. (b) Saito, A.; Yamashita, T.; Mariko, Y.; Nosaka, Y.; Tsuchiya, K.; Ando, T.; Suzuki, T.; Tsuruo, T.; Nakanishi, O. *Proc. Natl. Acad. Sci. U. S. A.* **1999**, *96*, 4592-4597.
30. Bhuiyan, M. P. I.; Kato, T.; Okauchi, T.; Nishino, N.; Maeda, S.; Tomonori G. Nishino; Yoshida, M. *Bioorg. Med. Chem.* **2006**, *14*, 3438-3446.
31. Islam, N.M.; Kato, T.; Nishino, N.; Kim, H. J.; Ito, A.; Yoshida, M. *Bioorg. Med. Chem. Lett.* **2010**, *20*, 997-999.
32. Mulder, G. J.; Meerman, J. H. Environ. *Health Perspect*. **1983**, *49*, 27–32.
33. (a) Michaelides, M. R.; Dellaria, J. F.; Gong, J.; Holms, J. H.; Bouska, J. J.; Stacey, J.; Wada, C. K.; Heyman, H. R.; Curtin, M. L.; Guo, Y.; Goodfellow, C. L.; Elmore, I. B.; Albert, D. H.; Magoc, T. J.; Marcotte, P. K.; Morgan, D. W.; Davidsen, S. K. Bioorg. *Med. Chem. Lett.* **2001**, *11*, 1553–1556; (b) Frey, R. R.; Wada, C. K.; Garland, R. B.; Curtin, M. L.; Michaelides, M. R.; Li, J.; Pease, L. J.; Glaser, K. B.; Marcotte, P. A.; Bouska, J. J.; Murphy, S. S.; Davidsen, S. K. *Bioorg. Med. Chem. Lett*. **2002**, *12*, 3443–3447.
34. Miller, T. A.; Witter, D. J.; Belvedere, S. *J. Med. Chem*. **2003**, *46*, 5097-5116.
35. De Schepper, S.; Bruwiere, H.; Verhulst, T.; Steller, U.; Andries, L.; Wouters, W.; Janicot, M.; Arts, J.; Van Heusden, J. *J. Pharmacol. Exp. Ther.* **2003**, *304*, 881-888.
36. Furumai, R.; Matsuyama, A.; Kobashi, M.; Lee, K-H.; Nishiyama, M.; Nakajima, H.; Tanaka, A.; Komatsu, Y.; Nishino, N.; Yoshida, M.; Horinouchi, S. *Cancer Res.* **2002**, *62*, 4916-4921.

Chapter 4

Design, synthesis and evaluation of various functional groups as HDAC inhibitors on monopeptide derivatives

1. Introduction

The increased focus on inhibitors of HDAC enzymes as targets for cancer treatment stems from their ability to alter several cellular functions. The search for compounds with antitumor activities to develop novel HDAC inhibitors with potency and safety is still going on and with no doubt, very promising area for cancer chemotherapy. Efficacy of HDAC inhibitors is generally considered to be depending upon the terminal metal binding domain which interacts with the active site, a linker domain which occupies the channel and a surface recognition domain which interacts with residues on the rim of the active site. Every functional domain in HDAC inhibitors can be optimized to increase the potency of the inhibitor and to generate isoform selectivity. Functional groups have a significant effect on the isoform selectivity of inhibitors. The residues that make up the active site are highly conserved but there are certain key differences between the active sites of the different isoforms that give certain functional groups the ability to discriminate between isoforms. Each class of functional group has a stereotypical selectivity profile, whereby most type of compounds with the same functional group will have similar isoform selectivity.[1] Targeting cap group modification and functional group optimization, a large number of structurally diverse HDAC inhibitors have been reported in the literatures and patented. Suberoylanilide hydroxamic acid (SAHA), (Figure 1) the structure of which is related to that of trichostatin A (TSA), is one of the early HDAC inhibitors[2] which inhibits cell growth, induces terminal differentiation in tumor cells[3-5] and prevents the formation of malignant tumors in mice.[6]

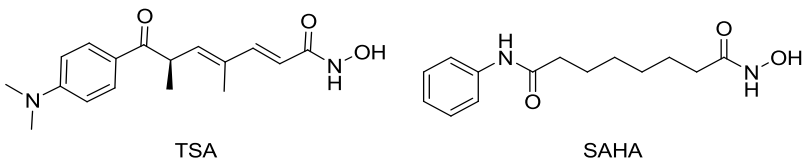

Figure 1. Structures of Suberoylanilide hydroxamic acid (SAHA) and trichostatin A (TSA).

SAHA has been approved by U.S. FDA (Food and Drug Administration) as an HDAC inhibitor against CTCL (Cutaneous T-Cell Lymphoma).[7]

In 2002, Frey, R. R. *et al.*[8] reported a series of trifluoromethylketones as HDAC inhibitors. The same group presented α-ketoamides and α-ketoesters as HDAC inhibitors.[9] The α–ketoamide shown in Figure 2 showed antiproliferative activity *in vitro*, as well as efficacy in a tumor model *in vivo*.

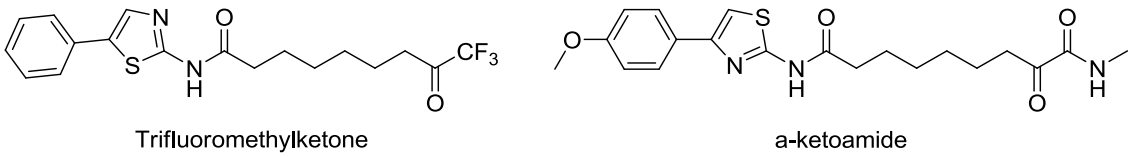

Figure 2. Structures of trifluoromethylketone and α–ketoamide.

Ketone derivatives were originally found in cyclic tetrapeptide inhibitors. This functional group was transposed to alkyl-like inhibitors inspired from SAHA. In their effort to obtain highly active and HDAC selective compounds, Jones *et al.*[10] prepared the compound shown in Figure 3 with nanomolar HDAC1, HDAC2 and HDAC3 selectivity. The compound was found active on several cancer cell lines and was successfully tested *in vivo* compared to SAHA and does not present off-target activities.

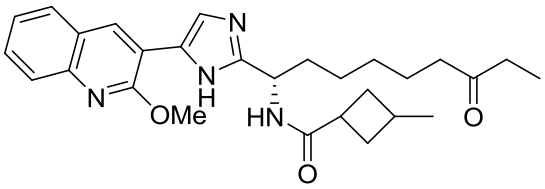

Figure 3. Ketone derivative as HDAC inhibitor.

Pina, I. C. *et al.*[11] reported sulfur derivative psammaplins group as HDAC inhibitors (Figure 4).

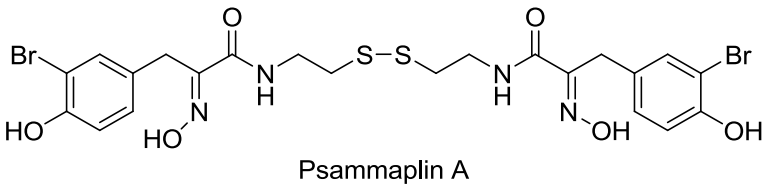

Figure 4. HDAC inhibitor having sulfur as functional group.

Suzuki *et al.* reported a series of thiol-based SAHA analogues (Figure 5) which act as novel HDAC inhibitors.[12] Thiols are thought to inhibit HDACs by coordinating the zinc ion which is required for deacetylation of the acetylated lysine substrate.

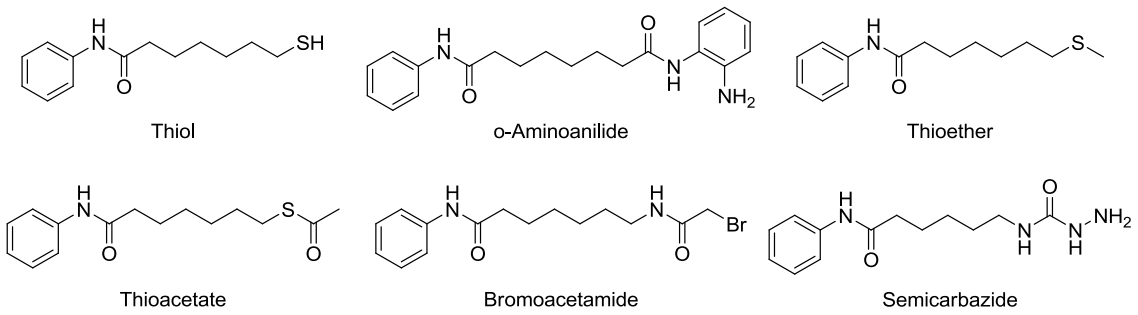

Figure 5. Thiol-based SAHA analogues as potent HDAC inhibitors.

In 2003, Kapustin, G.V. *et al.* [13] prepared phosphorus derivatives as HDAC inhibitors (Figure 6). The weak inhibitory activity of these compounds suggested that the transition state of HDACs may be different from the classical zinc containing enzymes.

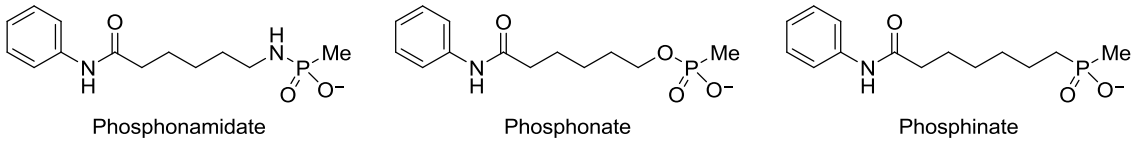

Figure 6. Phosphorus-based SAHA analogues.

Short-chain fatty acid analogues of butyric acid, such as sodium phenylacetate, sodium phenylbutyrate and the anticonvulsant valproic acid (Figure 7) have also been identified as antiproliferative agents and HDAC inhibitors.[14-17]

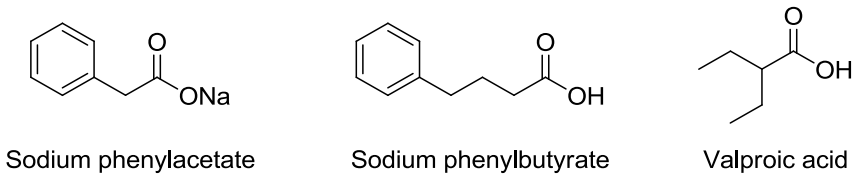

Figure 7. Short-chain fatty acid analogues of butyric acid.

But till date, only a few numbers of reports have been published where monopeptide derivatives having different functional groups are observed as HDAC inhibitors. SK-658 (Figure 8), a monopeptide derivative, has been reported as a new and strong inhibitor of HDAC1 with an IC_{50} value of 2.5 nM.[18]

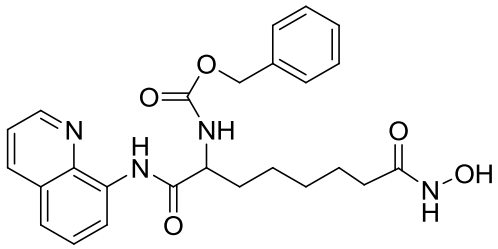

Figure 8. Structure of SK-658, a monopeptide HDAC inhibitor.

Jones, P. *et al.*[19] described a structurally novel series of HDAC inhibitors based on the natural cyclic tetrapeptide apicidin equipped with a varieties of functional groups (Figure 9). These HDAC inhibitors are equipotent with current clinical candidates.

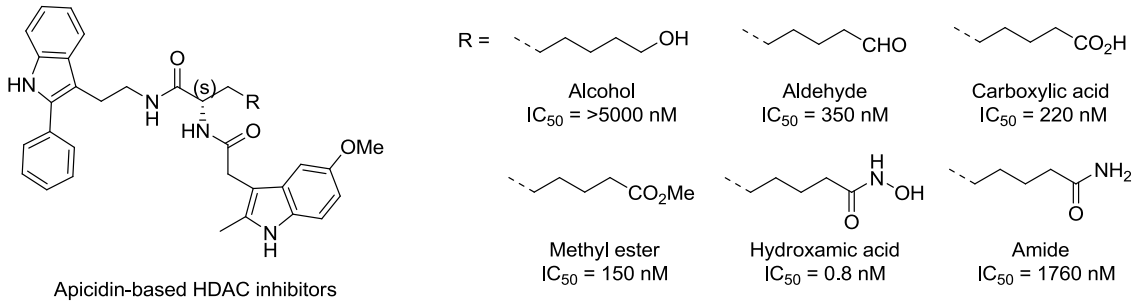

Figure 9. Structures of apicidin-based monopeptide HDAC inhibitors.

Suzuki, N. *et al.*[20] reported a series of boronic acid-based HDAC inhibitors bearing α–amino acid moiety. Among the synthesized compounds, three compounds (Figure 10) displayed potent HDAC-inhibitory activities.

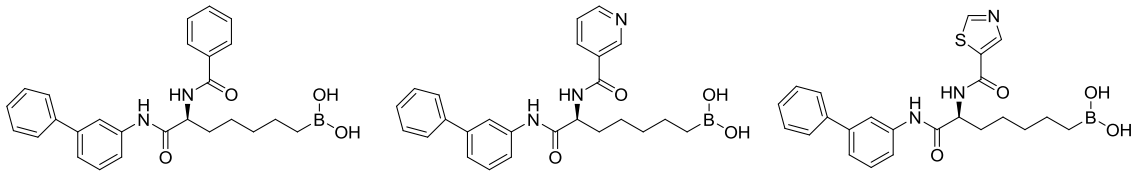

Figure 10. Boronic acid-based monopeptide HDAC inhibitors.

Suzuki, T. *et al.*[21] prepared thiolate analogues (Figure 11) as potent HDAC6 selective inhibitors based on the structure of an HDAC6-selective substrate. These compounds showed significant HDAC6 selective inhibition in both cellular and enzymes assay. They established that the presence of a bulky alkyl group in these compounds is important for HDAC6 selective inhibition.

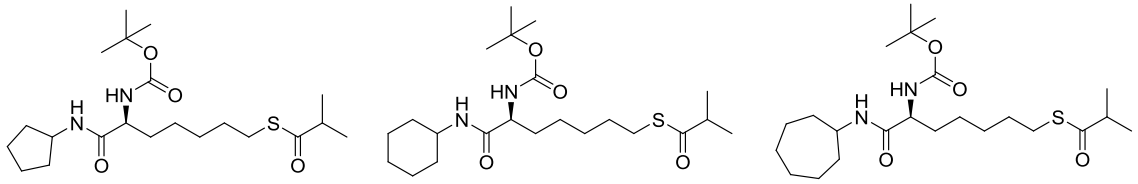

Figure 11. HDAC6-selective monopeptide HDAC inhibitors.

Following these findings, in the search for suitable functional groups, we designed and synthesized several mono-peptide HDAC inhibitors as analogues of SK-658.

2. Results and discussion

2.1. Design

SK-658 has the same linker and zinc binding group region as SAHA. SAHA has been reported to have an IC_{50} value measuring 200 nM.[18] Therefore, SK-658 is 80 fold more active than SAHA only due to the presence of double cap groups. This observation supports the facts that interactions between the surface of the enzyme and the cap groups of inhibitors are of great importance to selective inhibitor design. In order to compare the potency of some functional groups, we designed several HDAC inhibitors (Figure 12) as analogues of SK-658 in which hydroxamic acid group of SK-658 was replaced by thioester, S-S hybrid and methoxymethylketone groups.

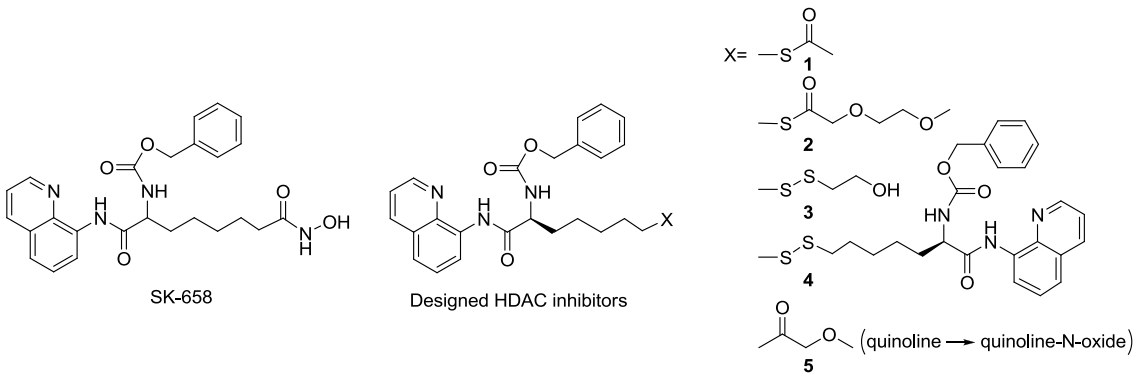

Figure 12. Structures of SK-658 and designed monopeptide HDAC inhibitors.

2.2. Synthesis

SK-658 analogues were successfully synthesized starting from 2-amino-7-bromoheptanoic acid. The condensation between 2-amino-7-bromoheptanoic acid **(1)**

and benzyloxycarbonyl chloride (Z-Cl) was carried out in NaOH and ether at 0^0C. The oily product, 2-(benzyloxycarbonylamino)-7-bromoheptanoic acid (Z-L-Ab7-OH) was then coupled with 8-aminoquinoline in dichloromethane (DCM) in the presence of DCC to get the crystalline solid compound Z-L-Ab7-QA **(2)**.The desired thioester compound Z-L-Am(Ac)-QA **(3)** was obtained by treating compound **2** with potassium thioacetate in DMF at room temperature (Scheme 1).

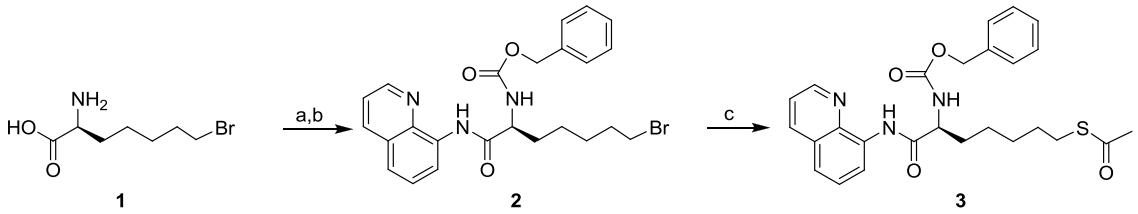

Scheme 1. Reagents and conditions: (a) Z-Cl, NaOH aq, ether, 0^0C, 3 h, 81%; (b) 8-aminoquinoline, DCC, DCM, 86%; (c) AcSK, DMF, 12 h, 68%.

The thioester, Z-L-Am(Ac)-QA **(3)** was treated with $MeNH_2$/MeOH in DMF to obtain the corresponding thiol. After removal of $MeNH_2$/MeOH by evaporation, the residue was again dissolved in DMF and reacted separately with 2-(2-methoxyethoxy)acetyl chloride and 2-marcaptoethanol to obtain Z-L-Am(AcEM)-QA **(4)** and Z-L-Am(betaME)-QA **(5)** respectively (Scheme 2).

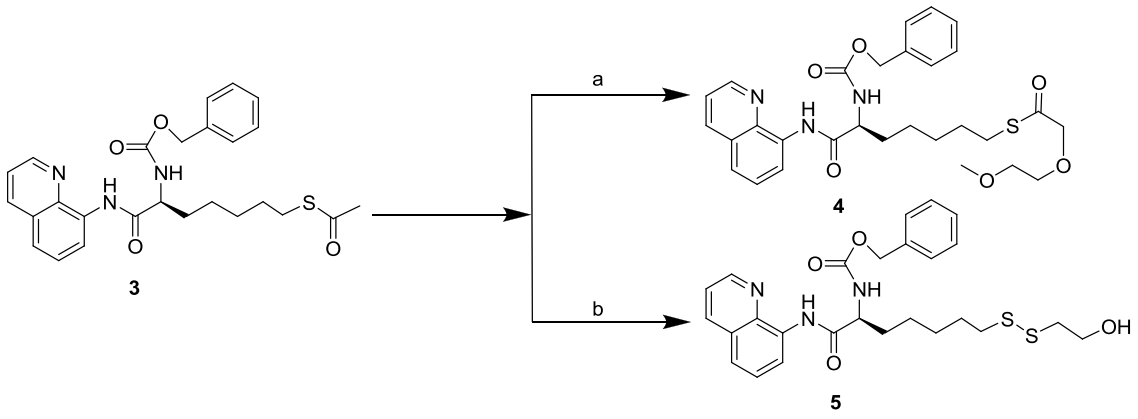

Scheme 2. Reagents and conditions: (a) 2-(2-methoxyethoxy)acetyl chloride, $MeNH_2$/MeOH, DMF, 36%; (b) 2-marcaptoethanol, $MeNH_2$/MeOH, DMF, I_2/EtOH, 61%.

The thioester, Z-L-Am(Ac)-QA **(3)** was again converted to the corresponding thiol in a similar manner as described for compound **4** and **5** and then dimerized to get (Z-L-Am7(S-)-QA)$_2$ **(6)** by treating with iodine dissolved in ethanol (Scheme 3).

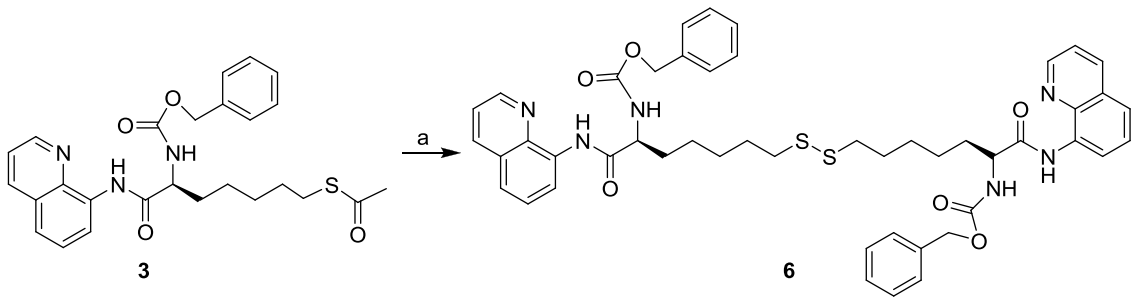

Scheme 3. Reagents and conditions: (a) $MeNH_2$/MeOH, DMF, I_2/EtOH, 86%.

For the synthesis of methoxymethylketone analogue, the carboxyl group of Boc-L-Ae9-OH (**7**) was first protected with 8-aminoquinoline and then the Boc-group was deprotected with HCl/dioxane. The protection of amino group was carried with Z-OSu. Both carboxyl and amino groups protected amino acid (**8**) was then treated with m-CPBA to obtain the correspondind epoxide (**9**) which was converted to hydroxy ether (**10**) by treating with sodium methoxide in methanol. Finally, the secondary alcoholic group of the hydroxy ether was oxidized to the keto-group by using Dess-Martin-periodinane (DMP) to obtain methoxymethylketone analogue Z-L-Ae9(Mmk)-QA (**10**) of SK-658 (Scheme 4).

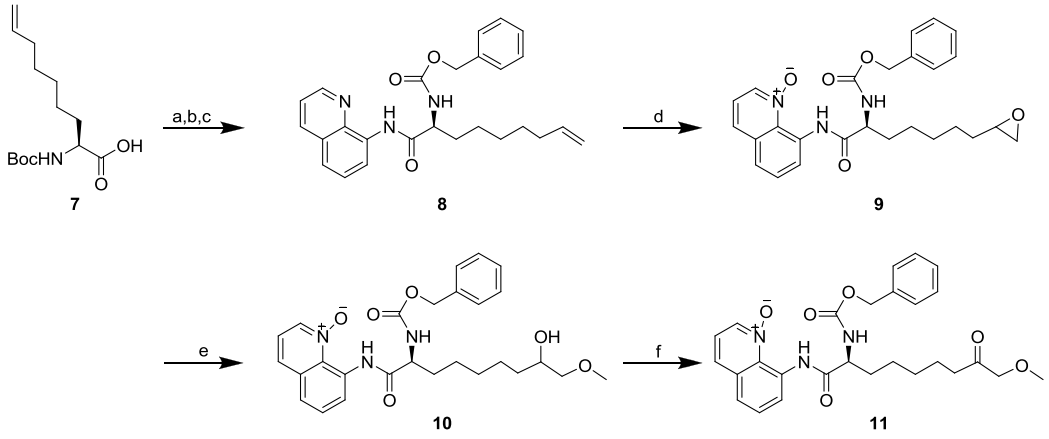

Scheme 4. Reagents and conditions: (a) 8-aminoquinoline, DCC, DCM, 81%; (b) 2 M HCl/dioxane, 2 h, 96%; (c) Z-OSu, Na_2CO_3 aq, acetone, 12 h, 84%; (d) m-CPBA, DCM, 15 h, 56%; (e) NaOMe/MeOH, 18 h, 69%; (f) DMP, DCM, 8 h, 40%.

All the synthesized compounds were characterized by high resolution FAB-MS. The purity of compounds was determined by HPLC analysis and all the synthesized cyclic tetrapeptides showed purity above 97%.

2.3. Evaluation of functional groups as HDAC inhibitors

The synthesized compounds were assayed for HDAC inhibitory activity using HDAC1, HDAC4 and HDAC6 enzymes prepared by 293T cells[22] with the aid of 0.1 mM of dithiothreitol (DTT) which is known to reduce S-S bond according to the reported methods but does not contribute to enzyme activity. In addition, to know the inhibitory activity of these compounds in cell based condition, we carried out p21 promoter assay according to the literature.[23] Detailed experimental procedure for the preparation and assay performed are being explained in experimental section of chapter 3. The results of HDAC inhibitory activity and the p21 promoter assay of the compounds are shown in Table 1.

Table 1. HDAC inhibitory activity and p21 promoter assay data of synthesized and reported compounds

No	Compounds	HPLC R_t (min)	IC_{50} (μM)			p21 promoter assay EC_{1000} (μM)
			HDAC1	HDAC4	HDAC6	
SAHA	-	-	0.29	0.34	0.27	1.2
SK-658	Z-L-Asu(NHOH)-QA	6.36	0.010	0.011	0.045	0.012
3	Z-L-Am7(Ac)-QA	7.68	0.047	0.018	0.034	0.049
4	Z-L-Am7(AcEM)-QA	8.19	0.019	0.018	0.029	0.061
5	Z-L-Am7(betaME)-QA	7.88	0.0049	0.0020	0.0032	0.082
6	$(Z\text{-}L\text{-}Am7(S\text{-})\text{-}QA)_2$	10.76	0.0082	0.0034	0.0075	7.8
11	Z-L-Ae9(Mmk)-QA	7.02				

Finally, we compared these functional groups with the reported compounds, SK-658 and SAHA which served as reference compounds. It is apparent from Table 1 that compounds **5** and **6** are more potent HDAC inhibitors than both SAHA and SK-658. This reveals that the extent of zinc binding affinities for these functional groups in mechanism of HDAC inhibition is highly effective than that of the reference compounds. Compounds **3** and **4** are more active than SAHA because of the introduction of double cap group in the inhibitors but less active than SK-658 due to less zinc binding affinities

for these functional groups towards HDAC inhibitors. The inhibitory activity of compound **11** was not received was not received during this dissertation.

3. Summary

In summary, we designed and synthesized monopeptide derivatives, SK-658 analogues having thioesters, S-S hybrid and methoxymethylketone groups as zinc ligands. All the functional groups showed potency as HDAC inhibitors. The disulfide hybrid showed inhibitory activity in nanomolar range in presence of DTT.

4. Experimental

4.1. General

Unless otherwise noted, all solvents and reagents were reagent grade and used without purification. Flash chromatography was performed using silica gel 60 (230-400) eluting with solvents as indicated. All compounds were routinely checked by thin layer chromatography (TLC) or high performance liquid chromatography (HPLC). TLC was performed on aluminium-backed silica gel plates (Merck DC-Alufolien Kieselgel 60 F_{254}) with spots visualized by UV light. Analytical HPLC were performed on a Hitachi instrument equipped with a chromolith performance RP-18e column. The mobile phases used were A: H_2O with 0.1% TFA, B: CH_3CN with 0.1% TFA using a solvent gradient of A to B over 15 min with detection at 220 nm with a flow rate of 2 mL/min. FAB-mass spectra and high resolution mass spectra (HRMS) were measured on a JEOL JMS-SX 102A instrument.

4.2. Synthesis of Z-L-Ab7-OH

To a cooled solution of 2-amino-7-bromoheptanoic acid (**1**) (2.23 g, 10 mmol) in 1 M aqueous sodium hydroxide (12 mL) containing ether (3 mL), Z-Cl (0.42 mL, 3 mmol) was added and stirred for 15 min. To this solution, 1 M aqueous sodium hydroxide (10 mL) and Z-Cl (1.7 mL, 12 mmol) were added in separate four portions in every 15 min with stirring. After completion of the reaction, the aqueous phase was washed with ether while pH of the aqueous layer was maintained in the basic region. The acid was extracted into ethyl acetate at pH 3-4 by using solid citric acid. The organic phase was

dried with anhydrous magnesium sulfate, filtered and evaporated to get the oily Z-L-Ab7-OH (3.57 g, 10 mmol, 100%). Analytical RP HPLC, R_t: 7.19 min, 81%.

4.3. Synthesis of Z-L-Ab7-QA (2)

To a cooled solution of Z-L-Ab7-OH (3.45 g, 9.7 mmol) in anhydrous DCM (20 mL), DCC (0.6 equiv, 1.20 g, 5.8 mmol) was added and stirred for 1 h. 8-aminoquinoline (1.39 g, 9.7 mmol) was added and stirred for 3 h. The reaction mixture was cooled again and DCC (0.6 equiv, 1.20 g, 5.8 mmol) was added and stirred for 12 h at room temperature. After completion of the reaction, DCM was evaporated and the residue was dissolved in ethyl acetate and successively washed with 10% citric acid, 4% sodium bicarbonate and brine respectively. The ethyl acetate solution was dried over anhydrous $MgSO_4$ and concentrated to remain an oily substance which was purified by silica gel chromatography using a mixture of chloroform and methanol (99:1) and crystallized with a mixture of ether and petroleum ether (1:6, v/v) to yield Z-L-Ab7-QA (**2**) (4.03 g, 8.34 mmol, 86%). Analytical RP HPLC, R_t: 8.07 min, 100%.

4.4. Synthesis of Z-L-Am7(Ac)-QA (3)

To a solution of Z-L-Ab7-QA (**2**) (3.81 g, 7.9 mmol) in DMF (63 mL), potassium thioacetate (1.5 equiv, 1.35 g, 11.8 mmol) was added and stirred for 12 h at room temperature. After completion of the reaction, DMF was evaporated and the residue was dissolved in ethyl acetate and successively washed with 10% citric acid and brine. The ethyl acetate solution was dried over anhydrous $MgSO_4$ and concentrated to remain an oily substance which was purified by silica gel chromatography using a mixture of chloroform and methanol (99:1) and crystallized with a mixture of ether and petroleum ether (1:6, v/v) to yield Z-L-Am7(Ac)-QA (**3**) (2.57 g, 5.36 mmol, 68%). Analytical RP HPLC, R_t: 7.68 min, 100%. HRMS (FAB, *m/z*): $(M+H)^+$ found: 480.1937 (calcd for $C_{26}H_{29}N_3O_4S$: 480.1957).

4.5. Synthesis of Z-L-Am7(AcEM)-QA (4)

To a cooled solution of Z-L-Am7(Ac)-QA (**3**) (1.17 g, 2.45 mmol) in DMF (25 mL), 40% solution of $MeNH_2$/MeOH (3 mL, 27 mmol) was added and stirred at room temperature for 5 h under argon. DMF was evaporated and the residue was dissolved in

pyridine (5 mL) to which 2-(2-methoxyethoxy)acetyl chloride (1 equiv, 2.45 mmol, 0.373 g) was added and stirred overnight at room temperature. After completion of the reaction, pyridine was evaporated and the residue was dissolved in ethyl acetate and washed with brine. The ethyl acetate solution was dried over anhydrous $MgSO_4$ and concentrated to an oily substance which was subjected to gel filtration to get the oily Z-L-Am7(AcEM)-QA (**4**) (0.37 g, 0.67 mmol, 27%). Analytical RP HPLC, R_t: 8.19 min, 100%. HRMS (FAB, *m/z*): $(M+H)^+$ found: 554.2350 (calcd for $C_{29}H_{35}N_3O_6S$: 554.2325).

4.6. Synthesis of Z-L-Am7(betaME)-QA (5)

To a cooled solution of Z-L-Am7(Ac)-QA (**3**) (0.80 g, 1.67 mmol) in DMF (17 mL), 40% solution of $MeNH_2$/MeOH (2 mL, 18 mmol) was added and stirred at room temperature for 5 h under argon. DMF was evaporated and the residue was dissolved in DMF (50 mL) to which 2-marcaptoethanol (10 equiv, 16.7 mmol, 1.17 mL) was added and stirred. To this reaction mixture, iodine (5.5 equiv, 2.33 g, 9.19 mmol) solution in ethanol was added drop wise. After completion of the reaction, DMF was evaporated and the residue was dissolved in ethyl acetate and washed with brine. The ethyl acetate solution was dried over anhydrous $MgSO_4$ and concentrated to an oily substance which was subjected to gel filtration to get the oily Z-L-Am7(betaME)-QA (**5**) (0.52 g, 1.01 mmol, 61%). Analytical RP HPLC, R_t: 7.88 min, 100%. HRMS (FAB, *m/z*): $(M+H)^+$ found: 514.1833 (calcd for $C_{26}H_{31}N_3O_4S_2$: 514.1834).

4.7. Synthesis of (Z-L-Am7(S-)-QA)$_2$ (6)

To a cooled solution of Z-L-Am7(Ac)-QA (**3**) (0.48 g, 1 mmol) in DMF (10 mL), 40% solution of $MeNH_2$/methanol (1 mL, 9 mmol) was added and stirred at room temperature for 5 h under argon. DMF was evaporated and the residue was dissolved in DMF (25 mL) to which iodine (1 equiv, 0.253 g, 1 mmol) solution in ethanol was added drop wise. After completion of the reaction, DMF was evaporated and the residue was dissolved in ethyl acetate and washed with brine. The ethyl acetate solution was dried over anhydrous $MgSO_4$ and concentrated to an oily substance which was subjected to gel filtration to get the crytallined solid (Z-L-Am7(S-)-QA)$_2$ (**6**) (0.38 g, 0.86 mmol,

86%). Analytical RP HPLC, R_t: 7.88 min, 100%. HRMS (FAB, *m/z*): $(M+H)^+$ found: 873.3457 (calcd for $C_{48}H_{53}N_6O_6S_2$: 873.3468).

4.8. Synthesis of Boc-L-Ae9-QA

To a cooled solution of Boc-L-Ae9-OH (**7**) (2.71 g, 10 mmol) in anhydrous DCM (20 mL), DCC (0.6 equiv, 1.24 g, 6 mmol) was added and stirred for 1 h. 8-aminoquinoline (1.44 g, 10 mmol) was added and stirred for 3 h. The reaction mixture was cooled again and DCC (0.6 equiv, 1.24 g, 6 mmol) was added and stirred overnight at room temperature. After completion of the reaction, DCM was evaporated and the residue was dissolved in ethyl acetate and successively washed with 10% citric acid, 4% sodium bicarbonate and brine. The ethyl acetate solution was dried over anhydrous $MgSO_4$ and concentrated to remain an oily substance which was purified by silica gel chromatography using a mixture of chloroform and methanol (99:1) to yield the solid Boc-L-Ae9-QA (3.24 g, 8.18 mmol, 82%). Analytical RP HPLC, R_t: 8.86 min, 100%.

4.9. Synthesis of HCl.H-L-Ae9-QA

Boc-L-Ae9-QA (3.24 g, 8.16 mmol) was dissolved in 2 M HCl/dioxane (40 mL) and the mixture was kept at room temperature for 2 h. The reaction was monitored by TLC. After completion of the reaction HCl/dioxane was evaporated and crystallized with a mixture of ether and petroleum ether (1:2, v/v) to yield HCl.H-L-Ae9-QA (2.90 g, 96%). Analytical RP HPLC, R_t: 6.12 min, 100%.

4.10. Synthesis of Z--L-Ae9-QA (8)

To a suspension of HCl.H-L-Ae9-QA (2.90 g, 7.86 mmol) in acetone (8 mL) and water (8 mL), sodium carbonate (6 equiv, 47.2 mmol, 5.0 g), and Z-OSu (1.96 g, 7.86 mmol) were added and stirred overnight at room temperature. After completion of the reaction, acetone was evaporated and the residue was dissolved in ethyl acetate and successively washed with 10% citric acid, 4% sodium bicarbonate and brine. The ethyl acetate solution was dried over anhydrous $MgSO_4$ and concentrated to remain an oily substance which was purified by silica gel chromatography using a mixture of chloroform and methanol (99:1) to yield the solid Z-L-Ae9-QA (**8**) (2.76 g, 6.40 mmol, 82%). Analytical RP HPLC, R_t: 9.15 min, 100%.

4.11. Synthesis of Z--L-Ae9(epoxide)-QA (9)

Z-L-Ae9-QA (0.86 g, 2.0 mmol) was dissolved in anhydrous DCM (10 mL) in ice bath and 3-chloroperbenzoic acid (m-chloroperbenzoic acid, m-CPBA) (2.0 equiv, 0.96 g 4.0 mmol) was added over 30 minutes. The mixture was stirred overnight. After the completion of the reaction, the reaction mixture was diluted to 40 mL by the addition of DCM. The resultant solution was washed with 4% $NaHCO_3$ and brine respectively. The DCM solution was dried over anhydrous $MgSO_4$, concentrated and was purified by silica gel chromatography using a mixture of chloroform and methanol (99:1) and crystallized with a mixture of ether and petroleum ether (1:4, v/v) to yield Z--L-Ae9(epoxide)-QA (**9**) (0.50 g, 1.12 mmol, 56%). Analytical RP HPLC, R_t: 7.38 min, 100%. HRMS (FAB, *m/z*): $(M+H)^+$ found: 464.2176 (calcd for $C_{26}H_{30}N_3O_5$: 464.2185).

4.12. Synthesis of Z--L-Ae9(OH, OMe)-QA (10)

To the epoxide (0.22 g, 0.50 mmol), 0.5 M NaOMe/MeOH (1 mL) was added in ice bath and was stirred at room temperature for 21 h. The reaction was quenched by the addition of acetic acid and water and methanol was evaporated. The residue was dissolved in ethyl acetate and washed successively with 10% citric acid, 4% $NaHCO_3$ and brine. It was then dried over anhydrous $MgSO_4$ and filtered. After evaporation of ethyl acetate, the residue was purified by silica gel chromatography using a mixture of chloroform and methanol (99:1) and crystallized with a mixture of ether and petroleum ether (1:3, v/v) to yield hydroxy ether, Z--L-Ae9(OH, OMe)-QA (**10**) (0.165 g, 0.34 mmol, 69%). Analytical RP HPLC, R_t: 6.78 min, 100%.

4.13. Synthesis of Z--L-Ae9(Mmk)-QA (11)

The hydroxy ether (0.15 g, 0.31 mmol) was dissolved in anhydrous DCM (6 mL) and Dess-Martin periodinane (DMP) (6 equiv, 0.80 g, 1.88 mmol) was added. The reaction mixture was stirred overnight at room temperature under argon atmosphere. The reaction was quenched by the addition of saturated $NaHCO_3$ solution (6 mL) containing $Na_2S_2O_3.5H_2O$ (3 equiv, 1.40 g, 5.64 mmol) and was stirred vigorously to get two clear layers. The DCM layer was separated and was washed with brine followed by drying

over $MgSO_4$. DCM was evaporated and the residue was purified by silica gel chromatography using a mixture of chloroform and methanol (99:1) to yield the methoxymethyl ketone (Mmk), Z--L-Ae9(Mmk)-QA (0.06 g, 40%) as an oil. Analytical RP HPLC, R_t: 7.02 min, 100%. HRMS (FAB, *m/z*): $(M+H)^+$ found: 494.2316 (calcd for $C_{27}H_{32}N_3O_6$: 494.2291).

5. Reference

1. Butler, K. V.; Kozikowski, A. P. *Curr. Pharm. Des.* **2008**, *14*, 505-528.
2. Breslow, R.; Marks, P. A.; Rifkind, R. A.; Jursic, B. PTC Int. Appl. WO 93/07148, April 15, 1993.
3. Yoshida, M.; Horinouchi, S.; Beppu, T. *BioEssays* **1995**, *17*, 423–430.
4. Richon, V. M.; Webb, Y.; Merger, R.; Sheppard, T.; Jursic, B.; Ngo, L.; Civoli, F.; Breslow, R.; Rifkind, R. A.; Marks, P. A. *Proc. Natl. Acad. Sci. U.S.A.* **1996**, *93*, 5705–5708.
5. Richon, V. M.; Emiliani, S.; Verdin, E.; Webb, Y.; Breslow, R.; Rifkind, R. A.; Marks, P. A. *Proc. Natl. Acad. Sci. U.S.A.* **1998**, *95*, 3003–3007.
6. Cohen, L. A.; Amin, S.; Marks, P. A.; Rifkind, R. A.; Desai, D.; Richon, V. M. *Anticancer Res.* **1999**, *19*, 4999–5005.
7. Mann, B. S.; Johnson, J. R.; Cohen, M. H.; Justice, R.; Pazdur, R. *The oncologist* **2007**, *12*, 1247-1252.
8. Frey, R. R.; Wada, C. K.; Garland, R. B.; Curtin, M. L.; Michaelides, M. R.; Li, J.; Pease, L. J.; Glaser, K. B.; Marcotte, P. A.; Bouska, J. J.; Murphy, S. S.; Davidsen, S. K. *Bioorg. Med. Chem. Lett*. **2002**, *12*, 3443–3447.
9. Frey, R. R.; Curtin, M. L.; Garland, R. B.; Wada, C. K.; Vasudevan, A.; et al. Presented at the 224th National Meeting of the American Chemical Society, Boston, MA, **2002**.
10. Kinzel, O.; Llauger-Bufi, L.; Pescatore, G.; Rowley, M.; Schultz-Fademrecht,C.; Monteagudo, E.; Fonsi, M.; Paz, O.G.; Fiore, F.; Steinkühler, C.; Jones, P. *J. Med. Chem*. **2009**, *52*, 3453-3456.
11. Piña, I.C.; Gautschi, J.T.; Wang, G.-Y.-S.; Sanders, M.L.; Schmitz, F.J.; France, D.; Cornell-Kennon, S.; Sambucetti, L.C.; Remiszewski, S.W. Perez, L.B.; Bair, K.W.; Crews, P. *J. Org. Chem*. **2003**, *68*, 3866-3873.

12. Suzuki, T.; Kouketsu, A.; Matsuura, A.; Kohara, A.; Ninomiya, S.; Kohda, K.; Miyata, N. *Bioorg. Med. Chem. Lett.* **2004**, *14*, 3313-3317.
13. Kapustin, G. V.; Fejer, G.; Grounlund, J. L.; McCafferty, D. G.; Seto, E.; Etzkorn, F. A. *Org. Lett.* **2003**, *5*, 3053-3056.
14. Chen, J. S.; Faller, D. V. *Curr. Cancer DrugTargets* **2003**, *3*, 219-236.
15. Gottlicher, M.; Minucci, S.; Zhu, P.; Kramer, O. H.; Schimpf, A.; et al. *EMBO J.* **2001**, *20*, 6969-6978.
16. Jeong, M. R.; Hashimoto, R.; Senatorov, V. V.; Fujimaki, K.; Ren, M.; et al. *FEBS Lett.* **2003**, *542*, 74-78.
17. Phiel, C. J.; Zhang, F.; Huang, E. Y.; Guenther, M. G.; Lazar, M. A.; et al. *J. Biol. Chem.* **2001**, *276*, 36734-36741.
18. Wang, D. F.; Wiest, O.; Helquest, P.; Lan-Hargest, H. Y.; Wiech, N. L. *J. Med. Chem.* **2004**, *47*, 3409-3417.
19. Jones, P.; Altamura, S.; Chakravarty, P. K. et al. *Bioorg. Med. Chem. Lett*. **2006**, *16*, 5948–35952.
20. Suzuki, N.; Suzuki, T.; Ota, Y. et al. *J. Med. Chem.***2009**, *52*, 2909-2922.
21. Suzuki, T.; Kouketsu, A.; Itoh, Y.; Hisakawa, S.; Maeda, S.; Yoshida, M.; Nakagawa, H.; Miyata, N. *J Med Chem.* **2006**, *49*, 4809-4812.
22. Furumai, R.; Matsuyama, A.; Kobashi, M.; Lee, K-H.; Nishiyama, M.; Nakajima, H.; Tanaka, A.; Komatsu, Y.; Nishino, N.; Yoshida, M.; Horinouchi, S. *Cancer Res.* **2002**, *62*, 4916-4921.
23. Bhuiyan, M. P. I.; Kato, T.; Okauchi, T.; Nishino, N.; Maeda, S.; Tomonori G. Nishino; Yoshida, M. *Bioorg. Med. Chem.* **2006**, *14*, 3438-3446.

Conclusions

In the present dissertation, the main objective was to find potent functional groups/zinc ligands which may have enhanced binding affinities for zinc in HDAC inhibition mechanism. The first strategy was to modify the epoxyketone moiety of 2-amino-8-oxo-9,10-epoxydecanoic acid (Aoe) of the cyclic tetrapeptide chlamydocin which is a very potent but irreversible HDAC inhibitor. In order to do so, several suitable amino acids with optimum side chain lengths and functionalities were necessary which could effectively mimic the Aoe of chlamydocin. The required amino acids were synthesized. The second strategy was to replace the hydroxamic acid group of SK-658, a potent monopeptide HDAC inhibitor, by different functional groups.

In the second chapter of this thesis, the author described in details the synthesis of several unusual amino acids. In the synthesis of different amino acids, commercially available diethyl (Boc-amino)malonate, diethyl 2-acetamidomalonate and several suitable alkylating agents were used. The side chain functional moiety of each amino acid was modified into separate different functional group that can act as effective functional groups/zinc ligands in the active site of HDACs. During this research a convenient method was developed for the synthesis of different amino acids.

In the third chapter of this thesis, the author reported the design, synthesis and evaluation of various functional groups of chlamydocin analogues. The author introduced new (azide, click product, acryloyl etc.) and known functional groups to the chlamydocin framework, cyclo(-L-AA-Aib-L-Phe-D-Pro-), (where AA bears different possible zinc ligands at the end of side chain) and successfully synthesized several compounds having azide, triazole, borate, acrylamide, chloroacetamide, oxyacetic hydroxamate and dioxyacetone as functional groups. The HDACs inhibitory activities of these functional groups were evaluated in the same molecular conditions and compared with chlamydocin and the reported compound CHAP15, a potent chlamydocin-hydroxamates. All the synthesized compounds were less potent inhibitors than that of both chlamydocin and CHAP15. This result reveals that the extents of binding affinities of these functional groups for zinc in HDAC inhibition mechanism are less than that of epoxyketone moiety of chlamydocin and hydroxamic acid of CHAP15.

In the fourth chapter of this thesis, the author reported the design and synthesis of SK-658 analogues. In the search for a suitable functional group/zinc ligand, the hydroxamic acid group of SK-658 was replaced with several functional groups, such as, thioesters, S-S hybrid and methoxymethylketone groups. The HDACs inhibitory activities of these functional groups were evaluated in the same molecular conditions and compared with the reported compounds SK-658 and suberoylanilide hydroxamic acid (SAHA). Two of the synthesized compounds were more potent HDAC inhibitors than that of both SK-658 and SAHA and two were less potent than SK-658 but more potent than SAHA.

The optimal functional groups or zinc ligands from these findings can be utilized as the preferred functional groups/zinc ligands for other HDAC inhibitors.

Acknowledgements

I would like to thank my supervisor Professor Norikazu Nishino (Kyushu Institute of Technology) for sharing his knowledge, experience and expertise selflessly and providing me the rare opportunity to learn, think and engage in this study which, I believe, will benefit me greatly for the rest of my life. I wish to thank him for arranging financial support throughout the work.

I express my sincere gratitude to Professor Tamaki Kato (Kyushu Institute of Technology) for his all time cooperation, valuable suggestions and proper guidance.

Many thanks to Akihiro Ito and Prof. Minoru Yoshida (RIKEN) for the analysis of our compounds against HDAC enzymes.

Heartiest thanks to Dr. Mohammed Parvez Ismail Bhuiyan for introducing me to my supervisor. I would like to thank Dr. Md. Nurul Islam and Md. Ashraful Hoque for their assistance, encouragement and discussion throughout my research.

Many thanks to the present and past members of Nishino Laboratory for their co-operation, encouragement and discussion.

Cordial thanks to the people of Japan for providing me financial support.

Finally, I would like to thank my parents who are my inspiration throughout my life. Thanks to my wife, Nasrin Nahar, as the source of all my strength to complete the study and research. Her ceaseless support, tolerance and encouragement were the significant contribution to the dissertation.

Md. Shahidul Islam

Department of Biological Functions and Engineering
Graduate School of Life Science and Systems engineering
Kyushu Institute of Technology
Kitakyushu, 808-0196
Japan

List of publications

1. Convenient Preparation of *N*-Methyl-L-Lysine and Incorporation to Histone Tail Peptides. Chi Hongfang, Md. Shahidul Islam, Nsiama Tienabe Kipassa, Tamaki Kato, and Norikazu Nishino. *Proceedings of the 46th Japanese Peptide Symposium (Peptide Science)* **2009**, 137-140.

2. Mechanism in Inhibition of Histone Deacetylase by Cyclic Tetrapeptides with Various Functional Groups. Md. Shahidul Islam, Md. Nurul Islam, Nsiama Tienabe, Naoto Oishi, Tamaki Kato, Norikazu Nishino, Akihiro Ito, and Minoru Yoshioda. *Proceedings of the 31st European Peptide Symposium (Peptides)* **2010**, 350-351.

3. Evaluation of Functional Groups as HDAC Inhibitors on Monopeptide Derivatives. Md. Shahidul Islam, Norikazu Nishino, Hyun-Jung Kim, Akihiro Ito, and Minoru Yoshida. *Proceedings of the 5th International Peptide Symposium*, **2010** (in the process of publication).

4. Evaluation of Functional Groups on Amino Acids in Cyclic Tetrapeptides in Histone Deacetylase Inhibition. Md. Shahidul Islam, Mohammed P. I. Bhuiyan, Md. Nurul Islam, Tienabe Kipassa Nsiama, Naoto Oishi, Tamaki Kato, Norikazu Nishino, Akihiro Ito, and Minoru Yoshida. Submitted to Amino Acid.

Presentations at conferences

1. Poster presentation: "Convenient Preparation of *N*-Methyl-L-Lysine and Incorporation to Histone Tail Peptides", Chi Hongfang, Md. Shahidul Islam, Nsiama Tienabe Kipassa, Tamaki Kato, and Norikazu Nishino. *46th Japanese Peptide Symposium,* Kitakyushu, Japan 2009.

2. Poster presentation: "Mechanism in Inhibition of Histone Deacetylase by Cyclic Tetrapeptides with Various Functional Groups" Md. Shahidul Islam, Md. Nurul Islam, Nsiama Tienabe, Naoto Oishi, Tamaki Kato, Norikazu Nishino, Akihiro Ito, and Minoru Yoshioda. *31st European Peptide Symposium,* Copenhagen, Denmark 2010.

3. Poster presentation: "Evaluation of Functional Groups as HDAC Inhibitors on Monopeptide Derivatives" Md. Shahidul Islam, Norikazu Nishino, Hyun-Jung Kim, Akihiro Ito, and Minoru Yoshida. *5th International Peptide Symposium,* Kyoto, Japan 2010.

Dedicated to my parents
and teachers